OPTIMIZING INFORMATION QUERYING AND DISSEMINATION IN WIRELESS NETWORKS

by

Joon Ahn

A Dissertation Presented to the
FACULTY OF THE USC GRADUATE SCHOOL
UNIVERSITY OF SOUTHERN CALIFORNIA
In Partial Fulfillment of the
Requirements for the Degree
DOCTOR OF PHILOSOPHY
(ELECTRICAL ENGINEERING)

August 2011

Dedication

To my dear wife *Hyejin*, my son *Nathan Hyunsuh*, and my parents for their love and support.

Acknowledgements

This dissertation is the result of many collaborations and valuable discussions with Prof. Bhaskar Krishnamachari. I would like to give my special thanks to my advisor, Bhaskar. He has consistently provided inspirations, encouragements, intuition, and patience, among many others. Without his extraordinary guidance and support, this dissertation would never be completed.

I would also like to thank Dr. Fan Bai and Dr. Lin Zhang. Discussions with Dr. Bai and the taxi trace data shared by Dr. Zhang were greatly helpful for the work presented in Chapter 6. I would like to thank my committee members of the Qualifying exam and Defense: Prof. John Silvester, Prof. Ramesh Govindan, Prof. Konstantinos Psounis, and Prof. Michael Neely. Their feedback was useful and helped to enhance the quality of this dissertation.

I would like to give my special thanks to my dear wife, Hyejin, for her selfless love, support, trust, and prayers for me. She has kept me concentrating and pursuing the goal. I thank my son, Nathan Hyunsuh, who gives me pure joy and energy to overcome difficult days.

For all these years, my parents have shown love to me and prayed for me always. Thank you, my parents. I would also like to thank my parents-in-law for their substantial help in the difficult times of me and my wife when my son was born.

I have many pleasant memories with my colleagues in Autonomous Networks Research Group, having discussions and fun in social gatherings. Avinash, Sundeep, Dongjin, Kiran, Shyam, Marco, Amitabha, Hua, Pai-Han, Yi Wang, Yi Gai, Scott, Marjan, Ying, Maheswaran, Sangwon, Suvil, Majed, and Kyoho, I will miss you all.

Finally, my friends have helped this not-so-short Ph.D.time that could be very boring, not so boring. Thank you my friends, Jeongyeup, Sanghyun, Joongsung, Hyunsuk, Jinho, Ki-young, Youngjin, and Moo-Ryong.

Table of Contents

List of Tables

List of Figures

Abstract

The recent advancement in semiconductor technologies brings more and more smart devices everywhere around us. Many emerging networks of such devices are envisioned to bring forward the era when we can gather information from everywhere, process them in real-time to make better decision on our activities, and tap into the necessary information from anywhere, whether at a standstill or moving around. In this dissertation, we consider two such promising networks — Wireless Sensor Networks (WSN) and Vehicular Networks — to see how they can effectively share the information they produce and consume.

First, we investigate how to search efficiently for the interesting information generated by monitoring the physical world through WSNs and look into the implication of our findings. We derive mathematical models for communication costs in information sharing (through search and replication) and optimize the energy-wise communication costs when the WSN operates as a distributed database system. The optimization results are then used to reveal the scaling laws of the network in terms of energy requirements.

As a second study we investigate how to effectively disseminate over a vehicular network the information (e.g. multimedia files) that a group of people want to consume while they are moving

around in the vehicles. We consider a hybrid network of vehicles in which vehicles are equipped with two kinds of radios: a high-cost low-bandwidth, long-range cellular radio, and a free high-bandwidth short-range radio. We formulate an optimization problem to maximize content dissemination from central servers to vehicles within a predetermined deadline while minimizing the cost associated with communicating over the cellular connection. We mathematically analyze the dissemination process and derive a closed-form optimal solution. We also develop a polynomial-time algorithm to obtain the optimal discrete solution better suited for practice and verify our results using real GPS traces of taxis.

Chapter 1

Introduction

It has been of great interest for people to obtain, share, and consume useful information efficiently and effectively. Thanks to the recent advancement in semiconductor technologies, we have a plethora of smart devices everywhere around us. In developed countries, people are starting to have multiple computers including portable laptop computers and mobile handheld devices. It is no longer in the realm of dreams or science fiction that we can gather information from everywhere, process them in real-time to make better decision on our activities, and tap into the necessary information from everywhere, whether at a standstill or moving around.

There are two emerging networks of devices that may bring forward the realization of this vision; one is the wireless sensor network (WSN) and the other is the vehicular network. The wireless sensor network is a new paradigm of collecting information from environments and monitoring the physical world, and the vehicular network is a new domain toward the world of ubiquitous connectivity to virtual information.

In this dissertation we consider mainly two problem domains in these two types of emerging networks. First, we investigate how to search efficiently for interesting information generated by monitoring the physical world and look into the implication of our findings. We optimize the communication search cost in WSN and derive the scaling laws of the network in terms of energy requirements. Second, we investigate how to effectively disseminate over the vehicular network the information that a group of people want to consume while they are moving around in the vehicles.

In this chapter, we introduce wireless sensor networks and vehicular networks, and their relevant preliminaries for this dissertation. Thereafter, we present the summary of our contributions and the organization of this dissertation.

1.1 Wireless Sensor Networks

Recently, semiconductor technology has been greatly developed so that devices of tiny form factor can be equipped with general processors, multiple sensors, wireless communication capabilities, and other features that previous sensors could not afford to have with such small form factor. Because of their small footprint and inexpensive cost, it has been envisioned to deploy a large number of such devices to gather, process, and deliver fine-grained information on the interested environments. The network of these sensing devices is referred to as Wireless Sensor Network (WSN) [8], and it has been under extensive study in recent years.

A sensor device in the wireless sensor network typically has multiple sensors for monitoring surroundings like temperature, humidity, pressure, acoustic, light, and vibration; a low-power embedded microprocessor for processing local sensing data and performing advanced computations like data compression and aggregation; and low data-rate low-power wireless transceivers for cooperating with other nodes and delivering the data. In some cases, it may have actuators such as speakers, buzzers, and LEDs to notify users directly, or localization system like Global Positioning System (GPS) for geotagging the captured data. The sensor device is powered by small batteries with supply voltage as small as 3V because of their form factor and their intended independence to the power grid so that WSN may be deployed for various environments.

For example, Tmote Sky is one of the popular devices in the WSN research community. It has a 16-bit TI MSP430 F1611 RISC microcontroller which features low active and sleep current consumption, a Chipcon CC2420 radio module for the IEEE 802.15.4 compliant wireless communication with 250kbps data rates in the 2.4GHz frequency, an internal Inverted-F microstrip omni-directional antenna that may reach up to 50 meters indoor, or 125 meters outdoor, and several integrated sensors for temperature, humidity, and light detection. Its storage consists of 10KB RAM and 40KB Flash memory.

Many applications of WSN consisting of such devices have been proposed, implemented, and studied to examine the usability and potential of sensor networks and to find out challenges and their solutions in various areas. The applications include industrial structure monitoring [69, 87, 96], habitat monitoring [57, 85, 112, 113, 116, 122, 136], environment monitoring [38, 54, 116, 124, 133], structure health monitoring [29, 67, 91, 111], remote surveillance [14, 55], personal health monitoring [40, 86], and so forth.

The wireless sensor networks are envisioned to be large scaled, composed of thousands, millions of the aforementioned tiny form-factor devices. Such large scale is considered to obtain the fine resolution monitoring to the extent that traditional sensing approaches would not imagine. However, this large scale and the form factor of each devices incur their own fundamental constraints and challenges:

Limited energy: Each sensor device operates typically with small batteries which are not replenishable except in some rare cases where the devices are powered by renewable energy such as solar power through solar panels. Even using energy harvesting technologies, devices face limited energy because of the natural fluctuation of the renewable energy and the small buffer for each device. The energy constraints require WSN to be extensively energy-efficient. Sensors are normally put into sleep mode most of time minimizing their duty cycle. Computation and communication should be energy-aware and minimize unnecessary operations. Otherwise, the lifetime of the network will be prohibitively short.

Limited computing power: The microcontroller in the device has limited computing power due to their small form factor and limited energy supply. This implies that it is not realistic to apply highly sophisticated techniques (for data compressions, aggregation, or classification) that demand intensive computation. The protocols and algorithms should be designed to be simple and effective for WSNs exploiting the collaboration of multiple devices, rather than relying on (extensive) computation on a single node.

Limited communication capability: The wireless transceiver in the sensor node is low-power and low-data rate. The energy consumption of wireless communication is much larger (in orders of magnitude) than that of computation. The energy cost is disproportionate with respect to the communication range r: r^2 (short range) vs. r^4 (long-range). In addition, due to dense deployment of nodes for fine-resolution monitoring, it is needed to reuse the frequency spatially avoiding the excessive packet collisions. Therefore, the communication range of each node is typically short. The communication strategy of WSNs should be carefully designed with these constraints in mind.

Hostile environment: Many applications of WSN involve monitoring various environments that tend to be highly dynamic, dangerous, or unfriendly to human intervention. In these environments, it is not uncommon that nodes fail due to energy depletion, overheat, HW/SW crashes, or natural loss. In addition to large number of sensor nodes, such hostile environments make it almost impossible to give close attention to individual nodes, making unattended autonomous operation a prime design goal of WSN.

Storage constraints: Each node has its own storage for program memory and data memory. Although it is not as critical as other constraints thanks to the advances in the semiconductor technologies, the size and speed of memory are relatively limited. More critical problem than individual storage constraints is about the data loss incurred by node failure. Proper data replication strategies have to be employed to prevent the complete loss of data.

1.2 Storage Models and Query Types in WSNs

In operating a wireless sensor networks, there are several schemes to answer users requests for sensed information. One popular way is that every node in the network sends its sensed data to one or a few sink nodes which are connected, potentially through another network such as Internet, to more powerful machines with enough storage resources. With this scheme, every users' queries can be resolved in these nodes locally, and the queries take no energy in any node in the WSN while processed. This scheme is called a External Storage scheme [42, 107]. Because each of the sensed data has to be delivered to the external node, every message incurs the cost of $O(\sqrt{n})$ when n number of sensor nodes are deployed uniformly in a 2D area. Although external queries cause no cost, the queries generated by internal sensor nodes experience the same cost of $O(\sqrt{n})$ to reach the external storage.

Another way is to use what is called a Local Storage scheme. In this scheme, each node keeps its sensed data, or what we call event information, in its local storage and the query should be propagated through the network to the desired node of its answers. Although this scheme does not incur any energy consumption for transferring its sensed data to some remote machine, the search communication cost of queries can be substantial, especially when the network has no information on which node having which data. Each of the external queries causes the communication cost of $O(\sqrt{n})$ when the location of the target local node is estimated with high accuracy. In the case of no information on the location, it may cause the cost of $O(n)$ if it resorts to flooding for search. Another problem is associated with node failures. When a sensor node stops working due to either failure or battery outage, the data stored in the node face the danger of their unrecoverable lost.

Data-Centric Storage [42, 107] is the scheme where the sensed data is stored either locally or at one or more remote locations within the network. Event information is obtained through queries that are issued on an on-demand basis. With this scheme, the problem of unrecoverable data lost in the local storage scheme can be greatly enhanced because the data no longer depends on a single node's reliability. The communication cost to store a copy of an event depends on the path length from the detector to the chosen carrier for the copy. The cost of query depends on many factors such as querying schemes, the number of copies of the interested events, the spatial distribution of the event copies, etc. And the querying cost is one of the subjects of this dissertation and investigated in Chapter 3.

We focus on *data-centric wireless sensor networks* that employ the data-centric storage scheme because it is inherently more scalable that others especially when the network is large-scaled. It is more scalable also when most of the sensed information is not essential, or there are multiple sinks that may need different subsets of the sensed information at different times. Moreover, the External Storage scheme has the hot-spot problem near and at the sink node, and the Local Storage scheme has the same problem near and at the source node of each event. However, the data-centric network can avoid these problems in some cases, and even can be operated successfully with an arbitrary number of nodes under some conditions.

In data-centric wireless sensor networks, queries can be classified in many ways, as follows:

Continuous queries vs. one-shot queries: Continuous queries request a long duration flow of packets for their responses while one-shot queries request a few number of packets for the response. The flow of response for continuous queries can be a back-to-back stream of packets (e.g. multimedia data) or a series of periodic reports from a given sensor to the querier.

Directed Diffusion proposed in [60, 61] is particularly useful with continuous queries because queries can be used to create the gradient which a long sequence of responding packets can efficiently follow to reach the querier. In order to save the energy expenditure, in-network compression or muti-node fusion can be adopted for the systems of continuous queries.

Random walk [9, 79, 114] mechanisms can be used to resolve simple one-shot queries with negligible overhead and minimal system complexity. Sadagopan *et al.* [102] have proposed ACQUIRE mechanism to efficiently deal with the one-shot queries. In ACQUIRE, an active query is resolved piece-by-piece from cached local information of each forwarder as it goes through the network. Once the query has been fully resolved, the complete one-shot response is sent back directly to the querier.

Queries vs. complex queries: While a simple query requests a response of a single attribute type (e.g. temperature) from a single sensor node, a complex query is associated with a combination of multiple simple sub-queries, or calls for aggregate information (e.g. average temperature) across multiple nodes.

Historical queries vs. real-time queries: Historical queries are the queries for historical data from the network, for example, "What was the maximum temperature over region A yesterday?"

The corresponding data can be stored in the nodes in the interested region, or even other nodes when the sensed data in the network is replicated over the network typically for the higher robustness and easier accessibility. Real-time queries request data from the current moment, which usually makes it harder for the network to post-process them for better functionality.

Because one of our goals in this dissertation is to derive the fundamental scaling laws of data-centric WSNs, we focus on rather less overhead-incurring type of queries that is of the simple historical one-shot queries. We investigate their communication costs in terms of energy expenditure, and the interaction between the communication cost and the storage requirement in the optimum regime of operation. Note that the energy and storage are among the precious resources in WSNs, as we discussed in Section 1.1.

1.3 Vehicular Networks

In Chapter 6, we consider the problem of efficient dissemination of some delay-tolerant content to a group of vehicles that share an interest in this content. The delay-tolerant contents can support a variety of services, ranging from traditional traffic information and weather forecast to futuristic mobile advertisement and music sharing. Such applications/services have been envisioned by industry as a key driving force for future vehicular networks [12].

One straightforward way to build a network for vehicles is to equip them with cellular radio transceivers to use the cellular data networks. The problem is, although they are widely deployed and becoming more spectrum-efficient with the ongoing transition to 4G systems, cellular infrastructure networks are feeling the strain of rapidly increasing data traffic due to new mobile platforms and applications. It is widely predicted that the volume of mobile data consumed by users will grow exponentially in the next decade. For example, it has been estimated in [32] that the global mobile data traffic will increase from 90,000 Terabytes per month in 2009 to 3,600,000 Terabytes per month in 2015, resulting in a dramatic increase of 39 times in 6 years; similarly, AT&T reported that its wireless data usage jumped almost 5,000% from 2006 to 2009 [90]. At the same time, it is also estimated that the growth of cellular infrastructures might fail to keep up with the pace of mobile data growth [26]. The outcome of exponentially growing mobile data significantly surpassing the limited supply of cellular data pipe is being vividly termed as *Mobile Data Tsunami*. As an early sign of mobile data tsunami, the recent event that newly introduced smart phones overloaded cellular systems in major cities was well documented [90].

The practical bandwidth constraints in cellular systems are not only due to limited wireless spectrum but also because of limited capacity of backhaul; while increasing the cellular capacity through additional spectrum or backhaul infrastructure is possible, it will incur significant capital and operational expenditure, further increasing the cost of cellular access charged to customers [97, 115].

One way to mitigate the dependence on the ever-crowded and expensive cellular bandwidth is to employ peer-to-peer communication network among vehicles and use the two networks judiciously. Due to recent development of the semiconductor technologies we can imagine near-future vehicles that are equipped with two different types of wireless radios – a high-usage-cost low-bandwidth, long-range cellular radio, and a free high-bandwidth, short-range WiFi-like radio. Recent trends in the automotive industry point to an emerging age of hybrid communication networks of vehicles consisting of cars equipped with both cellular radio devices as well as short range inter-vehicular radios such as those based on IEEE 802.11p/WAVE (wireless access for vehicular environments).

Therefore, we contend that, as the cellular bandwidth becomes increasingly crowded and more expensive, hybrid protocols that synergistically combine direct cellular access along with store-carry-and-forward routing through peer-to-peer communication will be proved as a bandwidth-efficient and cost-effective way for offloading the often congested cellular infrastructure.

1.3.1 Delay-Tolerant Networks for Sparse Vehicular Networks

The architecture and protocols of today's Internet have been highly successful in broad classes of networks. Those classes of networks share often implicit assumptions that are important to their overall performance. Some of these key assumptions are that an end-to-end path exists between a data source and its peers, that the maximum round-trip time between any node pairs in the network is not excessive, and that the end-to-end packet drop probability is small. The existing TCP/IP-based schemes may operate poorly in the networks where some of the assumptions are violated, particularly, for very long delay paths and frequent network partitions. As pointed out by [37], *challenged networks* are under such conditions, and becoming important, and may not be well served by the current end-to-end TCP/IP models. Such challenged networks include terrestrial mobile networks (e.g. vehicular networks), exotic media networks (e.g. interplanetary Internet), military ad hoc networks, and vehicular networks as described in more detail below.

Terrestrial Mobile Networks: These networks have as important components mobile nodes whose mobility can be closely controlled in some networks, or regarded as an uncontrollable (unknown) parameter in other cases. While the former networks may be partitioned in a periodic and predictable manner, the latter networks may become unexpectedly partitioned due to the node mobility or change in signal strength (e.g. RF interference).

Exotic Media Networks: Interplanetary networks and near-earth satellite communication networks are good examples for this kind of networks. The network is characterized by high latencies with predictable interruption or environment-induced outage, for example, from weather changes.

Military Ad Hoc Networks: Hostile environments are among key features of these networks. The networks can experience frequent disconnections because of mobility, environmental factors, intentional jamming, or higher priority data traffic.

Vehicular Networks: Most nodes are moving with high speed in these networks. This results in a very short-lived communication link between a pair of nodes, which makes conventional routings perform poorly whether they are proactive or reactive. Sparse vehicular networks [11] are in an even worse situation. Due to low market penetration of participating vehicles, each node (vehicle) in the communication graph will have very small number of neighboring nodes (even less than one) most of time. This low density causes several partition in the communication network besides the issue of the short-lived communication link.

These challenged wireless networks are characterized by combination of fragile network connectivity, link error probability, unreliable node longevity, bandwidth limitation, or communication path stability that are significantly worse than conventional networks common in the domain of Internet. The fragile network connectivity incurs end-to-end disconnection that is often more common than connection. This is due to high mobility, low duty-cycle system operations, or sparseness of network.

In the challenged networks, the aforementioned issues are often manifested in the resulting effect of very large and unpredictable delays for end-to-end communication. Among such networks, we call the networks where messages can traverse from a node to another node *over time*, *Delay-Tolerant Networks* (DTNs) in this dissertation. They are also known as disruption-tolerant networks, or intermittently connected networks particularly for the networks with mobile nodes, in some literature. Particularly, we focus on wireless delay-tolerant networks with mobile nodes because they correspond to vehicular networks that are of our main subjects.

Although full connectivity may not be obtained in the snapshot of DTN at any time, messages can be delivered to the destination through a sequence of independent, local forwarding decisions over time because it is assumed that the sequence of connectivity graphs over a time interval are overlapped. This can be easily understood by a simple illustration. Suppose there are three nodes A, B, C in a network. Link AB is up at every $t = 3i, i \in \mathbb{I}$ and down at other times. Likewise, link BC is up at every $t = 3i+2$. In this network, it is obvious that A cannot send any message to C in a single time slot. However, it is possible to deliver a message from A to C in 3 time slots: A sends the message to B at $t = 3i$, then B waits a time slot and send it to C at $t = 3i + 2$. Hence, the message is sent to a (relay) node, gets buffered for relatively long time, then sent to another node when the link become up. This forwarding scheme is often called *store-carry-and-forward*.

Authors of [37] have presented one of the pioneering works that have identified characteristics and challenges of DTN. They have also proposed a network architecture and application interface that structured around optionally-reliable asynchronous message forwarding, explicitly considering limited expectations of end-to-end connectivity and node resources.

In order to understand the hybrid networks of vehicles we first need to understand individual communication networks separately. Although the cellular data networks have sophisticated internals for radio signal handling, power management, etc., the packet communication in the MAC layer and above can be abstracted and modeled relatively simply because it is nevertheless a point-to-point communication between a mobile node and its associated base station.

Sparse vehicular networks, which are the one of main target networks in the dissertation, are one of delay-tolerant networks when they are deployed at the first few years. It is because the density of inter-vehicular network-enabled vehicles will be very low in the early years of adoption. From [11] the rate of populating vehicular network-enabled vehicles in US transportation system is at most around 7% per year in the ideal case that all the new vehicles are network-enabled. This implies that at least 15 years are needed to reach close to 100% market penetration of network-enabled vehicles. At this point, vehicular networks become more like ad hoc networks rather than delay-tolerant networks.

1.4 Contributions

1.4.1 Optimizing Querying in Data-Centric WSNs

In this study, we first derive closed-form expressions for the expected minimum search energy cost and replication cost considering data-centric wireless sensor networks deployed in a d-dimensional area. We use these cost expressions as basic tools when we investigate the optimum data replication strategy, which again is employed to reach the scaling laws. We focus on analyzing the energy costs with respect to two key parameters — the size of the network and the number of copies of the event information.

We then formulate an optimization problem whose aim is to select the optimal number of replicas that minimizes the total communication cost of querying and storage in terms of energy. We focus on the case in which replicated event information is stored at multiple storage points in the network in a randomized manner. Multiple replicas of an event can be either placed carefully at predetermined locations or randomly. The former approach is exemplified by hash-based data centric storage techniques introduced in Section 2.1.1 and can be efficient since queries can be sent directly to the storage location. However, randomized storage of replicated information is justified in some scenarios when there is a high overhead for maintaining shared predetermined location information across the entire network (due to dynamics such as changes, movements and failures of nodes in the network). Randomized storage can also provide for a more load-balanced storage over time, and, in some cases, provide greater security by making it difficult to identify and target nodes containing critical information.

With unstructured, randomized storage, however, the querying nodes must resort to some form of blind search. We focus on expanding ring queries; their performance depends on the amount of replicas (see Section 2.1.2 for more details). We also assume there can be limited storage at each sensor node in some networks. In such scenarios, the optimization must explicitly consider storage constraints. We therefore consider both constrained and unconstrained versions of this optimization problem.

We use this optimization problem as a tool to identify the conditions, in terms of the numbers of events and queries, under which query resolution can be performed in a scalable manner despite constraints on energy and storage. It turns out, though, that the storage constraints are less restrictive than the energy constraints. We therefore first derive the scalable operating conditions using an storage-unconstrained version of the optimization problem, and then use the constrained version to investigate in more detail the behaviors of the network as its size grows.

We find that operating a network in a scalable fashion essentially requires that the traffic load due to additional events and queries be outweighed by the improvement in energy and storage resources obtained as the network size increases. Note that the scaling of event and query activity with network size is application specific — e.g., in many applications there may be only a constant number of queriers regardless of the network size, but the number of events detected grows linearly with the covered area; in other applications, the number of querying nodes may increase in some fashion with the network size, while the events detected remain constant. Thus, our results suggest that only certain types of applications are inherently scalable, while others are not.

Another interesting finding is that networks deployed in higher dimensions are inherently more scalable. Thus, 3D uniform deployments are inherently more scalable than 2D uniform deployments, which in turn are more scalable than 1D uniform deployments. Intuitively, this happens because in higher dimensions the same number of nodes can be packed within a smaller diameter, resulting in a lower average energy consumption per store/query operation.

1.4.2 Optimizing Information Dissemination in Vehicular Networks

In this study, as a first step towards understanding the potential benefits of using delay-tolerant networks to offload the cellular networks, we scope our research interest only to highly mobile vehicular networks. Particularly, we consider the problem of efficient dissemination of some delay-tolerant content to a group of vehicles that share an interest in this content.

We assume that vehicles in the future could be equipped with two different types of wireless radios – a high-usage-cost low-bandwidth, long-range cellular radio, and a free high-bandwidth, short-range WiFi-like radio. In light of the fact that cellular radios in cars would allow only for unicast communication, and therefore incur a significant unit per-vehicle charge for content download, the use of the free short-range radio to assist in such a broad dissemination process becomes economically compelling. We formulate in this work an optimization problem with the goal of maximizing the number of vehicles that obtain the content within a given deadline while minimizing the expense of using the cellular infrastructure.

We analyze mathematically the content dissemination process using differential equations, and derive the optimum solution for the problem in closed-form by solving a convex optimization problem. We then investigate the behaviors of the system in terms under various optimal parameter settings to understand the key trade-offs. We also develop a polynomial-time algorithm to obtain the practical optimum solution to overcome the non-integrality limitations of our closed-form solution. Finally, in order to validate our analysis in a more credible setting, we have used a real large-scale vehicular mobility trace from a large metropolitan area (Beijing) in our study, one of the first studies to do so (a methodology adopted in another recent study [25]). We conclude that content can be spread effectively to most vehicles across a city in a reasonably timely manner with very low-cost use of the cellular infrastructure.

1.5 Organization

We present background of relevant studies in the literature in Chapter 2. In Chapter 3, we derive the expected communication costs of search and replication in wireless sensor networks. We use the developed cost models to optimize the number of replicas to minimize the expected cost for the expanding ring search and validate our results with realistic simulations in Chapter 4. Then, we investigate the scaling laws of data-centric wireless sensor networks with respect to the bounded energy in Chapter 5. In Chapter 6, we turn to the problem of efficient content dissemination in vehicular networks. Finally, we conclude in Chapter 7.

Chapter 2

Background

We present as background the studies in the literature that are relevant to this dissertation. We introduce querying schemes in the data-centric WSN in Section 2.1. The analysis studies for the querying schemes are introduced in Section 2.2. Scaling law studies for wireless sensor networks are introduced in Section 2.3. While the aforementioned studies are related to our WSN study presented from Chapter 3 to 5, the following sections are relevant to our vehicular networks study in Chapter 6. Section 2.4 introduces routing protocols for delay tolerant networks (DTNs) that include the sparse vehicular networks. Section 2.5.1 introduces several mobility models in the literature that are relevant to our study. In Section 2.6, we discuss related techniques on the content dissemination in vehicular networks. Related research on hybrid communication network is discussed in Section 2.7. Finally, we discuss about the positioning of our studies in Section 2.8.

2.1 Querying Schemes in Data-Centric WSNs

The querying strategies in wireless sensor networks can be broadly classified based on whether the network maintains specific structure for efficient search or not. In structured querying schemes for which specific structures are maintained in the network, a hash or index is used so that the querying node knows exactly where the nearest copy of the requested event information can be found. On the other hand, in unstructured querying schemes, the node issuing a query does not know in advance where any copy of the requested event information can be found. We refer to the network with the unstructured querying scheme as an *unstructured network*, the other one as a *structured network*. In this section, we present several prominent querying schemes in the literature for both structured and unstructured networks.

2.1.1 Structured Querying

There have been many interesting querying schemes that utilize the hash function or index to decide the location of generated data.

Li *et al.* [78] have proposed a structured querying mechanism called DIM of data-centric storage scheme that is based on hash techniques, especially for multi-dimensional range queries. The mechanism uses distributed indexes for multi-dimensional data derived from the geographic embedding of a classical index data structure, then use the GPSR geographic routing algorithm to direct the queries. They have shown that DIMs scale as $O(\sqrt{n})$, for insertion and query costs, with the network size n under several query distributions.

Ratnasamy *et al.* [98] have proposed Data-Centric Storage (DCS) mechanism that stores data within the sensor network in a structured manner in the sense that it requires some common knowledge for every node. In their mechanism sensed data are stored at nodes determined by the name associated with the data, using Geographic Hash Table (GHT) system that they have developed for DCS. GHT system hashes keys (e.g., event types) into geographic coordinates and store the key-value pair at the sensor node near the generated geographic coordinate. Hence, it is required that every node knows the predetermined hash functions and the geographic location of each and every node in the network. When these requirements are satisfied, this method can eliminate the flooding phase in certain data-centric routing protocols. Particularly, DCS is shown by the first-order analysis to be preferable for historic queries when WSN is large and there are many detected events among which many would not be queried for.

DIFS [43] is the spatially distributed index system, built on top of GHT, to provide efficient index construction and range searches. In order to support range queries, its hash system takes into consideration the location of detecting node in addition to the event value and name in determining the storage node for the event occurrence. One of its design goals is to provide the load balancing on communications over index nodes so that the network lifetime may be extended. In order to achieve this, DIFS decreases the value range covered by an index node when the index node covers wider spatial area. In DIFS, a multiply rooted hierarchical index is constructed to balance the amount of information that each node in the index structure is responsible for queries. Each node stores event information for a particular range of detected values within a particular geographic region. And, higher-level nodes cover smaller range of values from larger geographic regions while lower-level nodes cover a wider range of values from a smaller geographic region.

2.1.2 Unstructured Querying

For one-shot queries in unstructured networks there are three important querying mechanisms: flooding, controlled-flooding (using expanding rings), and random walks. These querying mechanisms have been extensively studied in the context of wireless sensor networks [2, 28, 30, 61, 83, 84, 102, 105].

Flooding is a simple unstructured querying scheme that needs no information at all about the existence and location (if it exists) of the target information. In this scheme query packets are flooded to be delivered to every node in the network. Upon receiving the query packet, each node retransmit the packet to its neighboring nodes through broadcast, if the node does not have information that the query desires. If it does, the node sends the query answer to the querier.

Flooding is a basic operation and has many applications in resource discovery in wireless networks. Examples include route discovery in several routing protocols of wireless networks [62, 95], sensor discovery in WSNs [61], and service discovery in wireless ad hoc networks [126].

With flooding it is guaranteed to find the target information (if it exists) and the shortest path to it, if there is no loss of packets. It can also support very dynamic networks such as networks with high nodal mobility. On the other hand, it can waste a great deal of resources such as bandwidth and energy. When the network is dense, it can cause high contention and interference that, in turn, may cause excessive retransmission eating up the bandwidth. Even if the target node is nearby, the query is flooded to the network because there is no easy way to stop the flood once it is initiated, which makes every node pay the transmission energy cost. Therefore, the communication cost is always $O(n)$ regardless of the target location.

Flooding may be controlled by limiting the number of hops so that the flooding packet will not be transmitted beyond the maximum number of hop counts, or restricting the flooding distance (when the location information is available to nodes) so that the query is contained in a certain geographical area.

Johnson *et al.* [63] consider *expanding ring* mechanism for their famous DSR protocol for the target discovery while enhancing the resource inefficiency of flooding. Expanding Ring Search (ERS) mechanism issues a sequence of controlled flooding from a querier. The radius of flood (usually expressed as the maximum hop count from the issuer) is restricted to cover only a part of network in the controlled flooding. In ERS, the radius is increasing after each round of flooding if the previous round fails to resolve the query.

Any expanding ring search can be characterized as a vector $u = \{u_1, u_2, \ldots u_m\}$ that describes the sequence of successive TTL values for controlled flooding in each step. For example, let $u = \{1, 5, 10\}$ for a network where the maximum hop count is 10. Then the expanding ring search would proceed as follows: first the nodes within 1-hop are searched for the event through a controlled flood with TTL value of 1. If no copies of the event are located in this first step, then all nodes within 5 hops are searched for the event through a larger controlled flood. If still no copies of the event are located in the second step, then all nodes in the network (within 10 hops) are searched. If at any step at least one copy of the event is located, the search terminates successfully at that step.

Because ERS can stop at a certain round without covering the entire network, it can save the network resources especially the target is close to the querier. However, it may cause more waste if the sequence vector is poorly configured and the target is located far from the querier. It is because the nodes near the querier have to be covered multiple times as ERS progresses.

Cheng *et al.* [30] have shown that two-ring and three-ring schemes can reduce the search cost compared to a single attempt of pure flooding, and have provided a general formula to determine good parameters for the two-ring and three-ring hop-based ERS schemes. They also have conducted a simulation study of ERS and claimed that it can obtain up to 10% energy saving without data caching/replication, compared to the pure flooding, while the delay increases significantly. However, the optimum sequence vector is not identified and utilized in their study. Chang and Liu [28] have developed a dynamic programming solution to obtain the optimal TTL sequence vector that minimizes the expected search cost in terms of transmission number when the event spatial distribution is known a priori.

Intuitively, the performance of a TTL-based expanding ring search improves with additional replicas. When there are more randomly placed replicas in a network, the likelihood that the event being searched for is located within a smaller number of steps, close to the sink, becomes higher. However, this reduction in the expected search energy cost comes at the expense of an increased energy cost for replication.

Random walk-based schemes have been considered in the literature as an alternative way to the flooding-based schemes. In simple random walk schemes, intermediate nodes retransmit the query packet to a random neighboring node instead of broadcasting it. This makes it possible for the network to use less amount of energy than flooding, and the bandwidth consumption is very small. On the other hand, sometime it may use more energy because nodes can retransmit more than once in random walk schemes. The delay until the time to find the target is also generally very large because the query packet moves like Brownian motion. Another weakness of the simple random walk is its tendency to revisit recently visited nodes. It can spend a significant amount of time in the vicinity of the starting node before exploring the rest of the network - causing significant delays and increased energy cost.

Shakkottai [105] have suggested three types of random walk-based search strategies: (a) a querier-only search, where the querier tries to locate the target by initiating random walk query; (b) a querier and target driven "sticky" search, where both the querier and the target node send a query and an advertisement both of which move as random walks; and (c) spatially-periodic caching, where the target information is spatially cached and the querier tries to locate any one of these caches.

An enhanced random walk scheme, called self avoiding random walk with k-memory, has been proposed in [2]. The scheme avoids the most recently visited k nodes that were part of its trajectory. The identity of the last k nodes is stored within the random walk query packet itself. If the random walk finds itself trapped at a node such that all its neighbors have been visited in the last k steps, only then does it violate this avoidance rule to escape, by picking one of the neighbors uniformly at random.

The authors of [84] have considered about launching k-random walks simultaneously to discover desired data in the peer-to-peer (P2P) overlay network. Although their scheme can be used in the wireless sensor network setting, their performance results cannot be directly applied to WSN because the locations of nodes in WSNs are spatially correlated, which is not true in P2P overlay networks.

Sadagopan *et al.* [102] have proposed ACQUIRE search scheme that combines random walks with controlled flooding attempting to achieve best of both worlds. The scheme is designed for one-shot complex queries for historic data, supporting replicated data. In ACQUIRE, each query that consists of several sub-queries is processed at each intermediate node by a sequence of local updates (via local floods) with d hops, then is forwarded to the next node following random walk. The look-ahead parameter d enables ACQUIRE to span from a random walk-based querying (with $d = 0$) to flooding-based querying (with $d = \infty$). The optimum d depends mainly on the query rate and data dynamics. Given the query rate, small d is better for low data dynamics while large d is better for high data dynamics.

The Comb-Needle technique proposed in [83] is similar to the sticky search [105] and the rumor routing scheme [19]. Here, queries build a horizontal comb-like routing structure while events follow a vertical needle-like trajectory to meet the "teeth" of the comb. Key tunable parameters are spacing between branches of the comb, and the length of the needle. It turns out that they are dependent on the query rate and event rate.

2.2 Performance Analysis for Querying in WSNs

As for the analytical modeling of query strategies which we deal with to deduce our scaling laws, there have been several interesting prior studies [83, 105, 107].

Shenker *et al.* [107] have suggested intuitive bounds for the communication costs of query and storage: $O(\sqrt{n})$ for both storing data to external storage and retrieving from the internal sensor nodes, $O(n)$ for flooding-based search in the local storage scheme, $O(\sqrt{n})$ for both structured querying and storing under the data-centric storage scheme, where n is the number of nodes in the network.

In the previous section, we saw Shakkottai [105] have suggested three random walk-based search strategies. They have also presented a comparison of their asymptotic performance. They have shown that the rendezvous-based sticky search has the best success probability over time using Brownian motion assumption in the regular grid network. Specifically, the probability that a query is unsuccessful is shown to decay as $(\log t)^{-1}$ for the querier-only search; $t^{-5/8}$ for the sticky search; and no faster than t^{-1} for the spatial caching scheme, where t is the average of random query time-out value.

Liu *et al.* [83] have analyzed the optimal parameter setting for the comb-needle search approach. For better performance in terms of average total cost per query, the comb inter-spacing and the length of needle should be smaller if the event to query ratio is larger. In the opposite case, the spacing and the length should be larger. If the query rate is larger than the event rate, or there are multiple queriers, a reverse-comb structure can have better performance. The reverse-comb structure consists of the vertical comb for queries and horizontal needles for events. In the comb-needle scheme, the query cost is $O(\sqrt{n})$ and, due to the inherent feature of the scheme, it is hard to improve the query cost by replicating the events.

An analytical comparison of the comb-needles approach and data centric storage is provided in [66]. Through the analysis based on a single-sink square-grid deployment, they have found that the structured hash-based data-centric storage generally performs better than both of the unstructured comb-needle mechanism when the query rates are high and event rates are low. In the case of high event rates, it is found that the comb-needle has better performance. They have also identified magic number thresholds ($\Theta \approx 39.78$) for event rates, for the aggregate queries that requires information from all relevant nodes. The threshold is independent of network size or query probability.

For the expanding-ring search, Chang and Liu [28] have found the way how to construct the series of controlled floods in order to minimize the expected search cost given the distribution of the event's location. They have found that the optimum sequence vector can be determined through the following dynamic programming that can be solved recursively for $0 \leq k \leq L-1$:

$$V(L) = 0 \tag{2.1a}$$

$$V(k) = \min_{k+1 \leq l \leq L} \{C_l + F(l|k)V(l)\} \tag{2.1b}$$

where L is the radius (in terms of hop counts) of the network, C_l is the cost of controlled flooding up to l hops, and $F(l|k)$ is the conditional tail distribution of the target given that the most recently used TTL value k has failed to locate the target. However, from their solution, it is not straightforward to obtain closed-form expressions for the optimum cost that may give intuition on the relationship between system parameters.

In [2], the performances of flooding, ERS, and random walks have been compared in real environments attempting to account for the non-idealities faced by the networks in real deployments. Considered metrics are delay, reliability, and transmission costs. Their simulation and experiment results suggest that flooding scheme is better suited for low-interference environments, while random walks might be a better option in networks with high interference.

2.3 Throughput-Wise Scaling Laws

There have been many interesting studies on the scalability of the wireless networks from the information-theoretic point of view [50, 51, 76, 77, 128]. The information-theoretic approaches make no particular assumption on the way that communications take place, focusing on the upper bounds on the throughput using order notation.

Gupta and Kumar [51] studied on the throughput capacity of multi-hop wireless networks where nodes are not mobile. They considered two types of communication models, namely, the protocol model and the physical model, for arbitrary networks and random networks. In arbitrary networks, they focused on optimum arrangement so that all n nodes are optimally placed in a disk of unit area, traffic patterns are optimally assigned, and each transmission's range is optimally chosen. In random networks, all n nodes are randomly located independently and uniformly, either on the surface of a three-dimensional sphere of are 1 m^2, or in a disk of area 1 m^2 in the plane.

Each node has a randomly chosen destination for transmission, and the radio range or power is same for all nodes.

The protocol model can be said an abstracted link layer model similar to what many network studies have been using due to its relative simplicity. In this model, a transmission is considered successful its transmitter and receiver are in the radio range, and there is no other active transmitter in the radio range (plus some guard zone) of the receiver. Presenting it more formally, suppose node X_i transmits to a node X_j, where X_i denote both a node and its location. Then, for the arbitrary networks, this transmission is successfully received by node X_j if

$$|X_k - X_j| \geq (1 + \triangle)|X_i - X_j| \tag{2.2}$$

for every other node X_k simultaneously transmitting over the same channel.

For the random networks, the transmission is successful if

$$|X_i - X_j| \leq r \qquad \text{and} \qquad |X_k - X_j| \geq (1 + \triangle)r \tag{2.3}$$

for every other node X_k simultaneously transmitting over the same channel. r can be considered as the common radio range.

A radio range does not need to be assumed for the arbitrary networks because optimum radio power for each transmission is used. The quantity $\triangle > 0$ models the situations where the interference range is larger than the transmission radio range.

The physical model for successful communications is essentially the signal-to-interference ratio model that represents more accurately the real world phenomena. In this model, a transmission is successfully received at the receiver if its power at the receiver side is larger than the ambient noise plus the sum of powers of irrelevant transmission at the receiver side after proper scaling. Presenting it more formally, let $\{X_k; k \in \mathcal{T}\}$ be the subset of nodes simultaneously transmitting at some time instant over the same channel. Let P_k be the power level chosen by node X_k. Then, the the transmission from a node $X_i, i \in \mathcal{T}$ is successfully received by a node X_j, for both arbitrary and random networks, if

$$\frac{\frac{P_i}{|X_i - X_j|^\alpha}}{N + \sum_{k \in \mathcal{T}, k \neq i} \frac{P_k}{|X_k - X_j|^\alpha}} \geq \beta \tag{2.4}$$

where N is the ambient noise power level and α is the path loss exponent so that the signal power decays with distance r as $\frac{1}{r^\alpha}$.

Gupta and Kumar found that the transport capacity of an arbitrary network under both protocol and physical models is $\Theta(W\sqrt{An})$ bit-meter per second under the optimum arrangement, where W is the transmission bandwidth in bets per second, and A is the area of network domain in square meters. Equivalently, the throughput is only $\Theta(\frac{W}{\sqrt{n}})$ bits per second for each node for a destination nonvanishingly far away.

They also found that the throughput capacity in a random network is more pessimistic. The throughput obtainable by each node for a randomly chosen destination is $\Theta(\frac{W}{\sqrt{n \log n}})$ bits per second under the protocol model. Under the physical model, higher throughput can be obtained but no better than the throughput capacity of arbitrary networks, i.e. $O(\frac{W}{\sqrt{n}})$.

Their results suggest that wireless multi-hop networks with immobile stations should suffer from unacceptably high decrease in throughput as the number of participant stations increases. Some solutions for the poor scalability may be to explicitly restrict the network size, or clustering the network and using wired transmissions for inter-cluster communications.

In the sequel [50] they extended the results for three-dimensional deployment of nodes. They found that the entire network can carry only $\Theta\left(W(Vn^2)^{\frac{1}{3}}\right)$ bit-meters per second at its best for an arbitrary network under the Protocol Model, and that the per-node throughput capacity is $\Theta\left(\frac{W}{(n\log^2 n)^{\frac{1}{3}}}\right)$ bits/sec for a random network. Similar results are reported for the physical model.

In [128] Xie and Kumar have tried to tackle the capacity problem of wireless networks that is of great interest in the information theory. Instead of studying the exact capacity region, they have studied the scaling law of transport capacity that is the supremal distance-weighted sum of rates for all source-destination pairs.

Consider a network in which n nodes are located on a plane, with minimum separation distance $\rho_{\text{min}} > 0$. Signals attenuates as $\frac{e^{-\gamma\rho}}{\rho^{\delta}}$ over a distance ρ, where $\gamma \geq 0$ is the absorption constant and $\delta > 0$ is the path loss exponent. And all receptions are assumed to be subject to additive Gaussian noise of variance σ^2.

In such network they found that the transport capacity grows like $O(n)$ when $\gamma > 0$ or $\delta > 3$. Note that the absorption constant γ is generally positive unless the medium is a vacuum. This scaling law becomes sharp meaning that the transport capacity order is $\Theta(n)$ if traffic can be load balanced across the network by multipath routing with bounded distance traversed at each hop.

Therefore, the multihop routing strategy is shown to be order-optimal for information transport under this high attenuation case.

2.4 Routing Protocols for DTNs

The initial effort for tackling delay-tolerant networks was placed on designing reliable and efficient routing protocols under a variety of assumptions on mobility [110, 134]. Because of the challenging characteristics of DTNs introduced in the previous chapter, conventional Internet routing protocols such as RIP and OSPF as well as popular ad hoc routing protocols like AODV and DSR have severe performance degradation, or simply fail to work in DTN. The reason for failure is the fact that the protocols try to establish complete end-to-end paths before sending data to the destination. In DTN, end-to-end paths are intermittent at best. But, many times, there is not a complete end-to-end path at all at any given point of time. Note that neither proactive nor reactive ad hoc routing protocols work successfully in DTN although the reactive protocols are designed particularly for dynamic networks. This is because the difference between the proactive and reactive is the timing at which the routes are figured out: in proactive schemes, it is figured out before the destination is identified while reactive schemes search out the routes after the destination is identified.

A great deal of research efforts have been devoted in exploring viable solutions for routing in this challenging DTNs. They can be classified into the following three categories.

2.4.1 Mobile Resource-Based Schemes

In this class of schemes systems employ mobile resources such as data mules or mobile agents as message ferries for more effective data exchanges. In [1] tour-boats and pleasure cruisers are used to carry and relay the monitored water quality data from the buoys deployed on a lake. Authors of [104] have presented an architecture that uses data mules to carry and relay the collected data in sparse sensor networks to wired access points. Such message ferries in these schemes are often added into the system mainly, if not solely, to "motion-relay" the data that would be otherwise stuck in the part of the network. Therefore, they can be considered as overhead of the system with extra cost, resulting in restriction on wide application of the system.

2.4.2 Prediction-Based Schemes

In these schemes inter-node contacts and nodal mobility are believed to be effectively predictable through the history of nodes' behaviors such as current positions, trajectories [73], contact history to other nodes [21, 22, 137], or landmarks [134]. The next hop that may not be currently available is decided using the predictions so as to maximize the chosen quality of service (QoS) metric (e.g. delay, delivery success ratio).

Authors of [81] and [137] have proposed utility routing schemes, in which each node maintains a utility value for every other node. The utility value is considered as the predictor of the future likelihood of two nodes' contact, and updated using the inter-contact times, that is the time between the consecutive contacts of the pair of nodes. With these schemes, a node forwards a copy of the message to encountered nodes only when their utility values are higher enough for the message destination. The routing protocol proposed in [22] also uses the past frequencies of contacts as well as past inter-contact times. For vehicular DTNs, [73] uses the current positions and trajectories of nodes to predict their future distances to destinations, which plays key role in their routing decision. Authors in [21] have proposed MaxProp routing protocol that also utilizes the historical contact data to predict the path likelihoods. However, they have gone beyond the simulation studies with artificial mobility models for the performance evaluations of their protocol, using 60 days' trace data from a real DTN network deployed on 30 buses. MobySpace routing algorithm proposed in [75] uses a high-dimensional Euclidean space constructed on nodes' mobility patterns to find better forwarders for the destination. The frequency of nodes' visits to each possible location is recorded as the basis of the future distance calculation in the constructed Euclidean space. While the above routing protocols focus on the prediction of whether or not two nodes would encounter, the authors in [134] have proposed predict-and-relay algorithm that also considers what time the nodes would meet each other. In their algorithm a time-homogeneous semi-Markov process model is employed to determine the probability distribution of future contact times.

2.4.3 Opportunity-Based Schemes

In this class of schemes nodes forward messages during nodes' contacts that are unscheduled or regarded as random. These schemes either assumes the contacts may not be effectively predicted, or the sophistication in prediction methods does not deserve their overheads. In order to fully exploit the given opportunity, most approaches in this category disseminates in the network multiple copies of each original message to encountering nodes, which generally gives higher delivery reliability and low latency. However, this benefits come at the cost of higher buffer occupancy and bandwidth consumption, which can be justified and reasonable when the network is sparse enough.

Direct transmission is one of the most simple strategy without overhead considered in [46, 104]. The source of the message does not use any relay nodes, but directly deliver the message to the destination when they meet together. There is only one copy for each messages and no overhead whatsoever in the network. But, without surprise, it has been shown that direct transmission is extremely slow [46].

Epidemic routing is a fundamental strategy and serves as basis in many schemes in this category [53, 64, 108, 118, 119, 137] In the epidemic routing data is flooded in the network and eventually reaches the destination. This strategy is guaranteed to find the the shortest paths when there is no contention for shared resources such as wireless bandwidth and buffer space in the nodes. Because it can be excessively wasteful of such resources, the performance of pure epidemic routing has been shown to degrade significantly especially when the network components have tight resource constraints [81, 109, 118]. However, under the assumption of sufficient buffer space and bandwidth, epidemic routing achieves the minimum end-to-end delay.

Many approaches have been devised to reduce the overhead and improve the performance of pure epidemic routing. Approaches in [108] focus on suppressing redundant transmissions and cleaning up valuable buffer space after a message has been delivered to its destination. In [118] and [137] the "gossiping" strategy is explored where a message is forwarded to encountering nodes with probability smaller than one. Harras *et al.* [53] have devised heuristics on hop limits and timeouts to improve the controlled message flooding. Spray-and-wait protocol proposed in [110] attempts to control the flooding overhead by limiting the number of message copies distributed in its first phase called *Spraying phase*. Then, it relies on the direct delivery waiting until any one of message-carriers meets the destination. Authors in [125] have investigated Network Coding ideas and found it could be useful to reduce the amount of transmitted bytes in the network.

Because node mobility is an essential factor of these opportunity-based schemes, they are also referred to as mobility-assisted routing, encounter-based forwarding, or store-carry-and-forward in the literature.

2.5 Mobility Models

In vehicular delay-tolerant networks, mobile node encounters are utilized for opportunistic data transfer, and thus the underlying mobility model has a great impact on their performance. In this section, we review the mobility models that have been extensively adopted in the literature.

2.5.1 Random Walk Model

In the random walk mobility model, each node moves as a random walker on a two-dimensional lattice, in the similar way that particles move as a Brownian motion. The time is discrete in this model and nodes transition at each time step. At each time step, each node hops to the neighboring points (up, down, left, right) or optionally stays in the same position with the same probabilities (1/4 without staying, 1/5 with staying). The transition is jointly independent of all previous transitions. When the node is on a boundary point, it may hop back to the same position instead of hopping out of the lattice, or hop to the point on the other side (as in two-dimensional torus topology). This model represents well the movement in Manhattan network where nodes moves from intersection to intersection with constant speeds in a city where all intersections are perpendicular and equally spaced.

The stationary distribution of node location is uniform in the random walk model. This can be easily seen from the fact that the 2D random walk can be decomposed into two independent 1D random walks that have same probability of hopping to the opposite directions, each of which results in the uniform stationary distribution of location [44]. In this model the diffusion speed is relatively slow.

2.5.2 Random Waypoint Model

The random waypoint mobility model [20] has been employed in many simulation studies in mobile ad hoc networks. In this model each node is assigned a sequence of waypoints to visit in the given area. For an arbitrary node, its first waypoint is chosen uniform at random over the given area, then the node travels to the waypoint at a constant speed which is chosen uniform at random within the given range of speed (v_{min}, v_{max}). The waypoint and the speed is jointly independent of each other and the start point. Upon arrival to the waypoint, the next waypoint of the node is chosen again uniform at random in the area, and its speed for this travel is also chosen uniformly at random in the speed range. Before starting the travel to the next waypoint, the node may pause optionally for a random amount of time. These random values (waypoint, speed, pause time) are jointly independent of each other and all the previous random values.

The stationary distribution of node location and speed in the random waypoint model are significantly different from the uniform distribution. Specifically, the location distribution is more and more concentrated toward the center of the region [16]. If the travel speed happens to be chosen to zero at some point of time, the node will become stuck in the current location and never be able to move again because it will never reach the next waypoint and get a new speed. Hence, the minimum speed of the speed range has to be strictly positive in order to prevent the average speed of nodes over time from falling to zero [131]. This does not mean that the nodes keep moving in this mobility model; nodes' idling can be represented with the optional pause time.

2.5.3 Random Direction Model

In the random direction model [15, 48], each node is assigned a sequence of random triple of direction, speed, and travel time. In the beginning each node is assigned a first travel direction uniformly at random, first constant speed uniformly at random from the given range (v_{min}, v_{max}), and the random finite travel time for this round. These three random values are jointly independent of one another and the start location of the node. If the node reaches a boundary of the given region, it may be reflected or appear on the other side treating the area wrapping around (like the 2D torus topology). When the travel time is expired, the new triplet of random values is chosen randomly which is jointly independent of each other and all the previous random values.

The station distribution of node location and direction have been proven to be uniform [88] for arbitrary distributions of direction, speed, and travel time. This result does not depend on the boundary actions – whether nodes are reflected or appear on the other side. Different from the random waypoint model, the minimum speed v_{min} has no problem being set to zero because the travel times are finite so that the node may be mobilized later.

2.6 Content Dissemination

In our study, we use differential equations to model content replication and dissemination. This is similar to [25], where differential equations are used to model the age of content updates and are found to be a good approximation for large networks. There have been several other prior studies on content dissemination and replication in vehicular networks.

In [41], the authors explore the latency performance of different frequency-based replication policies for sharing media files, in the context of vehicular networks with limited storage. They found that a random replication technique is sufficient when total storage capacity of the network is significantly larger than the required repository size from all media files. Otherwise, they found that there is a large parameter space where the frequency-based replication schemes provide superior performance. Unlike our study, they assume the network can be divided into cells, in each of which vehicles form a connected ad hoc network. However, it is assumed that traffic cannot get across the cell boundaries through multi-hop communications. The only way to transfer files across the cell boundaries is the mobility of vehicles that carry the files.

CarTorrent [74] and AdTorrent [89], present content dissemination mechanisms to distribute files and advertisements, respectively, in vehicular networks. In [99], the authors study how user impatience affects content dissemination.

2.6.1 Analysis of Epidemic Routing

Mobility-assisted epidemic routing in Delay Tolerant Network can be modeled as an infectious disease spread [10]. Many epidemiological modeling techniques used in medical research [35] has been borrowed by computer scientists to model the propagation of computer virus, such as eigenvalue analysis [121] or random graph analysis [39]. In our study, we find that ordinary differential equations (ODE) can be effectively used to model content replication and dissemination. This finding is in line with other recent study [24], which suggested a partial differential equation can be used to model the probability distribution for the age of latest content update. Note that the focus of [24] is on the distribution of *age* of the latest content update in mobility-assisted content dissemination, while ours is interested in the *state* of content update (i.e., whether the node is infected).

2.7 Hybrid Networks

In the past decade, extensive research has been done to study the technical feasibility of heterogeneous intergrated wireless networks. This research has focused largely on using limited-capability, limited-coverage wireless access technologies to supplement ubiquitous wireless telephony systems such as Universal Mobile Telecommunication Systems (UMTS, a.k.a, 3G).

Within their limited coverage area, wireless local area networks (WLANs) can provide a high throughput data service in comparison to cellular systems [92]. The integration of cellular system and WLAN system as a coherent heterogeneous network enables a better data service to customers by allowing handover between different wireless access technologies [103, 130]. The standardization effort has been undertaken by the IEEE 802.21 standard working group, which supports seamless handover between networks of the same type (i.e., horizontal handover) as well as handover between different network types (i.e., vertical handover) [47].

A hybrid wireless network architecture integrating both cellular systems and Mobile Ad hoc Networks (MANET) is also barely a new concept. One approach is to use MANETs to enhance the service provided by existing cellular infrastructure. For instance, the iCar network architecture [127] was proposed to place a number of Ad hoc Relay Stations (ARS) in a cellular network in attempt to address network congestion problem. Later theoretical analysis has shown that the iCar system not only increases the capacity of cellular network by offloading the data traffic to ad hoc networks [80, 127], but also increase the coverage of cellular system. Another approach is to occasionally use expensive cellular systems to guide the operations of MANETs. In CAMA network architecture [18], the important control information such as routing, security and localization is exchanged in cellular networks while the heavy-weighted data flow is delivered by MANET systems. This concept has been verified and evaluated using an empirical implementation in a WLAN testbed network [71]. Similar to these research works, we also follow the design philosophy of using resource-abundant distributed networks to offload the data traffic from costly cellular networks where some cells could be heavily congested; however, to our best knowledge, our study is the first to propose the idea of integrating delay-tolerant networks and cellular systems. In contrast to prior works which utilize connected multi-hop routes for real-time data service, our work focuses on using "store-carry-forward" approach for delay-insensitive service. Considering slow technology adoption process of vehicular communication devices [11], we believe that VANETs at early stage are likely to be delay-tolerant networks (rather than well-connected ad hoc networks).

There has been a growing interest in understanding the capacity of heterogeneous networks composed of cellular networks and ad hoc Networks. A number of theoretical studies have been dedicated to modeling the network capacity of such heterogeneous networks [31, 72, 82] and identifying the conditions under which the capacity gained via augmenting with ad hoc networks outweigh the penalty introduced by multi-hop relaying [117].

2.8 Positioning of Contributions

2.8.1 Wireless Sensor Networks Study

As discussed in Section 2.3, there have been many interesting studies on the scalability of the wireless networks in terms of throughput. However, our study investigates the scalability in another domain, namely, energy consumption, because energy is among the most precious resources in wireless sensor networks.

Some prior studies have looked at maximizing the energy efficiency in order to increase the lifetime of wireless sensor networks [56, 70, 129, 132]. But, they have focused on controlling the network topology given parameters such as network size. Some other studies have looked at the asymptotic energy-constrained network lifetime [58] or maximizing the network lifetime [17, 27, 65]. However, these studies pertain to continuous data-gathering applications.

As discussed in Section 2.2, there have been several interesting prior studies that have explored the analytical modeling of query strategies which we deal with to deduce our scaling laws. However, these studies have not developed scaling laws for data-centric storage and querying.

Further, all these prior studies do not address the question of application-specific conditions that determine fundamental limits on scalability of sensor networks.

2.8.2 Vehicular Networks Study

Unlike these pioneering works concentrating on network capacity analysis, our study formulates an optimization problem to maximize the contents dissemination upon the predetermined delay deadline while minimizing the cost associated with the cellular network. We find that, if some delay is allowed, contents can be spread to a large number of vehicles even with a very small number of accesses of the infrastructure, thus greatly reducing the usage of scarce cellular bandwidth and lowering the cost that content providers and end users need to bear.

Our work on vehicular heterogeneous networks is complimentary to the above studies on "pure" DTNs: (1) the network architecture in our study consists not only DTN system but also cellular system, though the usage of latter one is minimized; (2) we focus on the optimization of content replication and dissemination in VANETs to reduce the usage of scarce, costly cellular links while satisfying the customers' need using DTN as a cheap data pipeline, which is validated using real-world vehicular mobility traces; (3) our main objective is to establish an analytical framework to understand the fundamental tradeoff between the cost and delay requirement of content dissemination in the context of vehicular heterogeneous networks.

To evaluate the DTN protocols many previous studies have employed random mobility models, as discussed in Section 2.5.1. While the random models are useful for analytic analysis on the performance of the DTN protocols, they do not have to be relevant to the realistic situations. There have been some studies analyzing human mobility traces in the effort to derive more realistic mobility models. In [23], empirical studies have been conducted with human-carried wireless devices to derive statistical distributions of inter-contact time of encounters of nodes. Rhee *et* *al.* [100] have analyzed real human mobility traces and suggested that human walk patters follow Levy Walk model, which is more diffusive than Brownian motion but less diffusive than the random waypoint model. These studies analyzing human mobility traces are complimentary to our study, which is one of the first to use a real large-scale vehicular mobility trace in a major metropolitan area.

As discussed in Section 2.6, there have been several studies to explore or analyze the content dissemination process. Different from these studies, our focus in this work is on a novel cost optimization problem for disseminating content to the maximum number of vehicles within a given deadline, that leverages both the cellular infrastructure and peer-to-peer vehicular communication.

As discussed in Section 2.7, extensive research has been done to study the technical feasibility of hybrid integrated wireless networks. In common with these works, we too propose the integration of the cellular network with another mobile network, however in our context the other mobile network is a delay-tolerant network (DTN) that uses "store-carry-and-forward" approach for content dissemination. Also, unlike much of the prior focus on capacity improvements, our focus is primarily on maximizing content dissemination within a delay deadline while minimizing the cost of cellular access, though certainly our approach will also free up scarce cellular bandwidth.

Chapter 3

Modeling Search and Replication Costs in Wireless Sensor Networks[1]

In this chapter, we derive the expected communication costs of search and replication of event information in terms of the energy expenditure. In addition to the fixed transmission power (FTP) assumption, we also consider the random geometric graph (RGG) model where the nodes are deployed uniformly and independently at random. In this case, ensuring connectivity with high probability requires that the radio range be scaled with the network size so that each node has a logarithmic number of neighbors on average [49, 93, 94].

3.1 Assumptions

In this section, we introduce the common key assumptions employed for Chapters 3, 4, and 5, unless stated otherwise.

[1]This work was done jointly with Prof. Bhaskar Krishnamachari, and was first published as [5].

- N nodes are deployed with a constant density in a d-dimensional ball $\mathbb{B}^d$ space. The constant density implies that if the network size is increased, the deployment area grows proportionally. We consider mainly the fixed transmission power (FTP) model in which the radio range R is kept fixed, but the deployment is such that the network remains connected.

- The distribution of events is assumed to be uniform in the deployment area.

- A total of r copies of an event are maintained with the uniform distribution in the network by creating $r - 1$ additional replicas when the event is first sensed.

- Each query is a one-shot query (i.e. requires a single response, not a continuous stream), and is satisfied by locating a single copy of the corresponding event.

- We assume that the links over which transmissions take place are lossless (e.g., using blacklisting) and present no interference due to concurrent transmissions (e.g., due to low traffic conditions or due to the use of a scheduled MAC protocol). However, we relax this assumption for verification of our results in our simulation study (Section 4.4).

- For the FTP deployment model, the total energy cost for searching is assumed to be proportional to the total number of transmissions.

- We assume that the boundary effect is negligible. However, we relax this assumption in our simulation study (Section 4.4).

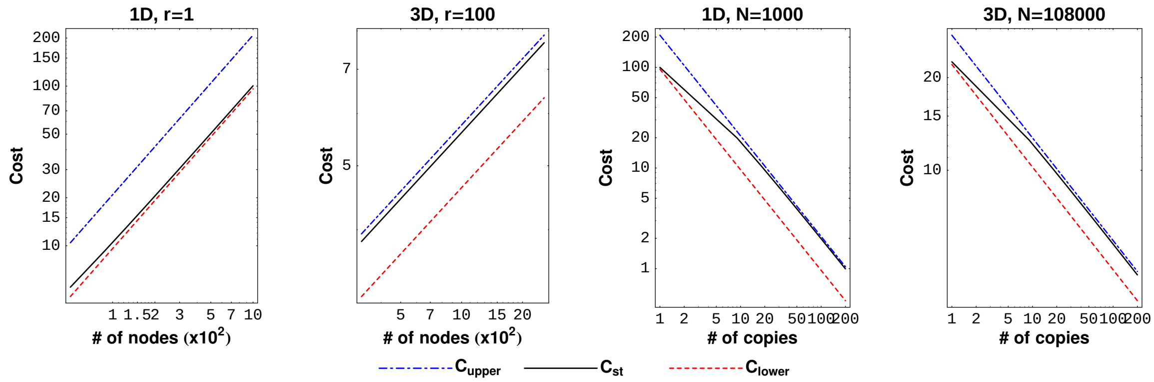

(a) (b) (c) (d)

Figure 3.1: Structured average search cost

3.2 Search Cost in Structured Networks under the FTP Model

We first consider structured networks where nodes are deployed with constant node density ρ in the d-dimensional ball. We further assume that the network is sufficiently dense so that all nodes within a distance kR of the sink can be reached in k hops. The nodes in the network are all located within L hops of the sink. When modeling the search cost we assume that the sink is located in the center of the region. In Section 4.4, we show by simulations that relaxing this assumption does not provide big differences. Let $V_d(x)$ denote the volume of a d-ball of radius x, $N_d(h)$ the number of nodes at most h hop away from the sink. The volume of the ball is known to be expressed as follows:

$$V_d(x) = f(d) \cdot x^d \tag{3.1}$$

where $f(d) = \frac{2\pi^{d/2}}{d \cdot \Gamma(d/2)}$.

In this dissertation, $\Gamma(\cdot)$ is the Gamma function. Then, the number of nodes at most h hop away from the sink is given by,

$$N_d(h) = \rho\, f(d) \cdot (hR)^d = \tau(d) \cdot h^d \tag{3.2}$$

where

$$\tau(d) \doteq \rho\, f(d)\, R^d \tag{3.3}$$

which is the average number of neighbors of a node. Hence, the total number of nodes N can be expressed as follows:

$$N = N_d(L) = \tau(d) \cdot L^d \tag{3.4}$$

Now we recall that there are r number of copies of an event distributed uniformly randomly in the network. Let the random variable X_{min} denote the hop distance to the nearest copy of them from the querier. Its tail distribution is as follows:

$$\begin{aligned} P\{X_{min} > x\} &= \prod_{i=1}^{r} P\{i\text{-th copy is not in } x \text{ hop neighbors}\} \\ &= \left(1 - \frac{N_d(x)}{N}\right)^r = \left(1 - \frac{x^d}{L^d}\right)^r \end{aligned} \tag{3.5}$$

Figure 3.2 illustrates how this distribution varies with the number of replicas in a typical network. As may be intuitively expected, this distribution shifts to the left (i.e. the nearest copy is located closer to the sink) as the number of replicas increases. This should result in a lower search cost with increasing replication size.

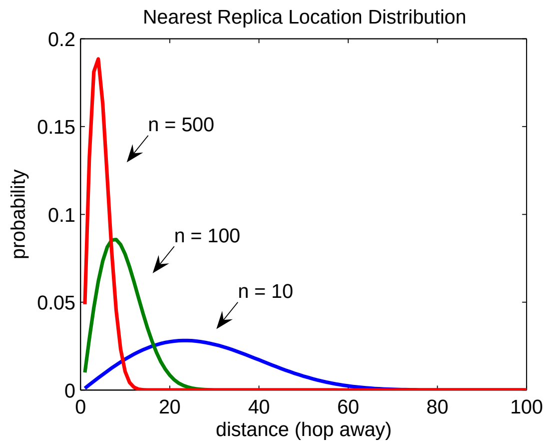

Figure 3.2: Illustration of the probability mass function for the nearest replica in a 2D network (L=100)

In the structured network, the search cost is related to a path of the lowest cost from a querier to the nearest node which has one of the copies. We assume the shortest path routing scheme so that the path would be their shortest path. Hence, the search cost is equal to the hop count from the querier to the nearest copy through the shortest path, which is denoted by X_{min}, plus the cost back to the querier. Hence, the expected search cost of the network deployed in d dimension is as follow:

$$C_{s,st}^{(d)} = 2\ E[X_{min}] \tag{3.6}$$

Using the tail distribution given in Equation (3.5) and approximating summation to integration, we have

$$\begin{aligned} E[X_{min}] &= \sum_{x=0}^{L} P\{X_{min} > x\} \approx \int_0^L \left(1 - \frac{x^d}{L^d}\right)^r dx \\ &= \frac{L \cdot \Gamma(\frac{1}{d})}{d} \cdot \frac{\Gamma(r+1)}{\Gamma(r + \frac{1}{d} + 1)} \end{aligned} \tag{3.7}$$

	$d=1$	$d=2$	$d=3$
$l\,(d)$	0.0961058	0.410714	0.68273
$u\,(d)$	0.208858	0.577974	0.849538

Table 3.1: The coefficients of lower and upper bounds of the search cost for the structured network. The number of neighbors $\tau(d)$ of a node is set to 10.

The last equality of Equation (3.7) can be achieved through the multiple application of Integration by Parts and the property of Gamma function; $\Gamma(x) = (x-1)\Gamma(x-1)$.

Using Lemma A.1 stated in the appendix and the equation $L = \frac{1}{\sqrt[d]{\tau(d)}} \cdot \sqrt[d]{N}$ (from Equation (3.4)), we can calculate the lower and upper bounds of the search cost:

$$C^{(d)}_{s,st}(N,r) \quad > \quad l(d) \cdot \frac{\sqrt[d]{N}}{\sqrt[d]{r}} \tag{3.8}$$

$$C^{(d)}_{s,st}(N,r) \quad < \quad u(d) \cdot \frac{\sqrt[d]{N}}{\sqrt[d]{r}} \tag{3.9}$$

where

$$l(d) \quad = \quad 2\,\frac{\Gamma(\frac{1}{d})\;exp\left(\frac{1}{d}\right)}{d\;\sqrt[d]{\tau(d)}}\left(\frac{d}{d+1}\right)^{\frac{3d+2}{2d}}$$

$$u(d) \quad = \quad 2\,\frac{\Gamma(\frac{1}{d})\;exp\left(\frac{1}{d}+\frac{12+d}{12(12+13d)}\right)}{d\;\sqrt[d]{e\,\tau(d)}}$$

Table 3.1 shows the numerically calculated values of $l(d)$ and $u(d)$ when the average number of one-hop neighbor $\tau(d)$ is 10 for 1, 2, and 3 dimensional deployments. As the table illustrates, the lower and upper bound are close and proportional to $\sqrt[d]{N}/\sqrt[d]{r}$ from the above double inequalities. Hence, we can approximate with good accuracy the search cost as follows:

$$C_{s,st}^{(d)} = \alpha_1 \cdot \frac{\sqrt[d]{N}}{\sqrt[d]{r}} \tag{3.10}$$

where $l(d) < \alpha_1 < u(d)$ (we can obtain the more accurate value of α using the curve fitting.)

Figure 3.1 verifies the accuracy of our model in various cases; (a) and (b) illustrate how the search cost varies as the number of nodes increases in 1D and 3D deployment, respectively. The number of copies of the event is 1 and 100 for (a) and (b), respectively. (c) and (d) show the search cost vs. the number of copies in 1D and 3D deployment, respectively. The number of nodes is 10^3 and 108×10^3 for (c) and (d), respectively. The bounds of the search cost are evaluated using Equation (3.8) and (3.9), and the search cost is evaluated numerically using Equation (3.6) with (3.7). All the four plots agrees that the search cost is almost proportional to the bounds in both relatively large and small networks, both 1D and 3D networks, and when r is small or large. As for 2D deployment, we have investigated extensively in Chapter 4 and [3], which also agree with the above.

3.3 Search Cost in Unstructured Networks under the FTP Model

We now consider unstructured networks. The search cost consists of the cost to locate the nearest copy and the cost to bring the data back to the querier using the shortest path. Since the latter cost is much smaller than the former, we here ignore the latter cost, which is equal to $E[X_{min}]$

given in (3.7). Hence, we derive the search cost expression using the optimal expanding ring-based flooding query [28, 68]. We consider the same d-Ball as a network deployment space as in Section 3.2.

3.3.1 Cost Modeling of Expanding Ring Searches

Any expanding ring search can be characterized as a vector $u = \{u_1, u_2, \ldots u_m\}$ that describes the sequence of successive TTL values for controlled flooding in each step. The vector is also referred to as the TTL sequence vector. To ensure that the entire area is covered in the worst case, u_m is set to L. For example, let $u = \{1, 5, 10\}$ for a network where the maximum hop count is $L = 10$. Then the expanding ring search would proceed as follows: first the nodes within 1-hop are searched for the event through a controlled flood with TTL value of 1. If no copies of the event are located in this first step, then all nodes within 5 hops are searched for the event through a larger controlled flood. If still no copies of the event are located in the second step, then all nodes in the network (within 10 hops) are searched. If at any step at least one copy of the event is located, the search terminates successfully at that step.

Because we assume that each transmission (and the corresponding receptions) incurs a unit cost, the cost of the controlled flooding incurred in the i^{th} search step is given as:

$$C_f^{(d)}(u_i) = 1 + N_d(u_i - 1) \tag{3.11}$$

where $N_d(h)$ is the number of nodes up to h hops away given in Section 3.2.

For a given search sequence vector u, assuming there are r total copies of the event in the network, the expected search cost is then

$$C_{s,un}^{(d)} = \sum_{i=1}^{m} C_f^{(d)}(u_i) \cdot Pr\{X_{min} > u_{i-1}\} \tag{3.12}$$

where $Pr\{X_{min} > u_0\}$ is defined to be 1 (since the search sequence starts with u_1, and it is guaranteed that there is at least one copy of the event being queried somewhere in the network).

3.3.2 Optimal Costs of Expanding Ring Searches

The cost evaluation of the optimal expanding ring-based flooding query requires the optimal TTL sequence. Chang and Liu [28] have developed a dynamic programming solution to solve this problem. This dynamic program uses the following recursive property.

Let the value function $V(n)$ be the minimum expected cost-to-go (over all choices of TTL values), given that the most recently used TTL value k did not locate the object. Then

$$V(L) = 0 \tag{3.13}$$

$$V(c) = \min_{c+1 \leq k \leq L} \{C_f(k) + F(k|c) \cdot V(k)\} \tag{3.14}$$

In the case of multiple replicas, we use the tail distribution $F(k|c)$ given as follows:

$$\begin{aligned} F(k \mid c) &= Pr\{X_{min} > k \mid X_{min} > c\} \\ &= \left(\frac{L^d - k^d}{L^d - c^d}\right)^r \end{aligned} \tag{3.15}$$

The optimal search sequence u^* is obtained by recursively calculating the value function, and then tracking back through the choices made at each step to determine the optimal TTL value for each stage. This search sequence can then be used in Equation (3.12) to determine the expected cost of the optimal strategy. However, this algorithmic approach does not yield a tractable closed form expression for this cost as a function of the number of replicas. We therefore derive lower and upper bounds on the cost, before developing an approximate expression for the optimal cost based on the bounds.

3.3.2.1 Lower Bounds

We first consider the lower bound of the optimal expected search cost. Suppose a querying node happens to know the hop distance X_{min} to the nearest copy of the desired event before disseminating queries. Then, the flooding cost up to X_{min} hops away is certainly the lower bound. The distribution of X_{min} is given in Section 3.2. Under our assumption the flooding cost up to h hops away is $C_f^{(d)}(h)$. Hence, the lower bound of the expected search cost is given by,

$$\begin{aligned} C_{s,lower}^{(d)} &= E[C_f^{(d)}(X_{min})] \\ &\approx \tau(d) \cdot E[X_{min}^d] \end{aligned} \tag{3.16}$$

In order to obtain the d-th moment of X_{min}, we make an approximation that X_{min} is continuous. The probability density function of X_{min} is given by,

$$f_{X_{min}}(k) = \frac{rd}{L^d} k^{d-1} \left(1 - \frac{k^d}{L^d}\right)^{r-1} \tag{3.17}$$

Then, the d-th moment is given by,

$$\begin{aligned} E[X_{min}^d] &= \frac{rd}{L^d} \int_0^L k^{2d-1} \left(1 - \frac{k^d}{L^d}\right)^{r-1} dk \\ &= \frac{L^d}{r+1} \\ &= \frac{1}{\tau(d)} \cdot \frac{N}{r+1} \qquad (\because (3.4)) \end{aligned} \tag{3.18}$$

Substituting Equation (3.18) into Equation (3.16) we have the following expression:

$$C_{s,lower}^{(d)} = \frac{N}{r+1} \tag{3.19}$$

3.3.2.2 Upper Bounds

Now, let us consider the upper bound of the optimal expected search cost. We note that any expected search cost with a specific search sequence vector (SSV) is the upper bound. We consider two search sequence strategies to obtain two upper bounds, from which we obtain a tighter upper bound in terms of order notation. Let us first consider the step-by-step expanding ring search (ERS) strategy where the SSV is $\{1, 2, 3, \ldots, L\}$. The expected cost of this strategy is given by,

$$
\begin{aligned}
C_{s,sbs}^{(d)} &= \sum_{k=1}^{L} C_f^{(d)}(k) P\{X_{\min} > k-1\} = \sum_{k=1}^{L} \left(1 + \tau(d)\cdot(k-1)^d\right)\left(1 - \frac{(k-1)^d}{L^d}\right)^r \\
&\approx \int_0^L \tau(d)\cdot k^d \left(1 - \frac{k^d}{L^d}\right)^r dk = \tau(d)\cdot \frac{L^{d+1}\,\Gamma(\frac{1}{d})\Gamma(r+1)}{d^2\,\Gamma(r+\frac{1}{d}+2)} \\
&< \frac{\tau(d)\cdot\Gamma(\frac{1}{d})}{d^2}\frac{L^{d+1}\cdot\Gamma(r+1)}{\Gamma(r+2)} \qquad (\because \Gamma(r+2) < \Gamma(r+\frac{1}{d}+2)) \\
&= \frac{\Gamma(\frac{1}{d})}{d^2\,\sqrt[d]{\tau(d)}}\cdot\frac{N^{1+\frac{1}{d}}}{r+1} \qquad (\because (3.4))
\end{aligned}
\tag{3.20}
$$

As a next step, let us consider the flooding strategy which can be considered as the one step ERS with SSV $\{L\}$. The expected cost of this strategy is given by,

$$
\begin{aligned}
C_{s,fld}^{(d)} &= C_f^{(d)}(L) = 1 + \tau(n)(L-1)^d \\
&\leq \tau(n)L^d = N
\end{aligned}
\tag{3.21}
$$

If we apply Lemma A.2 in the appendix using Equation (3.20) and (3.21) we can conclude that the optimal expected search cost $C_{s,un}^{(d)}$ is $O(N/r)$. With the result of the lower bound of the optimal cost in Equation (3.19) we reasonably approximate that the optimal search cost is proportional to its corresponding lower bound. Hence, we have

$$
C_{s,un}^{(d)} = \alpha_2 \cdot \frac{N}{r+1} \tag{3.22}
$$

where α_2 is constant w.r.t r and N, but a function of d.

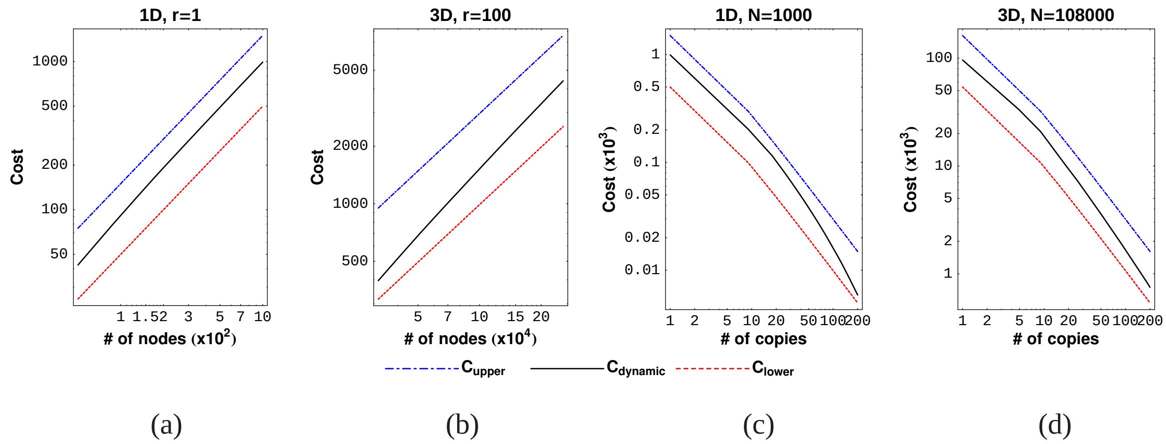

Figure 3.3: Unstructured average search cost

Figure 3.3 has similar plots as in Figure 3.1. The lower bound is using $C^{(d)}_{s,lower}$ in Equation (3.19), the upper bound is using $3C^{(d)}_{s,lower}$, and the search cost $C_{dynamic}$ is evaluated numerically using the dynamic programming algorithm proposed by Chang and Liu [28]. We can see that our approximation of the proportionality is quite close as for the structured search cost.

3.4 Replication Cost under the FTP Model

We now consider the expected replication cost. Since our replication strategy is to pick a destination uniformly at random, for each copy of the event, it has nothing to do with the querying structure, and so the replication cost is same for both structured and unstructured networks. Furthermore, under our assumptions, the number of transmissions required to move data between any pair of locations a distance x apart along the shortest path between them is approximately x/R. Thus, the expected cost of creating any replica is given by the ratio of expected distance between any pair of points in the area and the radio range R. Let $\Psi_B(x)$ denote the average length of line picked in $\mathbb{B}^d(x)$ with radius x, $\psi_B(x)$ the integral of all possible lines in the same $\mathbb{B}^d$, and $V_d(x)$ the volume of the ball which is dealt with in Section 3.2. And, let $\psi_C(x)$ denote the corresponding integral of lines in the d-cube $\mathbb{C}^d(x)$ with the width of x. Because $\mathbb{C}^d(\sqrt{2}LR) \subset \mathbb{B}^d(LR) \subset \mathbb{C}^d(2LR)$, $\Psi_B(LR)$ has the following bounds:

$$\frac{\psi_C(\sqrt{2}LR)}{V_B(LR)^2} < \Psi_B(LR) = \frac{\psi_B(LR)}{V_B(LR)^2} < \frac{\psi_C(2LR)}{V_B(LR)^2} \tag{3.23}$$

Letting $\bar{x} = (x_1, \ldots, x_d)$ and $\bar{y} = (y_1, \ldots, y_d)$, $\psi_C(x)$ is given by,

$$\begin{aligned} \psi_C(x) &= \overbrace{\int_0^x \cdots \int_0^x}^{2d} |\bar{x} - \bar{y}| dx_1 \cdots dx_d dy_1 \cdots dy_d \\ &= \triangle(d) \cdot x^{2d+1} \end{aligned} \tag{3.24}$$

where

$$\triangle(d) = \overbrace{\int_0^1 \cdots \int_0^1}^{2d} |\bar{x} - \bar{y}| dx_1 \cdots dx_d dy_1 \cdots dy_d$$

Let $\overline{\Psi_B}(LR)$ and $\underline{\Psi_B}(LR)$ denote the upper and lower bound of Inequality (3.23), respectively. From Equation (3.1), (3.4), and (3.24),

$$\underline{\Psi_B}(LR) = \frac{2^d \sqrt{2} \cdot \triangle(d)}{\sqrt[d]{\rho} \cdot f(d)^{2+\frac{1}{d}}} \cdot \sqrt[d]{N} \tag{3.25}$$

$$\overline{\Psi_B}(LR) = \frac{2^{2d+1} \cdot \triangle(d)}{\sqrt[d]{\rho} \cdot f(d)^{2+\frac{1}{d}}} \cdot \sqrt[d]{N} \tag{3.26}$$

Therefore, we can approximate the replication cost as follows:

$$\begin{aligned} C_r^{(d)} &= (r-1) \cdot \frac{\Psi_B(LR)}{R} \\ &= \alpha_3 \cdot \sqrt[d]{N} \cdot (r-1) \end{aligned} \tag{3.27}$$

where

$$\frac{2^d\sqrt{2}\cdot\triangle(d)}{f(d)^2\sqrt[d]{\tau(d)}} < \alpha_3 < \frac{2^{2d+1}\cdot\triangle(d)}{f(d)^2\sqrt[d]{\tau(d)}}$$

3.5 Costs under Uniform Random Deployment (RGG Model)

We now consider the uniform random deployment for both structured and unstructured networks, i.e. the RGG model. The RGG model has different assumptions regarding the radio radius and the unit transmission cost. The radio range R is assumed to be scaled proportionally with $\sqrt[d]{\log N}$ to ensure connectivity of the network with high probability. We also assume that the energy expenditure per transmission scales as R^η, where η is the path-loss exponent.

Therefore, the neighbor density τ is logarithmically increasing with N. Letting $\tau = \rho f(d) R^d = \theta_1 \log N$ with some constant θ_1, the radio range can be expressed as,

$$R = \sqrt[d]{\frac{\theta_1}{\rho\, f(d)}}\sqrt[d]{\log N} \tag{3.28}$$

Note that our analysis in the previous sections (Sect. 3.2, 3.3, 3.4) is still valid except that the costs derived therein are in terms of number of transmissions and the network radius L is now also a function of N. It should be noted that the number of transmissions is no longer proportional to the energy cost in the uniform random deployment because R is no longer constant with respect to N. Hence, we shall refer the derived search costs in the previous sections as $H_{s,st}$ and $H_{s,un}$ for structured and unstructured networks, respectively, and the replication cost as H_r in this section.

For structured networks, by substituting Equation (3.28) into (3.8) and (3.9), the bounds of $H_{s,st}$ can be expressed as,

$$l'(d) \cdot \frac{\sqrt[d]{N}}{\sqrt[d]{r \log N}} \; < \; H_{s,st}^{(d)} \; < \; u'(d) \cdot \frac{\sqrt[d]{N}}{\sqrt[d]{r \log N}} \tag{3.29}$$

where

$$\begin{aligned} l'(d) &= 2\, \frac{\Gamma(\frac{1}{d})\, exp\left(\frac{1}{d}\right)}{d\, \sqrt[d]{\theta_1}} \left(\frac{d}{d+1}\right)^{\frac{3d+2}{2d}} \\ u'(d) &= 2\, \frac{\Gamma(\frac{1}{d})\, exp\left(\frac{1}{d} + \frac{12+d}{12(12+13d)}\right)}{d\, \sqrt[d]{e\, \theta_1}} \end{aligned}$$

Now we introduce the transmission energy cost over a link of distance R given by,

$$E_t(R) = \beta R^{\eta} \tag{3.30}$$

where β is the transmit amplifier constant and η is the path-loss exponent. Generally, there should be a term for the distance-independent energy cost of transmitter and receiver electronics, but we assume it is negligible because we focus more on the search cost behavior of large networks[2].

Because the search cost is given by multiplying $H_{s,st}$ and $E_t(R)$, we can approximate it using its double inequalities as follows:

$$C_{s,st}^{(d)} = \alpha_4 \cdot \frac{\sqrt[d]{N(\log N)^{\eta-1}}}{\sqrt[d]{r}} \tag{3.31}$$

[2]For more accurate result for small size networks, we can add a constant for the electronics energy cost to the transmission energy cost model, which would lead to the desired result without difficulty.

where $\beta\left(\frac{\theta_1}{\rho f(d)}\right)^{\frac{\eta}{d}} \cdot l'(d) < \alpha_4 < \beta\left(\frac{\theta_1}{\rho f(d)}\right)^{\frac{\eta}{d}} \cdot u'(d)$.

With the analogous reasoning, we can obtain the search cost of unstructured networks and the replication cost under the RGG deployment as follows:

$$C_{s,un}^{(d)} = \alpha_2 \cdot \beta\left(\frac{\theta_1}{\rho f(d)}\right)^{\frac{\eta}{d}} \cdot \frac{N(\log N)^{\frac{\eta}{d}}}{r+1} \tag{3.32}$$

$$C_r^{(d)} = \alpha_5 \cdot (r-1)\ \sqrt[d]{N(\log N)^{\eta-1}} \tag{3.33}$$

where α_2 is as same as in Section 3.3, and

$$\frac{2^d\sqrt{2}\,\beta\,\theta_1^{(\eta-1)/d}\triangle(d)}{\rho^{\eta/d}\,f(d)^{2+\eta/d}} \;<\; \alpha_5 \;<\; \frac{2^{2d+1}\,\beta\,\theta_1^{(\eta-1)/d}\triangle(d)}{\rho^{\eta/d}\,f(d)^{2+\eta/d}}$$

We note that the costs of unstructured networks under the RGG deployment turns out to be dependent on d, while that of the FTP deployment is independent of d.

Chapter 4

Optimizing Data Replication for Energy-Efficiency Expanding Ring-Based Queries[1]

The data-centric network considered in this dissertation has two inevitable sources of energy consumption – searching and replication. In this chapter, we are more interested in the total energy cost consisting of the search and replication costs rather than individual costs. We investigate how to minimize the total cost through the number of replicas, and derive the data replication scheme for the optimized total cost. We consider the unstructured network with the expanding-ring search (ERS) scheme and assume that the node deployment space is two dimensional. Although omitted, the analysis for the structured network of general dimension can be done in a similar manner.

As for the node deployment, we consider only the fixed-radius constant-density node deployment in this chapter and the scaling law study in the next chapter. It is because the random deployment requires logarithmically increasing neighbor density to ensure connectivity with high probability [49, 93, 94]. Grid-like and other regularized random deployments ensuring a bounded distance

[1]This work was done jointly with Prof. Bhaskar Krishnamachari, and was first published as [68].

between nodes would satisfy the second model, though. One justification for not considering the random deployments in our scalability analysis is that this kind of deployment explicitly rules out the kind of scalability we are interested in exploring. In the uniform random deployment case, with a fixed spatial density of nodes, the radio range needs to be increasing as $\sqrt[d]{\log N}$ as the network size N increases in order to maintain connectivity. Thus, a finite per-node energy budget can never sustain an arbitrarily large deployment of this kind. In the case of constant radio range that we examine, however, we show that there are conditions under which such scalability is still possible.

We validate our analysis through a set of simulations in Section 4.4. These simulations are performed using a realistic wireless network topology generator [138]. Although we find that the node placement distributions and optimal search sequences can be significantly different between simulations and analysis, we find that the corresponding expected search and replication costs are quite similar and that the optimal replication number obtained through analysis matches the simulation results quite closely.

4.1 Search Cost

We use the search cost model developed in Section 3.3 given as follows:

$$C_{s,un} = \alpha_2 \cdot \frac{N}{r+1} = \alpha_2 \cdot \frac{aL^2}{r+1} \qquad (4.1)$$

L *(max TTL)*	c *(Curve-fit constant)*
10	1.47845
50	1.99568
100	2.07722
500	2.14608
1000	2.15476

Table 4.1: Best-fit constant for search cost approximation

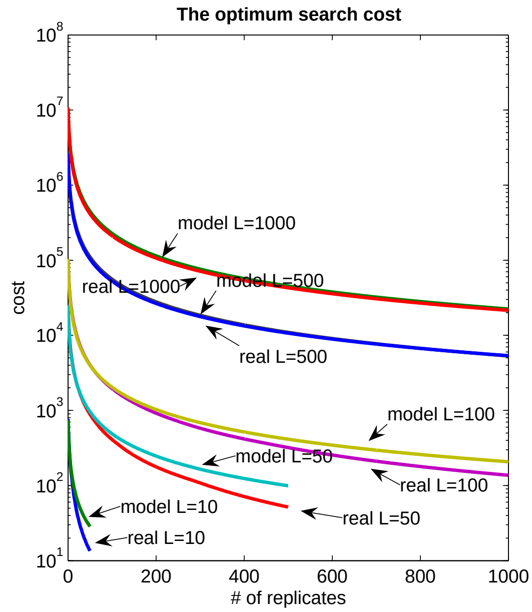

Figure 4.1: Approximation for optimal search cost

Note that L is the maximum hopcount defined in Section 3.2 and $a = \tau(2)$, which is the average number of neighbors in a 2D network.

The constant α_2 can be obtained using curve-fitting. As shown in Table 4.1, the constant is seen to converge to a value close to 2.15 as the size of the deployment area increases (i.e. for large L).

Figure 4.1 compares the search cost model with the numerically optimal search strategy (obtained using the dynamic programming method of Chang and Liu [28]). We see a close match, particularly when the network is large and the number of replicas is relatively small.

4.2 Replication Cost

Although we can use the approximate expression for the general dimension developed in Section 3.4, more direct method can be possible to obtain an exact closed-form expression for 2D networks.

Let $\hat{r}$ be the number of replicas of the original event, and they are assumed to be placed individually at each location through unicast routing on the shortest path between the random source and storage point. The expected distance between the two random points are presented in the subsequent subsections for circular and square regions.

4.2.1 Circular Area

For a circular region, there is a known geometric result referred to as disk line picking [123], which gives the expected distance between any two points in a unit circle to be:

$$\begin{aligned} E\left[d_{circle}\right] &= \frac{1}{\pi}\int_0^1\int_0^1\int_0^\pi \sqrt{r_1 + r_2 - 2\sqrt{r_1 r_2}\cos\theta}\, d\theta dr_1 dr_2 \\ &= \frac{128}{45\pi} \end{aligned}$$

Using this result, we get the following expression for the expected cost of creating $\hat{r}$ replicas of the event information in a circular region of radius LR to be:

$$C_{r,circle}(\hat{r}) = \frac{128LR\hat{r}}{45\pi R} = \frac{128L\hat{r}}{45\pi} \tag{4.2}$$

4.2.2 Square Area

Similarly, for a square, the expected distance in the square of width wR is

$$\begin{aligned} E[d_{square}] &= wR \underbrace{\int \cdots \int_0^1}_{4} \sqrt{(x_1 - y_1)^2 + (x_2 - y_2)^2} \underbrace{dx_1 \cdots dy_2}_{4} \\ &= wR \frac{2 + \sqrt{2} + 5 \ln \left(1 + \sqrt{2}\right)}{15} \approx 0.521405 wR \end{aligned}$$

From this, we get that

$$C_{r,square}(\hat{r}) \approx 0.52 w\hat{r} \tag{4.3}$$

4.3 Optimum Number of Replicas

We can formulate the problem of optimizing the number of replicas for each event as follows:

$$\begin{aligned} \textit{Minimize} \quad & C_{tot}(\bar{r}) \doteq \textstyle\sum_{i=1}^{m} q_i C_s(r_i) + \sum_{i=1}^{m} C_r(r_i - 1) \\ \textit{s.t} \quad & g(\bar{r}) = \sum_{i=1}^{m} r_i \leq S \\ & 1 \leq r_i \leq N, \quad \forall i \end{aligned} \tag{4.4}$$

Here q_i is the query rate for the i^{th} of m events, r_i is the number of copies of event i (note that $r_i - 1$ is the number of its replicas), and S is the total network storage capacity. For a circular region, the expressions for the search cost $C_s(r_i)$ and the replication cost $C_r(r_i - 1)$ are as given in Equations (4.1) and (4.2), respectively. We solve this problem using the method of Lagrange multipliers. The Lagrangian function for this inequality-constrained optimization problem can be expressed using a slack variable s as follows:

$$L(\bar{r}, \lambda) = C_{\text{tot}}(\bar{r}) + \lambda \left(g(\bar{r}) - S + s^2 \right) \tag{4.5}$$

It can be shown that the objective function is convex; hence, the following first-order conditions are sufficient for global minimization:

$$\frac{\partial L}{\partial r_i} = -\frac{q_i a L^2 c}{(r_i + 1)^2} + \frac{128L}{45\pi} + \lambda = 0 \tag{4.6}$$

$$\frac{\partial L}{\partial \lambda} = \sum_{i=1}^{m} r_i - S + s^2 = 0 \tag{4.7}$$

$$\frac{\partial L}{\partial s} = 2\lambda s = 0 \tag{4.8}$$

i) When the constraint is inactive we can solve directly from Equation (4.6), setting $\lambda = 0$:

$$r_i^* = \sqrt{\frac{45\pi a L c}{128}} \cdot \sqrt{q_i} - 1 \tag{4.9}$$

ii) When the constraint is active, (i.e. s=0, $\lambda \geq 0$), we get from Equation (4.6):

$$r_i^* = \sqrt{\frac{acL}{\frac{128}{45\pi} + \frac{\lambda}{L}}} \cdot \sqrt{q_i} - 1 \tag{4.10}$$

λ is a constant that can be solved by substituting the above equation into Equation (4.7), setting $s = 0$:

$$\lambda = \frac{acL^2 \left(\sum_{i=1}^{m} \sqrt{q_i}\right)^2}{(S+m)^2} - \frac{128L}{45\pi} \tag{4.11}$$

Substituting this back into (4.10), we get the following simplified expression:

$$r_i^* = \frac{\sqrt{q_i}}{\sum_{i=1}^{m} \sqrt{q_i}}(S+m) - 1 \tag{4.12}$$

To determine whether the constraint is inactive or active, it is sufficient to verify whether the sum of r_i^* obtained from Equation (4.9) is less than S. If not, then Equation (4.12) should be used to compute the optimal constrained r_i^*. A striking observation is that in both cases the optimal strategy is to have the replication number of each event to be proportional to the square root of the query. We note that this outcome is very similar to a result in unstructured peer-to-peer wired networks [33], which also argues for replicating content with a rate proportional to the square root corresponding frequency of access. However, there are key differences between that work and ours, including the type of search analyzed (expanding rings in a wireless network with a geometrically defined 2-D structure versus random walk on an arbitrary wired network graph), and the absence of replication cost.

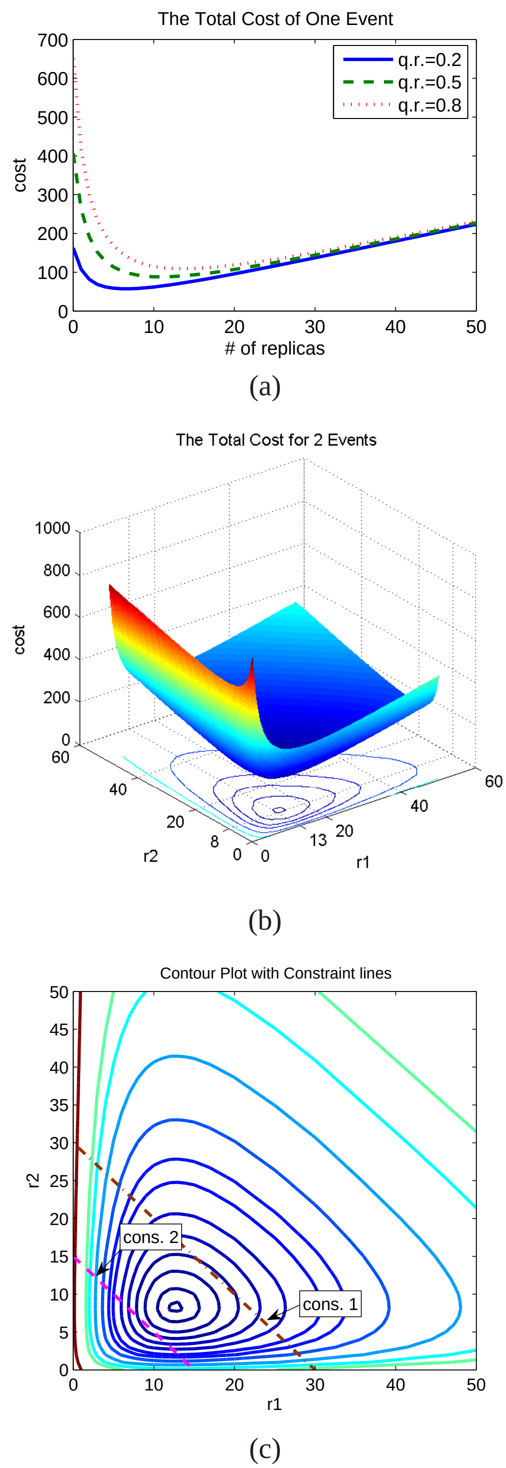

Figure 4.2: (a) Total expected cost for a single event showing that the optimal replication number varies as a function of query rates (b) a surface plot showing total expected cost for two events, and (c) a contour plot of the total cost for two events showing storage constraints (1, 2) and corresponding optimal solution points (A, B)

Figure 4.2(a) shows the total cost of querying and replication C_{tot} as a function of the number of replicas for different query rates for a single event. Figure 4.2(b) illustrates how the total cost may vary for the case of two events, as a function of the number of replicas for each event. Figure 4.2(c) shows the contours of this function, along with two sets of lines that represent different storage constraints. With the first storage constraint (a large value of S), there is sufficient storage available that the unconstrained optimal point A can be selected as the operating point, by allocating the corresponding optimal number of replicas for both events. However, under the tighter storage constraint 2 (smaller S), the original unconstrained optimal solution lies outside the feasible operation region. Hence, point B, which minimizes the function while maintaining storage feasibility, provides the optimal constrained solution in this case.

4.4 Realistic Simulations

4.4.1 Methodology

We use a realistic link layer model generator for wireless sensor networks [138], which determines the location of each node and the packet reception rate (PRR) of each pair of nodes. Table 4.2 shows parameters for our wireless sensor network topology to simulate on (corresponding to a dense deployment of Mica 2 motes). Given the realistic topology, our simulator performs the following procedures at each round:

1. Randomly choosing a source node which is considered to have the original event information

	Parameter	*Value*
Channel	path loss exponent	3.0
	shadowing std. deviation	3.8
	PL(d_0)	55.0
	d0	1
Radio	Modulation	3 (NCFSK)
	Encoding Option	3 (Manchester)
	Radio Output Power	-21.0
	Noise Floor	-105.0
	Preamble Length	2 bytes
	Frame Length	50 bytes
Topology	Number of nodes	1010
	Physical Terrain	(80, 80)
	Option	Uniform Deployment

Table 4.2: Radio parameters for simulation

2. Counting the actual replication cost for $r-1$ replicas chosen randomly

3. Randomly choosing a querier node in the given node pool.

4. Counting the actual search cost using the optimal search strategy.

Our numerical results are computed based on 10000 rounds for each r value.

4.4.2 Counting the Actual Replication Cost

The replication is done not by flooding, but rather through individual unicast transmissions from the source to the requisite number of random replication locations. We use the ETX (expected number of transmissions with retransmissions) metric [34] to define the routing strategy for the unicast transmissions. Specifically, the transmission on the edge from i to j costs $\frac{\beta}{PRR_{i,j}}$, where β is the cost of a single transmission, and $PRR_{i,j}$ is the packet reception rate from i to j, and a message between any pair of nodes in the network is routed along the shortest cost path between them. Here, we have assumed that acknowledgement packets (which are likely to be much shorter) are always received reliably. In the simulation results we count the actual replication cost by counting the actual total number of transmissions on the shortest unicast path and multiplying it by β.

4.4.3 Counting the Actual Search Cost

In order to find out the search cost, we need to find out the optimal search strategy. In order to use the optimal search strategy from the dynamic programming methodology [28], we need to know the distribution of number of nodes with respect to the hop distance from the querying node. However, it is not easy to determine the hop-distribution in the realistic wireless topology considered in the simulations, where the links are lossy and asymmetric. Even for a given topology, the number of nodes of i^{th} hop (for a single query event) is a random variable whose expectation is not easily obtained. Since we need to compute the distribution for any querying node in the network, it is particularly important to obtain an approximation that can be calculated simply. The approach we have taken is to look at the hop-distribution of the subgraph formed when all links with packet reception rates below 0.5 are blacklisted from the network. As a sanity check, we have compared the results obtained from this process with the average of the number of nodes at each hop from 100 simulation experiments where these are determined probabilistically

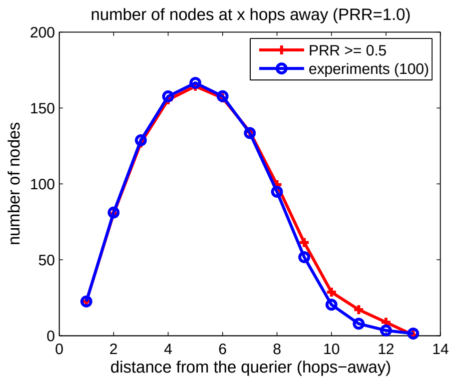

Figure 4.3: Experiment for the node number distribution

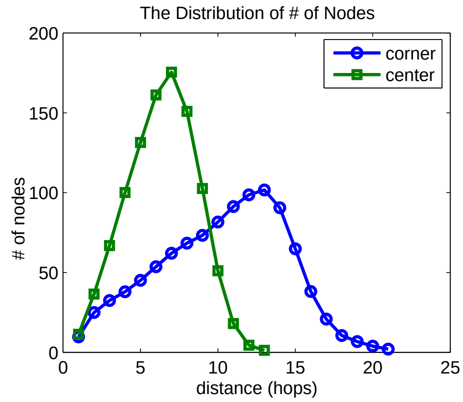

Figure 4.4: Distribution of the number of nodes as a function of distance from querier in a uniform square area deployment

in each run according to the PRR values at each edge. The two approaches show remarkably similar results (see Figure 4.3).

Let $H[i]$ denote the set of nodes that are reachable from the querying node at a distance of i hops. We use the following conditional tail distribution for the dynamic programming,(for $k \geq c$):

$$P\{X_{min} > k \mid X_{min} > c\} = \left(\frac{\sum_{i>k} |H[i]|}{\sum_{i>c} |H[i]|} \right)^r$$

Following the resulting optimal search strategy, the simulator floods a series of queries until it finds one of the copies of the event. Note that in our simulations, although two queries have the same TTL value, one query might find the event but the other might not, in the same network. It is because the coverage of first query is not necessarily same as that of the second one (because of the lossy wireless links).

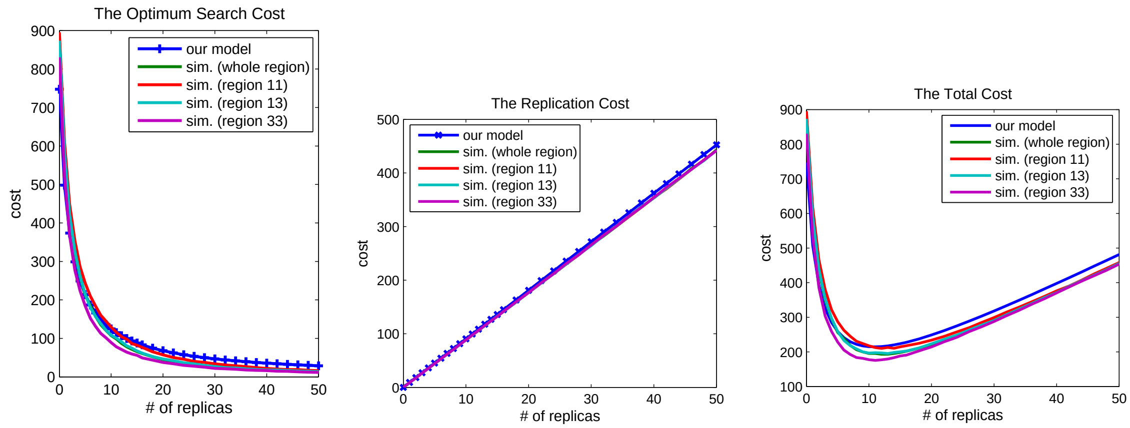

(a) Search costs (b) Replication costs (c) Total costs

Figure 4.5: Comparisons of analytical and simulated costs as a function of replication size

4.4.4 Results

In our simulations, we relax several assumptions from the mathematical analysis, so that (1) the querier can be any node in the network, (2) the network topology is not necessarily circular (it is the square area for our simulation), and (3) there might be the boundary effect. With these relaxations, the actual optimal search sequence of a node might be different from that of another node when they are considered as a querier at each time. For example, the optimal search sequence of a corner node is $\{2, 8, 12, 15, 17, 19, 20\}$, while that of a center node is $\{2, 4, 6, 7, 8, 9, 10, 11\}$ when there are two replicas of the queried event.

First of all, the theoretical values of our model are as follows;

$$C_{search}(r) = \frac{cN}{r+1} = \frac{1.48 \times 1010}{r+1}$$

$$C_{replication}(r-1) = \frac{128L(r-1)}{45\pi} = \frac{128 \times 10}{45\pi}(r-1)$$

where the node density variable $a \approx 10$ is obtained from the simulation (since this depends on radio and deployment settings), the value of $L \approx 10$ is obtained from $aL^2 = N = 1010$, and c is obtained accordingly from Table 4.1. Therefore, assuming the query rate is 1, the optimal number of replicas $\hat{r}^*$ is as follows by Equation (4.9);

$$\begin{aligned} \hat{r}^* = r^*_{th} - 1 &= \sqrt{\frac{45\pi}{128} qaLc} - 2 = \sqrt{\frac{45\pi}{128} \times 10 \times 10 \times 1.48} - 2 \\ &= 10.7852 \approx 11 \end{aligned}$$

The optimal number of replicas from the simulation is found to be $\hat{r}^*_{sim} = 12$ (see Figure 4.5c). Figure 4.5a shows the optimal search cost of the simulation and our model, and Figure 4.5b shows the replication cost. As we can see from these figures, our model meets the simulation results very well even with relaxed assumptions. The similarity of the results despite seeing very different hop distance distributions in the simulations suggests that the cost of the optimal search is quite robust to this distribution, particularly in the presence of replicas.

Chapter 5

Scaling Laws in Terms of Bounded Energy[1]

In this chapter, we drive the scaling laws for the data-centric wireless sensor networks based on the cost models and optimization method discussed in the previous chapters. We consider both unstructured and structured networks with bounded per-node storage budget. Although this bounded size of storage resource plays as a constraint in optimizing the total cost, it turns out that the storage constraints are less restrictive than the energy constraints. We therefore first derive the scalable operating conditions using an unconstrained version of the optimization problem, and then use the constrained version to investigate in more detail the behaviors of the network as its size grows.

[1]This work was done jointly with Prof. Bhaskar Krishnamachari, and was published as [4, 6].

5.1 Basic Optimization

We use mathematical models developed in Chapter 3 to quantify the cost of replication and search under structured and unstructured networks. From the costs, we have the common form of the total cost as follows:

$$C_t = \sum_{i=1}^{m} q_i C_s(r_i) + \sum_{i=1}^{m} C_r(r_i) \tag{5.1}$$

where $C_s(r_i)$ is the expected search cost of i^{th} event and $C_r(r_i)$ is its expected replication cost.

From the above, we get the following expressions for the expected total energy cost for all events which consists of search costs weighed by the number of queries and the replication costs:

1. Under the unstructured replication scheme, the total energy cost is

$$C_{t,u} = \sum_{i=1}^{m} c_2 \frac{N q_i}{r_i + 1} + \sum_{i=1}^{m} c_1 \sqrt[d]{N}(r_i - 1) \tag{5.2}$$

2. Under the structured replication scheme

$$C_{t,s} = \sum_{i=1}^{m} c_3 \frac{\sqrt[d]{N} q_i}{\sqrt[d]{r_i}} + \sum_{i=1}^{m} c_1 \sqrt[d]{N}(r_i - 1) \tag{5.3}$$

To simplify our expressions, with a slight abuse of notation, we shall make the following substitutions: in Equation (5.2), after dividing both sides by c_1, we let $C_{t,u}/c_1 \to C_{t,u}$ and $\frac{c_2}{c_1} q_i \to q_i$;

in Equation (5.3), after dividing both sides by c_1, we let $C_{t,s}/c_1 \rightarrow C_{t,s}$ and $\frac{c_3}{c_1}q_i \rightarrow q_i$. And the following expressions are the simplified versions;

$$C_{t,u} = \sum_{i=1}^{m} \frac{Nq_i}{r_i+1} + \sum_{i=1}^{m} \sqrt[d]{N}(r_i - 1) \qquad (5.4)$$

$$C_{t,s} = \sum_{i=1}^{m} \frac{\sqrt[d]{N}q_i}{\sqrt[d]{r_i}} + \sum_{i=1}^{m} \sqrt[d]{N}(r_i - 1) \qquad (5.5)$$

Now we can formulate the problem of optimizing the total cost as follows;

$$\text{Minimize} \quad C_t = \sum_{i=1}^{m} q_i C_s(r_i) + \sum_{i=1}^{m} C_r(r_i) \qquad (5.6)$$

We use the total energy cost in the network as the object function in stead of per-node energy for the optimization. Although naive replication-query schemes might make the system behave differently depending on which point of view is taken (total energy or per-node energy), the system behaviors for both point of views could be essentially same (in terms of O-notation) with a smarter replication-query scheme as discussed in Section 5.6. Moreover, the use of total energy gives at least the upper bound for the network scalability condition for any replication-query scheme.

We also ignore the storage constraints for now because it turns out that the constraints must not be active in order to ensure the scalability of the network. In Section 5.5 we incorporate the constraints to investigate more detailed behavior of the network as it grows.

The optimization formulation does require global knowledge of query rates for each event and hence the optimum may not be necessarily achieved by distributed heuristics in practice, but this is still a useful tool for our investigation on the performance of scalability as it provides the best-case scenario. For global optimization first-order conditions are sufficient because it can be shown that the objective functions for both the unstructured and structured scheme are convex. Solving the problem as in Section 4.3, we find that

$$r_i^* = \begin{cases} q_i^{1/2} N^{\frac{d-1}{2d}} - 1, & \text{(unstructured)} \\ \beta_s q_i^{\frac{d}{d+1}}, & \text{(structured)} \end{cases} \tag{5.7}$$

where

$$\beta_s = d^{-\frac{d}{d+1}} \tag{5.8}$$

Now we can derive the optimal expected total energy costs substituting Equation (5.7) into Equation (5.4) and (5.5) respectively as follows;

$$C_{t,u}^* = 2\sum_{i=1}^{m} \left(N^{\frac{d+1}{2d}} \sqrt{q_i} - \sqrt[d]{N} \right) \tag{5.9}$$

$$C_{t,s}^* = \sum_{i=1}^{m} \beta_s^{-\frac{1}{d}} \sqrt[d]{N} q_i^{\frac{d}{d+1}} + \sum_{i=1}^{m} \sqrt[d]{N} \left(\beta_s \, q_i^{\frac{d}{d+1}} - 1 \right) \tag{5.10}$$

5.2 Conditions for Scalability

In order to obtain useful insights regarding scalability, we simplify our expressions from this point on by assuming that the query rates for all events are uniform, i.e., $q_i = q, \forall i$. We now examine the scaling behavior of the total energy costs for both unstructured and structured networks.

Theorem 5.2.1. ***Total Cost of Unstructured Networks:*** *The total energy cost for unstructured networks grows with network size N as follows:*

$$C^*_{t,u} = \Theta\left(m \cdot \sqrt{q} \cdot N^{\frac{d+1}{2d}}\right) \tag{5.11}$$

Proof. The total energy cost is given from Equation (5.9) by,

$$\begin{aligned} 2\sum_{i=1}^{m}\left(N^{\frac{d+1}{2d}}\sqrt{q_i} - \sqrt[d]{N}\right) &= 2m\sqrt{q}N^{\frac{d+1}{2d}} - 2m\sqrt[d]{N} \\ &= \Theta\left(m\sqrt{q}N^{\frac{d+1}{2d}}\right) \end{aligned}$$

The last equality holds since $\frac{d+1}{2d} \geq \frac{1}{d}$ for all $d \geq 1$. □

Theorem 5.2.2. ***Total Cost of Structured Networks:*** *The total energy cost for structured networks grows with network size N as follows:*

$$C^*_{t,s} = \Theta\left(m \cdot q^{\frac{d}{d+1}} \cdot N^{\frac{1}{d}}\right) \tag{5.12}$$

Proof. It can be proven in the same way as the proof of Theorem 5.2.1 using the Equation (5.10)

□

To understand the implications of these theorems, it is helpful to consider some extreme cases of the scaling behavior of the number of events m and the query rate q. We consider allowing each of these parameters to scale as $\Theta(1)$ or $\Theta(N)$, giving us four possible combinations. In practice the scaling behavior of the events and queries with network size is determined by the application scenario. For instance, an application which requires the network (regardless of its size) to have only a single sink injecting queries for events would have that q is $\Theta(1)$, while a richer application involving increasing numbers of users with the network size could have that $\Theta(N)$. For many event monitoring applications, it is likely to be reasonable to assume that the number of observed events scales proportionally with the deployment area which for a constant density deployment would mean that m is $\Theta(N)$; however in other applications the scaling of m may be weaker, all the way down to the extreme of $\Theta(1)$ (which would imply that there only a finite number of events that can be detected regardless of the network size). The following table exhibits the scaling of total energy costs for the four cases under the unstructured networks.

	$m = \Theta(1)$	$m = \Theta(N)$
$q = \Theta(1)$	$\Theta(N^{\frac{d+1}{2d}})$	$\Theta(N^{\frac{3d+1}{2d}})$
$q = \Theta(N)$	$\Theta(N^{\frac{2d+1}{2d}})$	$\Theta(N^{\frac{4d+1}{2d}})$

Table 5.0: Illustration of the scaling of total energy costs for unstructured networks.

We generate a similar table below using Theorem 5.2.2 to illustrate the scenarios for structured networks.

	$m = \Theta(1)$	$m = \Theta(N)$
$q = \Theta(1)$	$\Theta(N^{\frac{1}{d}})$	$\Theta(N^{\frac{d+1}{d}})$
$q = \Theta(N)$	$\Theta(N^{\frac{d^2+d+1}{d^2+d}})$	$\Theta(N^{\frac{2d^2+2d+1}{d^2+d}})$

Table 5.1: Illustration of the scaling of total energy costs for structured networks.

We observe something striking about Tables I and II. In both tables, among the four cases, only when both q and m are $\Theta(1)$ do we observe that the total costs for the whole network scale as $O(N)$ for all dimension. In other words, only in this example case do we have $O(1)$ scaling of the per-node cost, i.e. bounded energy consumption per node. This motivates us to inquire about the general conditions under which a network can scale while ensuring that the energy requirement per node is kept bounded — a very important requirement from a practical perspective.

Theorem 5.2.3. ***Conditions for Scalability of Unstructured Networks:*** *For unstructured networks, the energy requirement per node is bounded if and only if*

$$m \cdot q^{1/2} \text{ is } O\left(N^{\frac{d-1}{2d}}\right)$$

Proof. The total optimal energy cost per node is the total cost divided by the number of nodes N. If the energy requirement per node is bounded, there exists $\mathcal{C}_0 > 0$ such that, from the per-node total cost given from Equation (5.9) divided by N (assuming $q_i = q, \ \forall i$),

$$C^*_{t,u}/N \ = \ 2mq^{1/2}N^{\frac{1-d}{2d}} - 2mN^{\frac{1-d}{d}} \ \leq \ \mathcal{C}_0$$

$$\Rightarrow \ m \cdot \left(q^{1/2} - N^{\frac{1-d}{2d}}\right) \leq \frac{\mathcal{C}_0}{2} N^{\frac{d-1}{2d}} \tag{5.13}$$

Since $\frac{1-d}{2d} \leq 0$ so that $N^{\frac{1-d}{2d}} \leq 1$, for $q \geq 4$, [2]

$$q^{1/2} - N^{\frac{1-d}{2d}} \geq 1 \tag{5.14}$$

Hence,

$$\frac{mq^{1/2}}{2} \leq m(q^{1/2} - N^{\frac{1-d}{2d}}) \tag{5.15}$$

$$\Rightarrow \quad mq^{1/2} = O\left(N^{\frac{d-1}{2d}}\right) \tag{5.16}$$

Conversely, if $mq^{1/2}$ is $O\left(N^{\frac{d-1}{2d}}\right)$,

$$\begin{aligned} & mq^{1/2} \ \leq \ \mathcal{C}_0 N^{\frac{d-1}{2d}} \\ \Rightarrow \quad & m \cdot \left(q^{1/2} - N^{\frac{1-d}{2d}}\right) \ \leq \ \mathcal{C}_0 \, N^{\frac{d-1}{2d}} \\ \Rightarrow \quad & 2mq^{1/2} N^{\frac{1-d}{2d}} - 2mN^{\frac{1-d}{d}} \leq 2\mathcal{C}_0 \end{aligned} \tag{5.17}$$

Note that the left side of inequality (5.17) is equal to the optimized per-node total energy cost. Therefore, the per-node total energy cost is bounded. □

Theorem 5.2.4. ***Conditions for Scalability of Structured Networks:*** *For structured networks, the energy requirement per node is bounded if and only if*

$$m \cdot q^{\frac{d}{d+1}} \text{ is } O\left(N^{\frac{d-1}{d}}\right)$$

[2]It can be proven for all $q > 0$, but the proof would be unnecessarily long and clumsy because r_i^* in Equation (5.7) becomes less than 1 which means we need to correct r_i^* to be one because r_i is at least one and the total cost is convex; therefrom, we need to make several trivial changes. We omit the corresponding proof due to the limited space and assume that $q \geq 4$ is reasonable enough.

Proof. It can be proven in the same way as the proof of Theorem 5.2.3 using the Equation (5.10).

□

We note that both $N^{\frac{d-1}{2d}}$ and $N^{\frac{d-1}{d}}$ from the above scalability conditions are increasing functions with respect to the dimension d. Therefore, we can see that networks deployed in higher dimensions are inherently more scalable.

5.3 Network Scaling on Fixed Energy Budget

We now consider having a fixed energy budget, and look into what conditions the network size must satisfy to ensure that events and queries within the finite deployment time duration can be resolved before energy depletion. Specifically, we will assume that there is an average energy budget e for each node, so that the total energy is $E = e \cdot N$.

Definition 5.3.1. *We say a network* ***operates successfully*** *if it can satisfy all queries for all events in a given deployment period before energy depletion. This requires that* $C_t \leq e \cdot N$.

The last case of each of the following two theorems has subcategories the proofs of which need to borrow knowledge in Section 5.5. We provide the subcategorization here for the sake of self-completeness of the theorems.

Theorem 5.3.2. ***Network Scaling on Fixed Energy Budget:*** *Given fixed average per-node energy e (i.e., the total energy allocated optimally among the nodes in the network grows linearly with the network size as $E = e \cdot N$), the following statements describe the conditions on the network size N, network dimension d, the number of events m and the number of queries per event q that ensure that the network can be operated successfully.*

1. *If $mq^{1/2}$ is $o(N^{\frac{d-1}{2d}})$ for unstructured networks ($mq^{\frac{d}{d+1}} = o(N^{\frac{d-1}{d}})$ for structured networks), then there exists a minimum network size $N_{min}(e)$ beyond which it can always be operated successfully.*

2. *If $mq^{1/2}$ is $\Theta(N^{\frac{d-1}{2d}})$ for unstructured networks ($mq^{\frac{d}{d+1}} = \Theta(N^{\frac{d-1}{d}})$ for the structured), then there exists an average per-node energy e^* such that for all $e < e^*$, it is not possible to operate a network of any size successfully, while for all $e \geq e^*$ it is possible to operate a network of any size successfully.*

3. *If $mq^{1/2}$ is $\omega(N^{\frac{d-1}{2d}})$ for unstructured networks ($mq^{\frac{d}{d+1}} = \omega(N^{\frac{d-1}{d}})$ for the structured), then there exists a maximum network size $N_{max}(e)$ beyond which the network cannot be operated successfully. Further,*

   (a) *If $mq^{1/2}$ is $o(N)$ for unstructured networks ($mq^{\frac{d}{d+1}} = o(N^{\frac{2d}{d+1}})$ for the structured), then N_{max} is a convex function of e*

   (b) *If $mq^{1/2}$ is $\Theta(N)$ for unstructured networks ($mq^{\frac{d}{d+1}} = \Theta(N^{\frac{2d}{d+1}})$ for the structured), then N_{max} increases linearly with e.*

(c) *If* $mq^{1/2}$ *is* $\omega(N)$ *for unstructured networks (*$mq^{\frac{d}{d+1}} = \omega(N^{\frac{2d}{d+1}})$ *for the structured), then* N_{max} *increases as a concave function of* e*.*

Proof. Because proofs for both structured and unstructured networks are similar, we provide here the proof for unstructured networks only.

1. $m \cdot q^{1/2} = \Theta(N^{\frac{d-1}{2d}-\epsilon})$ where $\epsilon > 0$. Then, the optimal total cost is given from Theorem 5.2.1 by,

$$\begin{aligned} C^*_{t,u} &= \Theta(m \cdot q^{1/2} N^{\frac{d+1}{2d}}) = \Theta(N^{1-\epsilon}) \\ &= \alpha N^{1-\epsilon} + o(N^{1-\epsilon}) \end{aligned}$$

   Since the total cost expenditure should be less than the given energy $e \cdot N$,

$$\begin{aligned} & \alpha N^{1-\epsilon} + o(N^{1-\epsilon}) \leq eN \\ \Rightarrow \quad & N^{\epsilon} \geq \frac{\alpha}{e} + \frac{o(N^{1-\epsilon})}{N^{1-\epsilon}} \end{aligned}$$

   Since $\epsilon > 0$ and the last term of RHS goes to zero, there exists $N_0 > 0$ such that $N \geq N_0$ implies this inequality holds, where N_0 is a fixed constant and can be considered as the minimum network size to make the network operate successfully.

2. If $m \cdot q^{1/2} = \Theta(N^{\frac{d-1}{2d}})$, then the total cost is given by,

$$C^*_{t,u} = \Theta(m \cdot q^{1/2} N^{\frac{d+1}{2d}}) = \Theta(N)$$

Hence, there exists $\alpha > 0$ and $\beta \geq \alpha$ such that

$$\alpha N \leq C^*_{t,u} \leq \beta N \ , \quad \text{for all } N \tag{5.18}$$

Let e^* be the infimum of such β so that $e^* = \inf\{\beta\} \geq \alpha > 0$. Such e^* always exists since the real number has the least-upper-bound property. Then, for $\forall e \geq e^*$,

$$E = e \cdot N \geq C^*_{t,u} \ , \quad \text{for all } N \tag{5.19}$$

And for $\forall e < e^*$, since e^* is the infimum,

$$E = e \cdot N < C^*_{t,u} \ , \quad \text{for some } N \tag{5.20}$$

3. Similarly, $m \cdot q^{1/2} = \Theta(N^{\frac{d-1}{2d}+\epsilon})$ where $\epsilon > 0$. Then, the optimal total cost is given by,

$$\begin{aligned} C^*_{t,u} &= \Theta(m \cdot q^{1/2} N^{\frac{d+1}{2d}}) = \Theta(N^{1+\epsilon}) \\ &= \alpha N^{1+\epsilon} + o(N^{1+\epsilon}) \end{aligned}$$

From the total cost expenditure constraints,

$$\begin{aligned} & \alpha N^{1+\epsilon} + o(N^{1+\epsilon}) \leq eN \\ \Rightarrow \quad & N^{\epsilon} \leq \frac{e}{\alpha} + o(N^{\epsilon}) \end{aligned}$$

For the sufficiently large initial per-node energy $e >> \alpha$, $\exists N_{max} > 0$ such that the last inequality above achieves the equality since the order of the LHS is bigger than that of

RHS. Hence, $N > N_{max}$ implies the negation of the above inequality so that the network cannot operate successfully.

As for the subcase a), We have another two subcases here. If $mq^{1/2} = O(N^{\frac{d+1}{2d}})$, then we can use the inactive optimal total energy cost given by Theorem 5.2.1. If $mq^{1/2} = \Omega(N^{\frac{d+1}{2d}})$, we should use the active cost given by Equation (5.26). Note that when $mq^{1/2} = \Theta(N^{\frac{d+1}{2d}})$, the storage constraints might be either active or inactive depending on the per-node storage s by Theorem 5.5.2. That is the reason why we investigate both active and inactive optimal total costs for the boundary situation.

First of all, let us consider the first case; $mq^{1/2} = \Theta(N^{\frac{d-1}{2d}+\epsilon})$, where $0 < \epsilon < \frac{d+1}{2d}$. When $0 < \epsilon \leq 1/d$, the optimal total cost is given by,

$$\begin{aligned} C^*_{t,u,inact} &= \Theta\left(mq^{1/2}N^{\frac{d+1}{2d}}\right) = \Theta\left(N^{1+\epsilon}\right) \\ &= \alpha N^{1+\epsilon} + o\left(N^{1+\epsilon}\right) \end{aligned}$$

where $\alpha > 0$ is constant with respect to N.

From the total cost expenditure constraints,

$$\begin{aligned} & \alpha N^{1+\epsilon} + o\left(N^{1+\epsilon}\right) \leq eN \\ \Rightarrow \quad & N^{\epsilon} \leq \frac{e}{\alpha} + o(N^{\epsilon}) \end{aligned} \tag{5.21}$$

For the sufficiently large initial per-node energy $e >> \alpha$, $\exists N_{max}(e) > 0$ such that it achieves the equality of Equation (5.21) since the order of the LHS of the equation is bigger than that of RHS. For large $N_{max}(e)$, N_{max} can be approximated as follows:

$$N_{max} = (1/\alpha)^{1/\epsilon} \cdot e^{1/\epsilon}$$

Since $1/\epsilon \geq d \geq 1$, this N_{max} is a convex function of e.

When $1/d \leq \epsilon < \frac{d+1}{2d}$, we can use the active optimal total cost. Through the similar reasoning, we can easily achieve the following equality with approximation for $e >> \alpha$.

$$N_{max} = (1/\alpha)^{\frac{d}{2d \cdot \epsilon - 1}} \cdot e^{\frac{d}{2d \cdot \epsilon - 1}}$$

Since $\frac{d}{2d \cdot \epsilon - 1} > 1$, this N_{max} is a convex function of e.

As for the other two subcases, we can prove them in the same way using the active optimal total cost equation.

□

Figure 5.1 illustrates the network size versus energy budget curves for the 2-dimensional deployment; the five cases are for the different cases in Theorem 5.3.2. The other dimensional networks, particularly those of one and three dimension, exhibit similar behavior. The figure is obtained numerically by equating the expressions for total cost with the energy budget $E = e \cdot N$, and solving for N as a function of e, under particular m and q scaling settings that satisfy each of the corresponding cases. (A very similar figure can be obtained for structured networks and is omitted due

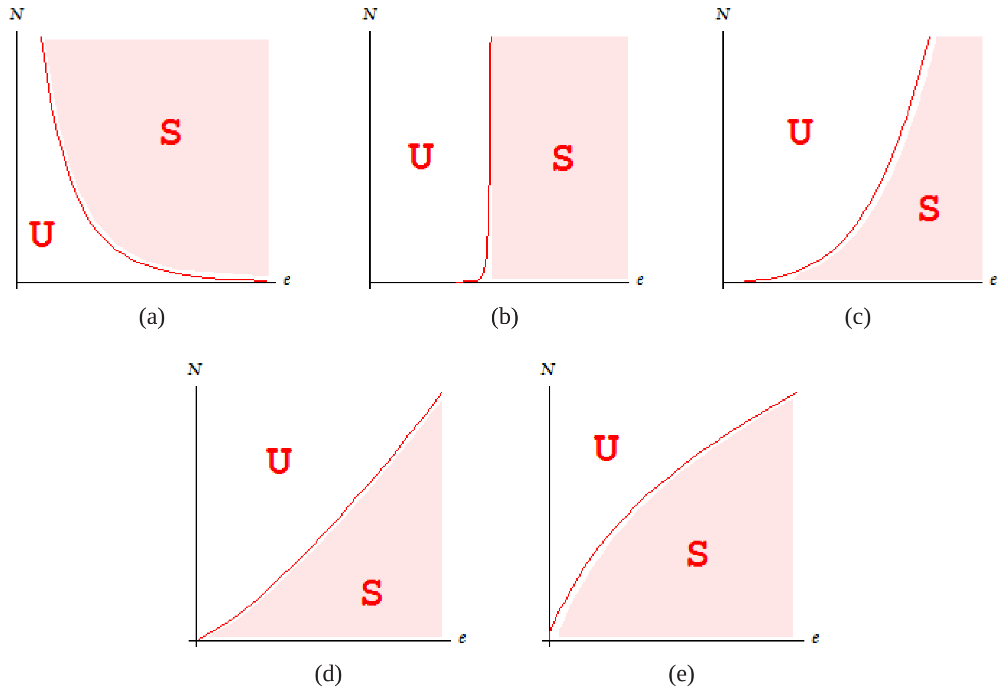

Figure 5.1: Network size conditions for successful operation with respect to per-node energy budget for different event-rate and query-rate scaling behaviors, for an 2D unstructured network; **S** denotes the successful region while **U** denotes the unsuccessful region. (a) case 1 of Theorem 5.3.2, (b) case 2, (c) case 3.a, (d) case 3.b, and (e) case 3.c

to lack of space). The regions marked S and U are where the network operates successfully and unsuccessfully, respectively.

We see that under case 1, there is a minimum network size that is needed to ensure successful operation, and this minimum network size decreases rapidly with increasing energy availability. In this case, the event and query activity remains low enough that adding nodes to the network is beneficial (as it increases the available total energy). Under the event-query activity case 2, there exists an per-node energy threshold such that below this threshold, no network can operate successfully, but beyond this threshold, networks of any size can be operated. Under cases 3.a, 3.b, and 3.c, we see that for a given energy budget there exist maximum network sizes beyond which successful operation is impossible. In these cases, adding nodes to the network is harmful

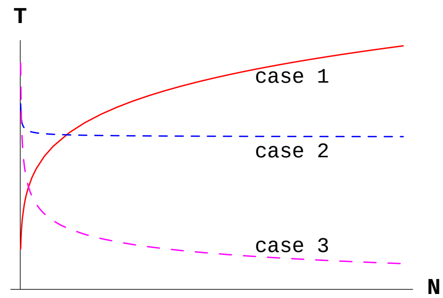

Figure 5.2: The network lifetime (T) vs. the number of nodes (N) of the unstructured network when both m and q are proportional to T

as each additional node introduces more consumption than resources. The key distinction between these cases is that under case 3.a, there is a convex growth that implies that adding energy resources to each node provides a super-linear improvement in the maximum network size that can be sustained; under case 3.b, the maximum network size grows linearly with the per-node energy budget; and under case 3.c, the concave growth of the curve implies that adding energy resources provide diminishing returns in maximum network size.

5.4 Scaling Implication in Terms of Lifetime of a Network

We now consider a relaxation of one of our key assumptions — that the network is being operated for a fixed duration. This allows us to examine how the lifetime of the network (the period over which all queries for all events can be resolved successfully) scales with the network size. In this connection we will assume that the total number of events since network initiation and the total number of queries per event ($m(t), q(t)$) are such that they are both non-decreasing functions of time, and at least one is a strictly increasing function of time.

Theorem 5.4.1. ***Lifetime Scaling on Fixed Energy Budget:*** *With a fixed average per-node energy budget of e, so long as the number of events and queries scale temporally so that $mq^{1/2}$ for unstructured networks ($mq^{\frac{d}{d+1}}$ for structured networks) is a monotonically increasing function of time, the lifetime of deployment T over which the network can operate successfully scales with the network size as per the following conditions:*

1. *if $mq^{1/2}$ is $o(N^{\frac{d-1}{2d}})$ for unstructured networks ($mq^{\frac{d}{d+1}} = o(N^{\frac{d-1}{d}})$ for the structured), then T increases with N.*

2. *if $mq^{1/2}$ is $\Theta(N^{\frac{d-1}{2d}})$ for unstructured networks ($mq^{\frac{d}{d+1}} = \Theta(N^{\frac{d-1}{d}})$ for the structured), then T is constant with respect to N.*

3. *if $mq^{1/2}$ is $\omega(N^{\frac{d-1}{2d}})$ for unstructured networks ($mq^{\frac{d}{d+1}} = \omega(N^{\frac{d-1}{d}})$ for the structured), then T decreases with N.*

Proof. Because proofs for both structured and unstructured networks are similar, we provide here the proof for unstructured networks only.

1. Suppose $m \cdot q^{1/2} = \Theta(N^{\frac{d-1}{2d}-\epsilon} \cdot f(T))$, where $\epsilon > 0$, $f(T)$ is a monotonically increasing function. Then, the optimal total cost is given from Theorem 5.2.1 by,

$$\begin{aligned} C^*_{t,u} &= \Theta(m \cdot q^{1/2} \cdot N^{\frac{d+1}{2d}}) = \Theta(N^{1-\epsilon} \cdot f(T)) \\ &= \alpha N^{1-\epsilon} \cdot f(T) + o(N^{1-\epsilon} \cdot f(T)) \end{aligned}$$

From the total cost expenditure constraints,

$$\begin{aligned} & \alpha N^{1-\epsilon} f(T) + o(N^{1-\epsilon} f(T)) \leq eN \\ \Rightarrow \quad & f(T) \leq \frac{e}{\alpha} N^{\epsilon} + \frac{o(N^{1-\epsilon} f(T))}{N^{1-\epsilon}} \end{aligned} \tag{5.22}$$

For large enough N, the second term of RHS of Equation (5.22) is negligible. Then, since $f(T)$ is monotonically increasing with respect to T, there exists T_{max} such that it satisfies the above equality; $T < T_{max}$ satisfies the inequality. Hence, $f(T_{max})$ can be approximated as follows:

$$f(T_{max}) = \frac{e}{\alpha} \cdot N^{\epsilon}$$

Since $f(T)$ is monotonically increasing, T_{max} increases with N.

The proofs for case 2) and 3) are analogous to the above case. □

These theorems are illustrated in Figure 5.2 through a numerical plot based on exact expressions. We can see that event-query scaling conditions determine whether the lifetime of the deployed network increases, decreases, or remains constant with respect to network size.

5.5 Storage Constraints

We now consider more practical situation adopting limited storage in each node in the network. We assume the total storage size of the network is $S = s \cdot N$, where s is the average storage size of a node. The optimization formulation is switched as follows:

$$\begin{aligned} \text{Minimize} \quad & C_t = \textstyle\sum_{i=1}^{m} q_i C_s(r_i) + \sum_{i=1}^{m} C_r(r_i) \\ \textit{s.t} \quad & \textstyle\sum_{i=1}^{m} r_i \leq S \end{aligned} \tag{5.23}$$

We solve this problem using the method of Lagrange multipliers. The Lagrangian function for this inequality-constrained optimization problem can be expressed using a Lagrange multiplier λ and a slack variable x as follows;

$$L(\bar{r}, \lambda, x) = C_t + \lambda \left(\sum_{i=1}^{m} r_i - S + x^2 \right) \tag{5.24}$$

The solution when the constraint is inactive (i.e. $\lambda = 0$) is as same as that of unconstraint version. When the constraint is active (i.e. $x = 0$, $\lambda \geq 0$), we get

$$r_{i,act}^{*} = \begin{cases} \frac{S+m}{\sum_{j=1}^{m} \sqrt{q_j}} \sqrt{q_i} - 1, & \text{(Unstructured)} \\ \frac{S}{\sum_{j=1}^{m} q_j^{\frac{d}{d+1}}} \, q_i^{\frac{d}{d+1}}, & \text{(Structured)} \end{cases} \tag{5.25}$$

Now we can derive the optimal expected total energy costs with the active constraint substituting Equation (5.25) into Equation (5.4) and (5.5) as follows;

$$C^*_{t,act} = \begin{cases} \sum_{i=1}^m \sqrt[d]{N}\left(\frac{(m+S)}{\sum_{j=1}^m \sqrt{q_j}}\sqrt{q_i} - 2\right) \\ \qquad + \sum_{i=1}^m \frac{\sum_{j=1}^m \sqrt{q_j}}{m+S}\sqrt{q_i}\, N, & \text{(Unst.)} \\ \sum_{i=1}^m \sqrt[d]{N}\left(\frac{S}{\sum_{j=1}^m q_j^{\frac{d}{d+1}}}\, q_i^{\frac{d}{d+1}} - 1\right) \\ \qquad + \sum_{i=1}^m \frac{\sqrt[d]{\sum_{j=1}^m q_j^{\frac{d}{d+1}}}}{\sqrt[d]{S}}\, q_i^{\frac{d}{d+1}} \sqrt[d]{N}, & \text{(Structured)} \end{cases} \tag{5.26}$$

When the available storage in the network exceeds the sum of the unconstrained optimal number of copies for all events, we have an efficient region where the network can achieve the smallest total energy cost of querying (and replication). Otherwise, even the optimal energy cost shoots up resulting in quite an inefficient performance of querying. Hence, from a scalability perspective, it is desirable to ensure that the per-node storage requirements remain bounded irrespective of the network size. This is equivalent to requiring that the average storage size s be constant with respect to the network size N.

Definition 5.5.1. *We say that a network* ***scales efficiently with bounded storage*** *if*

$$\exists N_0 \in \mathbb{N} \;\; s.t. \;\; \sum_{i=1}^m r^*_{i,inact} < S = s \cdot N, \;\; \textit{for} \;\; \forall N > N_0 \tag{5.27}$$

With the same reason in Section 5.2, we assume $q_i = q, \; \forall i$. The following theorems are the scaling results that quantify the above condition for unstructured and structured networks.

Theorem 5.5.2. ***Conditions for Efficient Operation of Unstructured Networks with Bounded Storage:*** *For unstructured networks, if condition (5.27) holds, then* $m \cdot q^{1/2}$ *must be* $O\left(N^{\frac{d+1}{2d}}\right)$*. Further, if* $m \cdot q^{1/2}$ *is* $o\left(N^{\frac{d+1}{2d}}\right)$*, then condition (5.27) holds.*

Proof. If condition (5.27) holds, then the following holds for all $N > N_0$ using Equation (5.7):

$$\begin{aligned} \sum_{i=1}^{m} r^*_{i,inact} \;&=\; m\,q^{1/2} N^{\frac{d-1}{2d}} - m \;\le\; sN \\ \Rightarrow\quad m\,(q^{1/2} - N^{\frac{1-d}{2d}}) \;&\le\; s\,N^{\frac{d+1}{2d}} \end{aligned} \tag{5.28}$$

As in the proof of Theorem 5.2.3, $q^{1/2} - N^{\frac{1-d}{2d}} \ge 1$. Hence, Equation (5.28) implies

$$m \le \frac{sN^{\frac{d+1}{2d}}}{q^{1/2} - N^{\frac{1-d}{2d}}} \le sN^{\frac{d+1}{2d}} \tag{5.29}$$

Equation (5.28) can be expressed as follows, for $\forall N > N_0$,

$$mq^{1/2} \;\le\; sN^{\frac{d+1}{2d}} + mN^{\frac{1-d}{2d}} \;\le\; sN^{\frac{d+1}{2d}} + sN^{1/d} \quad (\because\ (5.29))$$

Since $d \ge 1 \Rightarrow \frac{d+1}{2d} \ge \frac{1}{d}$, $mq^{1/2} = O\left(N^{\frac{d+1}{2d}}\right)$.

On the other hand, if $m\,q^{1/2}$ is $o\left(N^{\frac{d+1}{2d}}\right)$, then $\exists N_0 \in \mathbb{N}$ s.t $N > N_0$ implies

$$
\begin{aligned}
& m\, q^{1/2} < sN^{\frac{d+1}{2d}} \\
\Rightarrow \quad & m\, q^{1/2} - m\, N^{\frac{1-d}{2d}} \le m\, q^{1/2} < sN^{\frac{d+1}{2d}} \\
\Rightarrow \quad & \sum_{i=1}^{m} r^{*}_{i,inact} = mq^{1/2} N^{\frac{d-1}{2d}} - m < sN = S
\end{aligned}
$$

□

Theorem 5.5.3. ***Conditions for Efficient Operation of Structured Networks with Bounded Storage:*** *For structured networks, if condition (5.27) holds, then* $m \cdot q^{\frac{d}{d+1}}$ *must be* $O(N)$*. Further, if* $m \cdot q^{\frac{d}{d+1}}$ *is* $o(N)$*, then condition (5.27) holds.*

Proof. It can be proven in the same way as proof of Theorem 5.5.2 using the structured case of Equation (5.7). □

We note that the bounded-energy conditions of Theorem 5.2.3 and 5.2.4 are stricter than the above bounded-storage conditions, respectively. Even if the bounded-storage condition is satisfied, the per-node energy might not be bounded so that the scalability of network cannot be guaranteed. If the bounded-energy condition is satisfied, however, the bounded-storage condition will be automatically satisfied resulting in the scalable network in terms of the querying energy expenditure. In other words, introducing the limited storage does not produce any impact on the previous scalability conditions (Theorem 5.2.3, 5.2.4). However, as we mentioned earlier, it provides an effect on the case 3 of Theorem 5.3.2 making it possible to be subcategorized into three more cases as the theorem already claims. It is because the optimal expected total energy cost for each of the unstructured and structured network now has one more possibility — the active storage constraints.

Let us first consider unstructured networks. In the active constraint region, the optimal total energy cost is given from Equation (5.26) substituting $S = sN$ and $q_i = q, \forall i$ by,

$$\begin{aligned} C^*_{t,u,act} &= sN^{\frac{d+1}{d}} - mN^{1/d} + \frac{m^2 qN}{m+S} \\ &= \Theta\left(N^{\frac{d+1}{d}} + m^2 q\right) \end{aligned} \quad (5.30)$$

Since it is reasonable to consider that the number of events m is smaller than the total network storage S, $S = sN$ is dominant compared to m. Thus, $\frac{m^2 qN}{m+S} = \Theta\left(m^2 q\right)$, and so Equation (5.30) holds.

For structured networks, we can also conclude that the optimal total energy cost is as the following using the same reasoning.

$$C^*_{t,u,act} = \Theta\left(N^{\frac{d+1}{d}} + m^{\frac{d+1}{d}} \cdot q\right) \quad (5.31)$$

These new optimal total costs lead to the following statements in Theorem 5.3.2.

1. If $mq^{1/2}$ is $\omega(N^{\frac{d-1}{2d}})$ and $o(N)$ for unstructured networks ($mq^{\frac{d}{d+1}} = \omega(N^{\frac{d-1}{d}})$ and $o(N^{\frac{2d}{d+1}})$ for structured networks), then the maximum network size N_{max} is a convex function of e

2. If $mq^{1/2}$ is $\Theta(N)$ for unstructured networks ($mq^{\frac{d}{d+1}} = \Theta(N^{\frac{2d}{d+1}})$ for the structured), then N_{max} increases linearly with e.

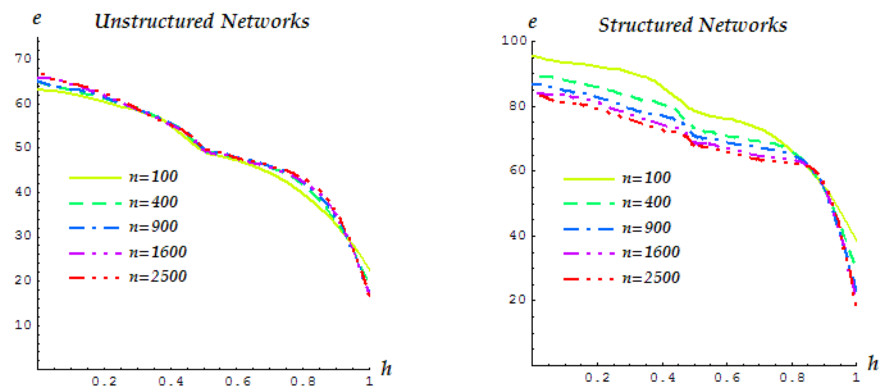

(a) Unstructured networks (b) Structured Networks

Figure 5.3: Average energy consumption vs. normalized hop distance from the center of the square grid network: each line corresponds to a different number of nodes

3. If $mq^{1/2}$ is $\omega(N)$ for unstructured networks ($mq^{\frac{d}{d+1}} = \omega(N^{\frac{2d}{d+1}})$ for the structured), then N_{max} increases as a concave function of e.

5.6 The Hot-Spot Problem

In the previous sections we have considered the total energy in the network for the analysis instead of the per-node energy. Certainly, it might be true for some cases that the network scales in a very different way in terms of the per-node energy. For example, consider a naive replication-query scheme where, at the moment a node senses an event i, the node creates and sends r_i^* replicas in the network, and the nodes which have the replicas serve as source nodes forever. It is easy to see that each source node serves the unbounded number of queries (for structured networks), or the sensing node sends the unbounded number of replicas (for unstructured networks) as the number of nodes in the network increases if the number of queries for the event i is unboundedly increases with the increasing number of nodes. In this situation, also referred to as the *hot-spot problem*, the network is not scalable because some individual nodes have unbounded energy requirements although the total energy requirement across the network remains constant.

However, there is a smarter yet simple replication-query scheme to avoid the hot-spot problem. For example, consider the following scheme: if a node senses an event i, it creates a replica and sends it to a random node in the network with the information that additional $r_i^* - 1$ replicas should be disseminated. The receiving node creates another replica and sends it to a random node with the information of $r_i^* - 2$ replicas, and so forth until all r_i^* replicas disseminated. When a source node n_s that has one of the replicas receives a query for the event, it doesn't only send back the event information to the querier n_q, but also transfer the ownership of the replica to the querier so that n_s is no longer the source of the event, but n_q is now. Note that this ownership transferring process does not incur any additional energy cost. With this scheme there is no special node in the network so that the expected energy consumption for each node is same ignoring the boundary effect. It does not even need the ownership transfer to occur at every query; it would be sufficient to transfer the ownership only when the remaining energy becomes less than a certain percentage of the amount when it has received the ownership. Likewise, many alternatives can be envisioned.

In order to examine the boundary effect, we also have conducted simulations on 2D square grids for both structured and unstructured networks with the above replication-query scheme in which the ownership of replica is transferred at every query.

In the simulations, the number of events is 30 and the number of queries for each event is $2\sqrt{N}$ (where N is the number of nodes) for unstructured networks so that the scalability condition of Theorem 5.5.2 is satisfied. For structured networks, the number of events are 60 and the number

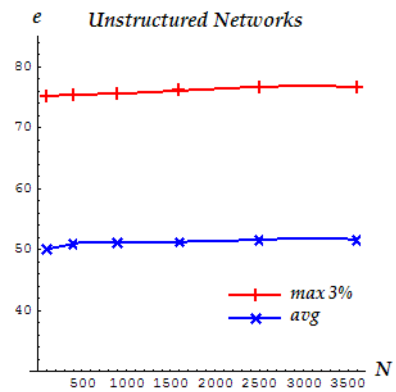

(a) Unstructured networks

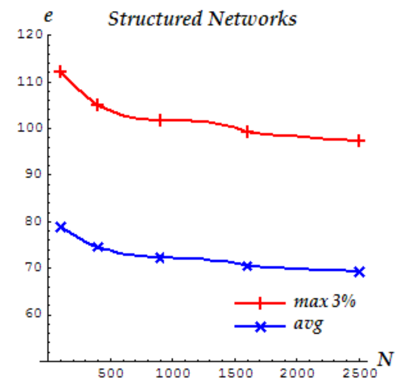

(b) Structured networks

Figure 5.4: Average energy consumption vs. the number of nodes in the network: the red line with cross marks is for the average consumption over the highest 3% nodes in energy consumption, and the blue line with x marks for average over all nodes

of queries is $N^{3/4}$ satisfying the condition of Theorem 5.5.3. The storage of each node is assumed to be large enough to accommodate all the given replicas. Other assumptions are as same as for the analysis. Figure 5.3 shows the average energy consumptions in terms of the normalized hop distance from the center of square grid networks. The key observation is that although energy consumption patterns are not uniform everywhere in the network (peaking close to the center), the ratio of the peak energy consumption to the average energy remains bounded (almost a constant) as the size of the network is increased. This is because the energy consumption as a function of the relative location remains essentially the same regardless of network size. Figure 5.4 also shows this - the ratio between the average requirement of the top 3% most-energy-consuming nodes and the average energy consumption in the whole network remains nearly constant. This shows that boundary effects are not dominant, and validates our argument that the asymptotic scalability results based on total energy consumption also hold when considering per-node energy constraints, so long as such a load-balanced replication-query scheme is used.

5.7 Discussion

Thus far we have studied the scaling laws for data-centric WSNs where replicas are placed individually before queries are issued, and no additional copies are made within the network while event information is being forwarded. It is an interesting open question to find out their effects on the scaling laws when copies of events are allowed to be made at the intermediate nodes as the event is forwarded. We call this process on-demand replication.

The details of storage and querying with on-demand replication is as follows: at first, a number of initial replicas are placed within the network before any query is generated as before. Meanwhile, additional copies of events are made in an on-demand fashion at intermediate nodes whenever the event information is forwarded either during the initial replication, or during the reply to a query. The replicas generated at the intermediate nodes can serve as sources of the event for future queries. Note that there is effectively no separate cost for this on-demand replication. The initial replication for r_i target nodes, in fact, produces a Steiner tree whose leaves are the target nodes and its internal nodes have the on-demand replicas if each node in the tree has enough storage to store the replica. When the number of nodes in the tree exceeds the fair share of the event in the network, only the fair share amount of nodes in the tree are selected to have replicas for the internal nodes in the tree. The fair share for event i is assumed to be proportional to $q_i / \sum_k q_k$ on average. This occurs because some of the nodes in the tree eventually exhaust their storage, being filled up with other events' replicas. After the first phase, additional replicas are to be produced in the nodes of the path that a reply follows whenever a query for the event is issued. It can be shown that the structure of replicas grows as the dynamic Steiner tree ([59]) in this phase. Further, the number of total replicas of a certain event also does not exceed the fair share on average because of the bounded per-node storage.

The analysis we have given in the previous sections does not cover this scheme because (1) on-demand replicas do not incur energy cost for replication, but help the search cost decreased; and (2) the replicas are not necessarily deployed uniformly. However, we provide the problem formulation for optimizing the communication energy cost of the system as follows:

$$\begin{aligned} \underset{\mathbf{r}=(r_1,\ldots,r_m)}{\text{Minimize}} \quad & \sum_{i=1}^{m}\sum_{j=1}^{q_i} \tilde{C}_s^i(r_i, j-1, \frac{q_i}{\sum_k q_k} sN) + \tilde{C}_r(\{r_i | 1 \le i \le m\}) \\ s.t \quad & \sum_{i=1}^{m} r_i \le sN \end{aligned} \tag{5.32}$$

where r_i is the number of target nodes for the initial replication for event i, $\tilde{C}_s^i(x, y, z)$ is the expected search cost for event i when the replicas of event i is in the subset of nodes of the tree structure, which starts as a Steiner tree for x randomly chosen leaves. Then, the tree grows as a dynamic Steiner tree for y additional leaves keeping the fair share z number of replicas. $\tilde{C}_r(\cdot)$ is the expected joint cost for initial replication for all events. Note that multicast can be used for this initial replication to further decrease the cost.

While the exact analysis for the above optimization is hard because of the complex dynamics and non-uniformity of the on-demand replication, we can still provide a bound on the energy cost which gives a necessary condition for scalability that applies to any replication scheme. The bound can be derived by assuming the best possible replication scheme which produce the maximum number of replicas being disseminated uniformly over the network without incurring any replication energy cost. We assume that the storage of each node is bounded as in the practical system, and the network has a large number of events so that the number of replicas of each event cannot grow on average more than a number which is much less than the total number of nodes in the network. This assumption prevents the trivial case where every node eventually acquire a replica. The optimum number of replicas for each event can be obtained using the following optimization formulation:

$$\begin{aligned} \underset{\mathbf{r}=(r_1,\ldots,r_m)}{\text{Minimize}} \quad & \sum_{i=1}^{m} q_i C_s(r_i) \\ s.t \quad & \sum_{i=1}^{m} r_i \leq sN \end{aligned} \tag{5.33}$$

The optimizer turns out to be exactly same as given in Equation (5.25).

Theorem 5.7.1. ***Necessary Condition for Scalability of Unstructured Networks:*** *For unstructured networks, the energy requirement per node is bounded only if*

$$m\sqrt{q} = O(\sqrt{N})$$

Proof. Because it is assumed that $q_i = q \, \forall i$, the optimum number of replicas for the best possible replication scheme is sN/m. Substituting the optimum number for each event into the search cost expression, it can be proven in a similar way as in Theorem 5.2.3. □

Theorem 5.7.2. ***Necessary Condition for Scalability of Structured Networks:*** *For structured networks, the energy requirement per node is bounded only if*

$$mq^{\frac{d}{d+1}} = O(N^{\frac{d}{d+1}})$$

Proof. It can be proven in the same way as the proof of Theorem 5.7.1. □

Based on the optimization, Theorems 5.7.1 and 5.7.2 describe the *necessary* conditions for the scalability for unstructured and structured networks, respectively, with the assumption that the query rate is same for each event, i.e $q_i = q \; \forall i$, as in previous sections.

Chapter 6

Content Dissemination in Heterogeneous Vehicular Networks[1]

In this chapter, we investigate the efficient dissemination of some delay-tolerant content to a group of vehicles that share an interest in this content. The delay-tolerant contents can support a variety of services, ranging from traditional traffic information and weather forecast to futuristic mobile advertisement and music sharing.

We first formalize optimization problems for the efficient content dissemination in Section 6.1. In Section 6.2, we derive one of our key measures, the expected number of satisfied vehicles by the dissemination, using ordinary differential equation (ODE) based modeling. The core optimization problem and its solution is then investigated in Section 6.3. Then, we develop an algorithm to calculate the practical optimum solution overcoming the limitation of the analytical solution in Section 6.4. We introduce the Beijing taxi traces and use them to verify our analysis in Section 6.5.

[1]This work was done jointly with Prof. Bhaskar Krishnamachari, Dr. Fan Bai, and Dr. Lin Zhang, and first reported as [7].

6.1 Problem Formulation

We consider a heterogeneous vehicular network consisting of cars with both short-range and cellular radios, over which m-types of content need to be disseminated to m-groups of vehicles. The i-th group of vehicles are interested in the i-th type of content. The goal is to efficiently disseminate these contents to their corresponding groups of nodes from the infrastructure exploiting both long-range and short-range communication methods.

One extreme way of the dissemination is to send the contents to each one of vehicles in interest through the long-range radio only. This method incurs significant access fees proportional to the number of the interested vehicles although the associated delay would be small. On the other extreme is to send the message to one vehicle only in each interested group through the long-range radio, and let it spread to other vehicles through encounters via the short-range radio. In contrast to the first approach, this incurs the minimum access fees, but the delay for reaching a large number of nodes would be substantial. In between, the delay would decrease as the number of vehicles that obtain the messages directly through the long-range radio (we call them *seed nodes*) is increased, with a corresponding increase in access cost. Thus the number of seed nodes tunes a fundamental tradeoff between delay and cost.

Our goal in this problem is, then, to maximize the expected number of vehicles obtaining the contents in their interest such that the access cost is as low as possible, subject to the long-range radio access cost constraint and tolerable delay constraint. For more specific presentation, let us suppose m types of messages to disseminate from the infrastructure. Let n denote the total number of nodes in the network, and p_i is the proportion of the nodes that are interested in the

i-th type of messages. We use interchangeably the terms node and vehicle, and messages and contents, respectively, in this chapter. Each long-range radio access incurs a unit cost which is assumed one in this dissertation while k_i is the number of seeds for the i-th type of message. Hence, the total cost $c(\vec{k})$ is the sum of all k_i-es, where $\mathbf{k} = (k_1, k_2, ..., k_m)$ is called *seed vector*. Let $s_i(k_i, t)$ denote the expected number of satisfied nodes for i-th type content at time t when the number of seed node is k_i. We assume that the seeds are deployed at time 0.

Then the problem formulation is as follows:

$$
\begin{aligned}
\textit{PF1}: \underset{\mathbf{k}=(k_1,\ldots,k_m)}{\text{Maximize}} \quad & f(\mathbf{k}) = \textstyle\sum_{i=1}^{m} s_i(k_i, d) - w \cdot c(\mathbf{k}) \\
s.t \quad & c(\mathbf{k}) = \textstyle\sum_{i=1}^{m} k_i \leq C \\
& 0 \leq k_i \leq n_i = p_i n, \ \forall i \in M \\
& \mathbf{k} \in \mathbb{N}^m
\end{aligned}
$$

where $M = \{1, 2, \ldots, m\}$, the cost budget is C, the tolerable delay is $d > 0$ units of time, and $w > 0$ is the total cost weight. The total cost weight reflects the importance of the cost in the sense that deploying one more seed should bring at least w number of satisfied nodes on average.

The objective function $f(\mathbf{k})$, which is referred to as *system utility* in this dissertation, is essentially the extra benefits induced by the short-range radio. It is easy to see that the system utility is the expected number of satisfied vehicles through the short-range radio alone, when the total cost weight $w = 1$.

6.2 Modeling Dissemination

In this section, we derive the expected number $s_i(k_i, t)$ of satisfied nodes obtaining i-th type of content at time t when only k_i seeds are initially deployed at time 0.

6.2.1 Terminology and Assumption

We first define the symbols used in our analysis as well as state the assumptions.

1. We assume that a node may encounter α proportion of all nodes on average for the time interval in interest;

2. For any pair of nodes, we assume that the inter-encounter time[2] follows an exponential distribution with rate β;

3. We also assume that the inter-encounter times of pairs of nodes are jointly independent and identical;

The assumption (1) is self-explainable. The assumptions (2) and (3) make our analysis mathematically tractable, and they have been found reasonable when vehicles follow conventional mobility models such as random waypoint model ([106]). At the same time, we acknowledge that these two assumptions might not be always realistic so that we relax both of them in our trace-driven simulation; though neither assumption is perfectly honored in the empirical traces of Beijing taxis, our simulation results still reasonably agree with our theoretical results.

[2]The *inter-encounter time* of a given pair of nodes is defined as the time duration from the time that the given pair of nodes encounter to the next consecutive time that the pair encounter again.

In our study, we take an *interest-only* caching policy: A node sends the previously obtained messages only to the nodes that are interested in the same type of the messages. In this dissertation, we focus on this caching policy because it can avoid the non-ignorable storage costs for keeping uninterested data incurred otherwise. A different solution is to allow vehicles carry contents which the vehicle users might not be interested. It is obviously the latter solution could provide an even better performance than the interest-only solution at the cost of extra storage space. The analysis of the latter cache policy is out of our scope, which merits an independent study.

Note that atomic contact among vehicles is assumed, implying that the message exchange between a pair of vehicles could be completed during their encounter process. As shown in [36, 135], it is reported that 30-70 MB data could be transfered as vehicle encounters (with normal driving speeds). Thus, we believe that most types of light-weighted contents (weather forecast, traffic information, mobile advertisement) could be successfully transmitted during short encounters between vehicles.

6.2.2 ODE model

We observe that the expected number of satisfied nodes behaves like the number of infected nodes in epidemic routing ([120]). The differences are that the initial number of sources (i.e. the number of seeds in this dissertation) is more than one, and that the other nodes that a node may ever encounter are not all nodes but a fraction of them. The previous work has introduced largely two methods to analyze the number of infected nodes; one is using the Markov chains and the other is using the ordinary differential equations (ODE) ([45, 52]). We use the ODE method with some modification for our analysis.

First, consider the expected number of newly satisfied nodes $\triangle S$ between time t and $t+dt$, where dt is infinitesimal. There are two groups of nodes at time t; a group of satisfied nodes and a group of unsatisfied nodes. The number of nodes in the former group is $s_i(k_i, t)$ as defined, and that of the latter is $n_i - s_i(k_i, t)$, where $n_i(= p_i n)$ is the number of nodes that are interested in the type i message.

Let us define the *inter-encounter time between the two groups* as the time elapsed until any node in one group meets any node in the other group after such encounter of inter-group nodes happens. Then, the inter-encounter time between the satisfied and the unsatisfied follows the Exponential distribution with rate $\beta\times$*(# of pairs of ever-encounter inter-group nodes)*, because the inter-encounter time of each pair of nodes that ever meets is i.i.d. Exponential (Assumptions (2) and (3)) and each node meets a fraction of other nodes (Assumption (1)).

Therefore, the expected number of newly satisfied nodes, $\triangle S$, is as follows:

$$\begin{aligned}\triangle S &= s_i(k_i, t + dt) - s_i(k_i, t) \\ &= \alpha\beta s_i(k_i, t)\,(n_i - s_i(k_i, t)) \cdot dt \end{aligned} \tag{6.1}$$

Note that the expected number of ever-meeting pairs of inter-group nodes is approximately[3] $\alpha s_i(k_i, t)\,(n_i - s_i(k_i, t))$.

From (6.1) and the fact that the number of seeds is k_i, we have the following ODE system;

$$\frac{\partial s_i(k_i, t)}{\partial t} = \alpha\beta s_i(k_i, t)(n - s_i(k_i, t)) \tag{6.2a}$$

$$s_i(k_i, 0) = k_i \tag{6.2b}$$

It turns out that this ODE system has the closed-form solution as follows:

$$s_i(k_i, t) = \frac{n_i}{1 + (n_i/k_i - 1)\exp(-n_i\alpha\beta t)} \tag{6.3}$$

6.3 Optimization

In this section, we derive theoretically the solution of the optimization problem proposed in Section 6.1. In order to gain better intuition about the system behavior, we relax the optimization

[3]This is because we approximate the expectation of the square of the number of satisfied nodes at time t to the square of the expectation of the number of satisfied, which is not rigorously true with the finite number of nodes. However, it becomes more accurate and eventually exact as $n \to \infty$ because the variance goes to zero. We shall also see when we validate with the real traces, this is still a useful approximation.

problem ignoring the integral constraint on the numbers of seeds k_i. Therefore, we focus on the following optimization problem $PF2$ in this section:

$$PF2 : \underset{\mathbf{k}}{\text{Maximize}} \quad f(\mathbf{k}) = \textstyle\sum_{i=1}^{m} s_i(k_i, d) - w \cdot c(\mathbf{k}) \tag{6.4a}$$

$$s.t \quad c(\mathbf{k}) = \textstyle\sum_{i=1}^{m} k_i \leq C \tag{6.4b}$$

$$0 \leq k_i \leq n_i = p_i n, \ \forall i \in M \tag{6.4c}$$

We first show that the problem is a convex optimization problem, then, solve the problem using the method of Lagrange multipliers. In the process, we further relax some constraints for easier derivation, and then, provide the condition under which the solution derived with the relaxation is valid for the original problem $PF2$.

6.3.1 Convexity of the Problem

The expected number s_i of the satisfied nodes is concave with respect to the number of seeds k_i because its first derivative is non-negative and its second derivative is non-positive as follows:

$$\frac{\partial s_i(k_i, d)}{\partial k_i} = \frac{n_i^2 z_i}{k_i^2(1 + (n_i/k_i - 1)z_i)^2} \geq 0, \qquad \forall k_i \in (0, n_i]$$

$$\frac{\partial^2 s_i(k_i, d)}{\partial k_i^2} = -\frac{2n_i^2 z_i(1 - z_i)}{k_i^3(1 + (n_i/k_i - 1)z_i)^3} \leq 0, \qquad \forall k_i \in (0, n_i]$$

where we use the following for concise presentation;

$$z_i = e^{-n_i \alpha \beta d} \tag{6.5}$$

Therefore, the objective function $f(\mathbf{k})$ is a linear combination of concave functions, which implies that the function itself is concave. From the concavity of the objective function and the fact that all constraints are linear, we can see that the problem is a convex optimization problem.

6.3.2 Optimum Number of Seeds

We use the Lagrange dual of the convex optimization problem to obtain the optimum solution. We further ignore the constraints in Equation (6.4c) for now for the concise presentation of the derivation. But, we shall provide the conditions under which the obtained solution in this section is valid for the problem $PF2$.

The Lagrangian of the problem is as follows:

$$L(\mathbf{k}, \lambda) = f(\mathbf{k}) - \lambda \left(c(\mathbf{k}) - C \right) \tag{6.6}$$

where λ is the Lagrange multiplier and $\lambda \geq 0$.

Since the primal problem is concave, it is well-known that the parameter set $(\widehat{\mathbf{k}}, \widehat{\lambda})$ that minimize $\sup_{\mathbf{k}} L(\mathbf{k}, \lambda)$ maximizes the primal. Because the Lagrangian is also concave with respect to $\mathbf{k}$, we have the following conditions for such $(\widehat{\mathbf{k}}, \widehat{\lambda})$;

$$\frac{\partial L(\mathbf{k}, \lambda)}{\partial k_i} = \frac{n_i^2 z_i}{(k_i + n_i z_i - k_i z_i)^2} - \lambda - w = 0 \quad \forall i \tag{6.7a}$$

$$\frac{\partial L(\mathbf{k}, \lambda)}{\partial \lambda} = \lambda \left(\sum_{i=1}^{m} k_i - C \right) = 0 \tag{6.7b}$$

As can be seen from Equation (6.7b), we have two cases; one for $\lambda = 0$ (*i.e.* $\sum k_i < C$) and the other for $\sum k_i = C$. When $\sum k_i < C$, the constraint (6.4b) is inactive meaning that the solution of the constrained optimization problem is indeed that of its unconstrained version. Suppose $\widetilde{\mathbf{k}}$ is the unconstrained optimum solution, and let $\widetilde{C}$ be the unconstrained optimum total cost, given by;

$$\widetilde{C} \doteq c(\widetilde{\mathbf{k}}) = \sum_{i=1}^{m} \widetilde{k}_i \tag{6.8}$$

Then, $\widetilde{C} = c(\widetilde{\mathbf{k}}) < C$, and so, the optimum solution $\widetilde{\mathbf{k}}$ automatically satisfies the constraint (6.4b) in this case.

On the other hand, the constraint (6.4b) is active in the case where $\sum k_i = C$. It means that the unconstrained solution of the optimization problem requires more cost than allowed in general, that is, $C \leq \widetilde{C}$. In other words, the system does not afford the unconstrained optimum seed vector, resulting in fewer numbers of seeds to meet the constraint. Therefore, the system utility $f(\mathbf{k})$ would be smaller than its maximum possible.

Now we provide the solution of the constrained optimization problem as follows:

$$\widehat{k}_i = \begin{cases} \widetilde{k}_i = \dfrac{n_i\sqrt{z_i}}{1-z_i}\left(\dfrac{1}{\sqrt{w}} - \sqrt{z_i}\right), & \text{if } \widetilde{C} < C \qquad (6.9a) \\ \breve{k}_i = \dfrac{n_i\sqrt{z_i}}{1-z_i}\left(\dfrac{C+A}{B} - \sqrt{z_i}\right), & \text{if } \widetilde{C} \geq C \qquad (6.9b) \end{cases}$$

where

$$A = \sum_{i=1}^{m} \frac{n_i z_i}{1-z_i}, \qquad B = \sum_{i=1}^{m} \frac{n_i\sqrt{z_i}}{1-z_i} \tag{6.10}$$

And, $\widetilde{C}$ can be obtained from Equations (6.8) and (6.9a). The derivation for the solution is not terribly difficult, and so, we omit it in this dissertation for more concise presentation. We note

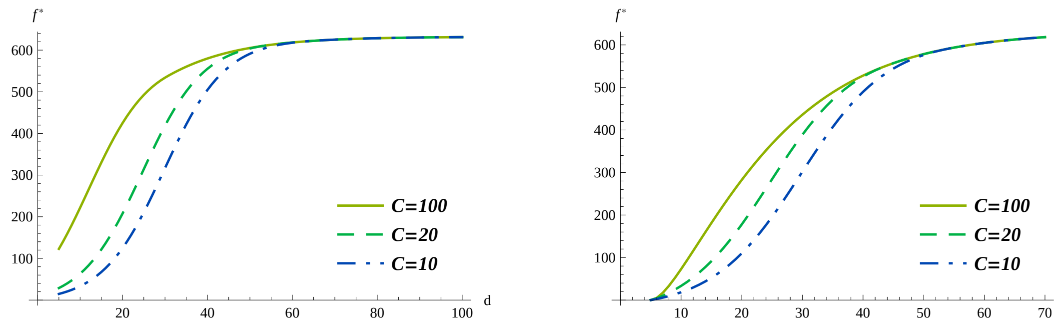

(a) $w = 0.5$ (b) $w = 2$

Figure 6.1: Optimum utility vs. delay budget

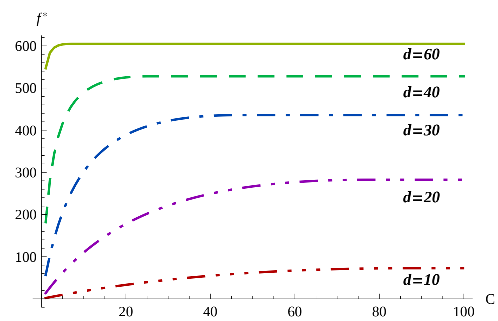

Figure 6.2: Optimum utility vs. cost budget $(w = 2)$

that the solution in Equation (6.9) still ignores the constraint (6.4c). However, we show that the solution is indeed the solution of $PF2$ under the conditions in Theorems 6.3.1 and 6.3.2.

Theorem 6.3.1. *Suppose* $\widetilde{k}_i$ *and* $\widetilde{C}$ *are defined as in Equations (6.9a) and (6.8), respectively. Also, suppose* $z_i = \exp(-n_i \alpha \beta d)$*. Then, under any one of the following conditions,*

$$\mathbb{C}_1 : \quad \{0 < w < 1, 0 < z_i \leq w\}$$

$$\mathbb{C}_2 : \quad \{w = 1, 0 < z_i < 1\}$$

$$\mathbb{C}_3 : \quad \{w > 1, 0 < z_i \leq 1/w\}$$

the optimum numbers of seeds, k_i^*, of the optimization problem $PF2$ are, if $\widetilde{C} < C$,

$$k_i^* = \widetilde{k}_i \tag{6.11}$$

Proof. We note that $\widetilde{k}_i$ is the solution of $PF2$ when $\widetilde{C} < C$ if we ignore the constraint (6.4c). Hence, what we need to show is that $\widetilde{k}_i$ is in the interval $[0, n_i]$ under any of the conditions $\mathbb{C}_1, \mathbb{C}_2$, or $\mathbb{C}_3$ so that the constraint is satisfied.

We can represent $\widetilde{k}_i$ as follows:

$$\widetilde{k}_i = \frac{n_i\sqrt{z_i}}{1-z_i}\left(\frac{1}{\sqrt{w}} - \sqrt{z_i}\right) = n_i \cdot y(z_i) \tag{6.12}$$

where

$$y(z_i) \doteq \frac{\sqrt{z_i/w} - z_i}{1 - z_i} \tag{6.13}$$

Then, we only need to show $0 \leq y(z_i) \leq 1$ under any of the three conditions.

When $0 < w \leq 1$, we can see that $y(z)$ is monotonically non-decreasing in $(0, 1)$ because its first derivative is non-negative in that interval as follows:

$$\frac{dy(z)}{dz} = \frac{1 - w + (\sqrt{z} - \sqrt{w})^2}{2\sqrt{wz}(1-z)^2} \tag{6.14}$$

Hence, we can easily see $0 = y(0) < y(z) \leq y(w) = 1$ under the condition $\mathbb{C}_1$.

Under the condition $\mathbb{C}_2$, we can see $0 \leq y(z_i) \leq 1$ from the following:

$$0 = y(0) < y(z) < \lim_{z \to 1} y(z) = 1/2 < 1 \tag{6.15}$$

Note that we cannot use $y(1)$ because it is not defined at $z = 1$.

Now consider the last condition $\mathbb{C}_3$. When $w > 1$, we can easily see that $y(z) < 1$ for $0 < z < 1$ from Equation (6.13). And it is not difficult to see that $y(z) > 0$ for $0 < z < 1/w$. And, these imply that $0 \leq \widetilde{k}_i \leq n_i$ under $\mathbb{C}_3$. □

Theorem 6.3.2. *Suppose $\breve{k}_i$ and $\widetilde{C}$ are defined as in Equations (6.9b) and (6.8), respectively. Also, suppose $z_i = \exp(-n_i \alpha \beta d)$.*

Then, if any of the conditions $\mathbb{C}_1, \mathbb{C}_2$ and $\mathbb{C}_3$ holds, and also if

$$\sum_{j=1}^{m} \frac{n_j \sqrt{z_j}}{1 - z_j} \leq C \leq \widetilde{C}$$

, the optimum numbers of seeds, k_i^*, of the optimization problem $PF2$ are,

$$k_i^* = \breve{k}_i$$

Proof. $\breve{k}_i$ is the solution of $PF2$ when $C \leq \widetilde{C}$ if we ignore the constraint (6.4c). Hence, we only need to show $\breve{k}_i \in [0, n_i]$ under the conditions.

First, we will show that $\breve{k}_i \leq n_i$.

$$\begin{aligned} \widetilde{C} \geq C \quad & \Rightarrow \quad \sum_{i=1}^{m} \frac{n_i \sqrt{z_i}}{1 - z_i} \left(\frac{1}{\sqrt{w}} - \sqrt{z_i} \right) = \frac{B}{\sqrt{w}} - A \geq C \\ & \Rightarrow \quad \frac{1}{\sqrt{w}} \geq \frac{C + A}{B} \end{aligned}$$

where A and B are defined in Equation (6.10).

This implies, together with Equation (6.9) and the proof of Theorem 6.3.1, that $\breve{k}_i \leq \widetilde{k}_i \leq n_i$.

Now let us show that $\breve{k}_i \geq 0$. Since $C \geq \sum_j \frac{n_j \sqrt{z_j}}{1 - z_j}$,

$$\begin{aligned} \breve{k}_i \quad & \geq \quad \tfrac{n_i \sqrt{z_i}}{1-z_i} \left[\tfrac{1}{B} \left(\sum_j \tfrac{n_j \sqrt{z_j}}{1-z_j} + A \right) - \sqrt{z_i} \right] \qquad (6.16) \\ & = \quad \tfrac{n_i \sqrt{z_i}}{B(1-z_i)} \sum_j^m \tfrac{n_j \sqrt{z_j}}{1-z_j} \left(1 + \sqrt{z_j} - \sqrt{z_i} \right) \geq 0 \end{aligned}$$

where (6.16) follows since $\sqrt{z_j} - \sqrt{z_i} \geq -1$ for all j and i. □

6.3.3 Optimum System Utility

In this section, we investigate the system behavior when the seed vector is optimum $\mathbf{k}^*$. We first derive the optimum expected number of satisfied nodes and the optimum system utility, and look into how they depend on the system parameters, such as the cost budget C, delay budget d, *etc.*, through numerical evaluations.

The optimum number s_i^* of satisfied nodes can be derived from Equations (6.3) and (6.9), given by

$$s_i^*(d,C) = \begin{cases} \sum_{i=1}^{m} \frac{n_i}{1-z_i}\left(1-\sqrt{wz_i}\right), & \text{if } \widetilde{C} < C \quad (6.17a) \\ \sum_{i=1}^{m} \frac{n_i}{1-z_i}\left(1-\frac{B}{C+A}\sqrt{z_i}\right), & \text{otherwise} \quad (6.17b) \end{cases}$$

where z_i, A, and B are given in Equations (6.5) and (6.10) respectively.

The optimum system utility is from Equations (6.4a), (6.9), and (6.17), as follows:

$$f^*(d,C) = \begin{cases} \sum_{i=1}^{m}(1-\sqrt{wz_i})s_i^*(d,C), & \text{if } \widetilde{C} < C \quad (6.18a) \\ \sum_{i=1}^{m}\left(1-\frac{C+A}{B}w\sqrt{z_i}\right)s_i^*(d,C), & \text{otherwise} \quad (6.18b) \end{cases}$$

Because of the complexity of the above equations, it is hard to obtain a good intuition on the optimum system behavior from the equations themselves. So, we resort to the numerical evaluations of the equations for better intuition. When it comes to numerical evaluation, the equations are very simple and easy to calculate. However, we need proper parameter values for evaluations in order to have relevant results.

We use the values we obtain from the real traces of vehicles in Section 6.5; the number of nodes $n = 632$, the inter-encounter rate $\beta = 3.663 \times 10^{-6}$ per second, and $\alpha = 0.191$. And we focus on a single type of content in this section. From the proof of Theorem 6.3.1, we can see that some system property may be different when $w < 1$ than when $w > 1$. So, we compare the system behaviors for $w = 0.5$ and $w = 2$ when appropriate.

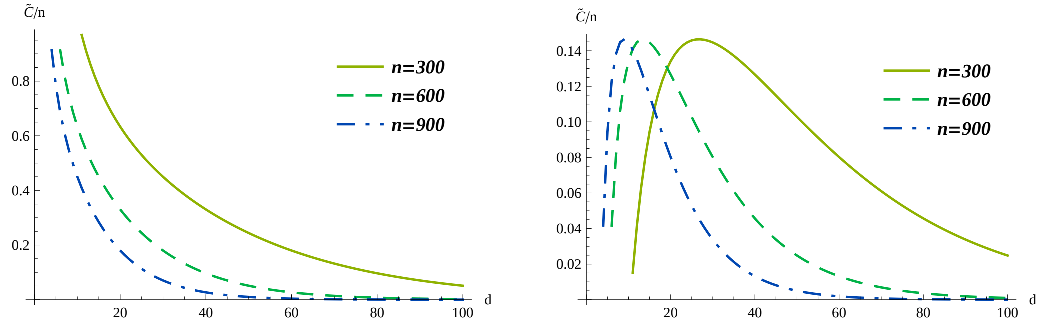

Figure 6.3: Unconstrained optimum total cost vs. delay budget

Figure 6.1 shows the optimum utility with respect to the delay d when the allowed cost C are small, medium, and large. When d is small or large, we can see that the system utility has ignorable sensitivity on the value of C. But, when d is in between, the difference can be quite huge. As for the influence of w, the utility shows similar tendency regardless of w although the utility is more sensitive to C when $w = 0.5$.

Now we look into the optimum utility with respect to the allowed cost C in more detail through Figure 6.2. From the figure, we can see that the utility increases up to some point and stays there afterwards as C increases, for each d values. From the analysis, we know that the C value from which the utility is constant is actually $\widetilde{C}$. When d is small, the optimum utility increase for a large range of C, but the slope is very small, which means the sensitivity of the utility to C is small. As d increases, $\widetilde{C}$ decreases while the sensitivity increases. However, when d is large enough, only a small number of seeds is needed to satisfy most of the nodes, and so the cost constraint become less important. Note that we omit the plots for $w = 0.5$ because they look similar to those of $w = 2$ (Figure 6.2).

Figure 6.3 shows more directly how the unconstrained optimum total cost $\widetilde{C}$ changes as the allowed delay d changes. While the cost monotonically decreases as d increase when $w = 0.5$, the cost reaches its maximum and decreases when $w = 2$. In fact, the optimum cost monotonically decreases when $w \leq 1$. The system behavior changes significantly at $w = 1$ because one more seed does not require more than one more satisfied node when $w \leq 1$, and so the system utility never decreases as the seed number increases. However, when $w > 1$, deploying one more seed requires more satisfied nodes besides itself, which may make the utility decreases especially when the delay budget is very small or very large. When the cost is very important (high w) and the allowed delay is very small, our model suggests it is sometimes better not to disseminate the content at all depending on other system parameters like the inter-encounter time.

We can also see that smaller portion of total nodes are needed to obtain the seeds for the optimum performance as the number of nodes increases.

As for the influence of parameters α and β, we can see they only appear in z_i with d from Equation (6.18), and d only appears with α and β. Therefore, α and β act like shrinking or stretching the performance plot in the direction of d as they increase or decrease, respectively.

6.4 Practical Solutions

In the previous section, we explored the optimum behavior of the system theoretically. While the theoretical analysis brings better intuition of the system, it is also true that the solution is not either exact nor ready to use in practical systems because it is a continuous solution derived from the relaxed version of the problem (ignoring the integral constraint). The practical systems require integer values for the seed numbers. Hence, in this section, we develop a polynomial algorithm to obtain the exact discrete solution for $PF1$.

Algorithm 1 OPTIMIZER(C, m)

$\mathbf{k}$:= m-sized array initialized to be all zero.
for $(c = 0; c < C; c+ = 1)$ **do**
  $i^* := 0$
  $\delta_{max} := -\infty$
  for $(i = 1; i \leq m; ++i)$ **do**
    $\delta := f(\{\mathbf{k}[1], \ldots, \mathbf{k}[i] + 1, \ldots, \mathbf{k}[m]\}) - f(\mathbf{k})$
    if $(\delta > \delta_{max})$ **then**
      $i^* := i$
      $\delta_{max} := \delta$
  if $(\delta_{max} \leq 0)$ **then**
    $\mathbf{break}$
  $\mathbf{k}[i^*] + = 1$
return $\mathbf{k}$

Algorithm 1 gives the optimum seed vector, each i-th element of which is integer-valued and in the range $[0, n_i]$. In a nutshell, the algorithm starts with zero seeds for all types, then increment the seed number of the type that gives the maximum increase in the system utility, as long as the total access cost is not over budget and the increase in the system utility is positive. Its correctness is proven in Theorem 6.4.1. The time complexity of the algorithm is $O(m^2C)$, where m is the number of types of content, and C is the allowed cost.

Theorem 6.4.1. *Algorithm 1 returns the optimum solution of $PF1$.*

Proof. We first note that the system utility function can be represented w.r.t $\mathbf{k}$ as follows:

$$f(\mathbf{k}) = \sum_{i=1}^{m} s_i(k_i, d) - w \sum_{i=1}^{m} k_i \tag{6.19}$$

$$= \textstyle\sum_i \underbrace{(s_i(k_i, d) - wk_i)}_{\doteq f_i(k_i)} = \sum_i f_i(k_i) \tag{6.20}$$

From Section 6.3.1, we know that f_i is concave w.r.t the number of seeds, which implies

$$\triangle f_j(k+1) \leq \triangle f_j(k), \quad \forall k \geq 0, k \in \mathbb{N}; \forall j \in M \tag{6.21}$$

where $M = \{1, 2, \ldots, m\}$, and

$$\triangle f_j(k) \doteq f_j(k) - f_j(k-1) \tag{6.22}$$

Now suppose $\mathbf{k}^*$ is the outcome of Algorithm 1, and $\widetilde{\mathbf{k}}$ is an arbitrary legitimate vector of number of seeds for *PF1* (*i.e.* $\widetilde{C} = \sum_i \widetilde{k}_i \leq C$). It is easy to see that Algorithm 1 ensures that $C^* = \sum_i k_i^* \leq \lfloor C \rfloor \leq C$, and so $\mathbf{k}^*$ is a legitimate seed vector. We shall show that $\mathbf{k}^*$ gives the system utility at least as high as that of $\widetilde{\mathbf{k}}$ so that $f(\mathbf{k}^*) \geq f(\widetilde{\mathbf{k}})$.

i) If $\mathbf{k}^* = \widetilde{\mathbf{k}}$, we have nothing to prove.

ii) When $\widetilde{\mathbf{k}} \preceq \mathbf{k}^*$, $\widetilde{k}_i \leq k_i^*$ for all $i \in M$. Then,

$$f(\mathbf{k}^*) - f(\widetilde{\mathbf{k}}) = \sum_{j \in J} \sum_{i=1}^{k_j^* - \widetilde{k}_j} \triangle f_j(\widetilde{k}_j + i) \geq 0 \tag{6.23}$$

where $J = \{j \in M | \widetilde{k}_j < k_j^*\}$.

It is non-negative because $\triangle f_j(k_j^*) \geq 0, \forall j$ due to the line 11 of Algorithm 1, and $\widetilde{k}_j + i \leq k_j^*$, which implies from Equation (6.21)

$$\triangle f_j(\widetilde{k}_j + i) \geq \triangle f_j(k_j^*) \geq 0 \tag{6.24}$$

Hence, $f(\mathbf{k}^*) \geq f(\widetilde{\mathbf{k}})$.

iii) When $\widetilde{\mathbf{k}} \succeq \mathbf{k}^*$ (*i.e.* $\widetilde{k}_i \geq k_i^*, \forall i$) but $\widetilde{\mathbf{k}} \neq \mathbf{k}^*$, it is easy to see the following:

$$C^* < \widetilde{C} \leq \lfloor C \rfloor \leq C \tag{6.25}$$

This implies the algorithm has executed the line 11, which again implies with Equation (6.21),

$$\triangle f_l(k_l^* + c) \leq 0, \quad \forall l \in M, \forall c \geq 1 \tag{6.26}$$

Hence, letting $J = \{j \in M | \widetilde{k}_j > k_j^*\}$,

$$f(\widetilde{\mathbf{k}}) - f(\mathbf{k}^*) = \sum_{j \in J} \sum_{i=1}^{\widetilde{k}_j - k_j^*} \triangle f_j(k_j^* + i) \leq 0 \tag{6.27}$$

iv) Consider the remaining cases. For all these cases, we have at least a pair of $(i, j) \in M^2$ such that $\widetilde{k}_i < k_i^*$ and $k_j^* < \widetilde{k}_j$.

Before proceeding, we show a couple of useful inequalities for this proof.

$$\triangle f_x(k_x^* + 1) \leq \triangle f_y(k_y^*), \quad \forall y \neq x \tag{6.28}$$

If this is not true, Algorithm 1 would have incremented k_x to be $k_x^* + 1$ instead of incrementing k_y when $k_x = k_x^*$ and $k_y = k_y^* - 1$.

From Equations (6.21) and (6.28),

$$\triangle f_x(k_x^*+1) \leq \triangle f_y(k), \quad \forall k \leq k_y^*; \forall y \in M \tag{6.29}$$

Let us define δ as follows:

$$\delta = \min\{|\widetilde{k}_i - k_i^*|, |\widetilde{k}_j - k_j^*|\} \tag{6.30}$$

And Let $\mathbf{k}^{(1)}$ such that $k_i^{(1)} = \widetilde{k}_i + \delta$, $k_j^{(1)} = \widetilde{k}_j - \delta$, and $k_l^{(1)} = \widetilde{k}_l, \forall l \neq i, j$, which implies $\mathbf{k}^{(1)}$ is also legitimate from $C^{(1)} = \sum_i k_i^{(1)} = \widetilde{C} \leq C$. Now, consider

$$\begin{aligned} f(\mathbf{k}^{(1)}) - f(\widetilde{\mathbf{k}}) &= \sum_{l=1}^{\delta} \triangle f_i(\widetilde{k}_i + l) - \sum_{l=1}^{\delta} \triangle f_j(\widetilde{k}_j - l + 1) \\ &= \sum_{l=1}^{\delta} \Big(\triangle f_i(\widetilde{k}_i + l) - \triangle f_j(\widetilde{k}_j - l + 1) \Big) \end{aligned} \tag{6.31}$$

Because $\widetilde{k}_i + l \leq k_i^*$ and $k_j^* \leq \widetilde{k}_j - l + 1$ for $\forall l \in [1, \delta]$, we have the following inequality from Equation (6.29):

$$\triangle f_j(\widetilde{k}_j - l + 1) \leq \triangle f_i(\widetilde{k}_i + l) \tag{6.32}$$

This implies that the RHS of Equation (6.31) is non-negative. Hence, $f(\mathbf{k}^{(1)}) \geq f(\widetilde{\mathbf{k}})$, and $k_i^{(1)} = k_i^*$ or $k_j^{(1)} = k_j^*$, which means at least one more element in $\mathbf{k}^{(1)}$ is same as that of $\mathbf{k}^*$ than $\widetilde{\mathbf{k}}$, augmenting the system utility.

Now, we keep doing this augmentation process from the resultant seed vector of each process until there is no such pair (i, j). We need no more than m rounds of this process to reach this state. Then, letting $\mathbf{k}^{(f)}$ denote the final resultant seed vector, we have one of the following exhaustive cases; (a) $\mathbf{k}^{(f)} = \mathbf{k}^*$, (b) $\mathbf{k}^{(f)} \preceq \mathbf{k}^*$, and (c) $\mathbf{k}^{(f)} \succeq \mathbf{k}^*$. In each of the cases, from i), ii) and iii),

$$f(\mathbf{k}^*) \geq f(\mathbf{k}^{(f)}) \geq f(\widetilde{\mathbf{k}}) \tag{6.33}$$

□

6.5 Simulation Based on Taxi Traces

In this section, we present how the contents dissemination behaves in the more realistic setting. We consider a single type of content in this section because the process of the dissemination does not depend on other contents as shown in Section 6.2.

6.5.1 Beijing Taxi Traces

We use the GPS traces of taxis in Beijing gathered from 12:00am to 11:59pm on Jan. 05, 2009 in the local time. The number of subject taxis is 2,927. The number of the GPS points in the trace is 4,227,795 typically one per minute per vehicle. The GPS points span from $32.1223°$ N to $42.7413°$ N in latitude, and from $111.6586°$ to $126.1551°$ in longitude. Figure 6.4a shows the GPS traces of randomly chosen 10 taxis as an example.

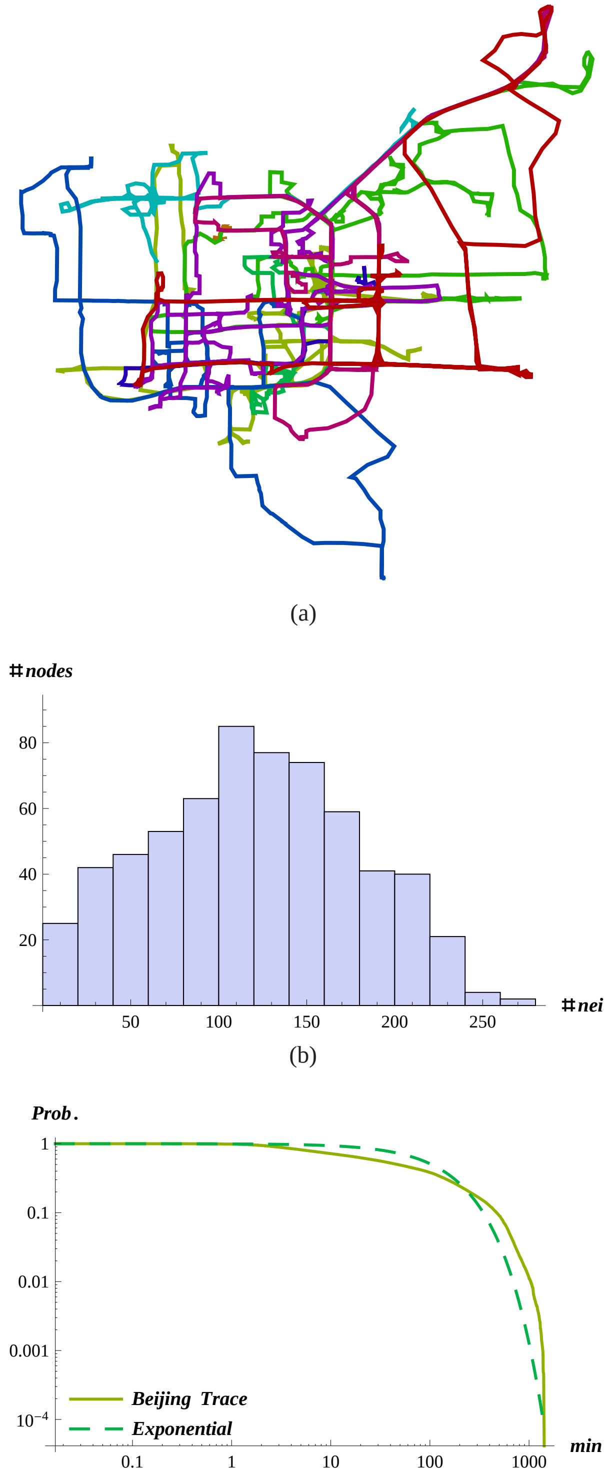

(a)

(b)

(c)

Figure 6.4: Properties of beijing taxi traces: (a) geographical movements of 10 sample taxis, (b) histogram of number of neighbors of a node, (c) tail distribution of the inter-encounter times

6.5.2 Encounter Processes

In order to perform a simulation for the contents dissemination through the short-range radio, we need traces of encounters of all pairs of nodes; that is, when which vehicle can communicate with which other vehicle. We can extract these traces from the GPS traces by assuming a radio model. In this dissertation we assume the circular radio model to decide if two given vehicles encounter each other so that they can communicate directly. The circular radio model has the radio range r so that any two vehicles of distance within r can directly communicate with each other successfully. We use $r = 300$ meters as the literature ([13]) suggests.

Suppose a set of error-free time-ordered GPS traces of a pair of vehicles is given. In order to obtain the time-ordered traces of encounters for the pair, we have compared their geodesic distances in some sequence of times. Instead of employing a time sequence of identical intervals, we have checked the distance after the minimum time τ_{min} (Equation (6.34)) that the pair can encounter each other next, if the current distance is large enough, for the faster processing and more accurate results. When the current distance is small, we have checked their new distance after a predetermined small time step.

Since the logs of GPS locations are not synchronized, we cannot simply take the locations of the pair from the logs at a given time. So, we have interpolated the locations of each vehicle assuming that the GPS traces are dense enough so that a vehicle can be approximated to move in a straight line between a consecutive pair of GPS locations in the traces.

The minimum time τ_{min} for the next encounter is given by

$$\tau_{min} = \frac{1}{2s_m}(\textsc{GeoDist}(pos(P_1, t), pos(P_2, t)) - r) \tag{6.34}$$

where GEODIST gives the geodesic distance between the given pair of GPS positions, $pos(P_i, t)$ calculates the estimated position of vehicle i at time t from the set of its GPS traces P_i by interpolating the positions, and s_m is the maximum speed of vehicles in the traces.

We then obtain the time-ordered set of encounters of all pairs by executing the aforementioned algorithm for each pair and sorting their combined result.

We note that the input sets of GPS traces to the algorithm are required to be error-free. However, we have found, as expected, that some GPS units of vehicles experienced errors in some time intervals, so either some erroneous log was reported or there was no data at all in the interval. After removing those erroneous GPS points, we have checked if this removal incurs some side effects. We have found that the removal makes some vehicle untraceable in some non-ignorable time intervals. In other words, some vehicles have no valid GPS points reported for long intervals. And it is difficult to approximate their positions for the duration by interpolating the valid positions. Hence, we resort to excluding those vehicles from the simulation.

After all, we have selected 632 vehicles, each of which satisfies the following criteria:

- The GPS points indicating the speed of 80 mph or more are considered erroneous and removed. It is because the speed of more than 80 mph is hard to reach and rarely exercised in the Beijing area.

- The valid GPS points of each vehicle are logged somewhat regularly in time when it is moving so that any two consecutive GPS points of the vehicle do not have distance more than 400 meters if their time difference is more than 3 minutes.

- The encounter graph of vehicles forms a well connected graph so that the number of neighbors of a node is at least 2. The encounter graph is defined in Definition 6.5.1.

The second condition makes sure that the vehicle has not moved actively when it skipped two consecutive regular GPS reports. We set the distance of 400m so that we can have better understanding on the timing of encounters (with some tolerance) in the interval of the reports, when the radio range is 300m. The last condition is to remove loner vehicles. We note that the loner vehicles have almost no interaction with others at all, which means they are in the very different activity region. But, we are interested in the dissemination over the nodes of similar activity region.

Definition 6.5.1 (Encounter Graph)**.** *An* ***encounter graph*** $G(V, E)$ *of vehicles is a graph such that each vehicle is represented by a node* $v \in V$*, and any two nodes* $v_1, v_2 \in V$ *has a link* $e(v_1, v_2) \in E$ *between them if and only if they can communicate with each other (*i.e. *encounter) at any point in the interested time interval.*

The encounter graph of the 632 nodes has 38,139 links; the minimum number of neighbors of a node is 2, the maximum is 261, and the median is 120. Their average number is 120.693. This value is used in later sections for evaluating our model for the number of satisfied nodes. Figure 6.4b shows the histogram of the number of neighbors of a node.

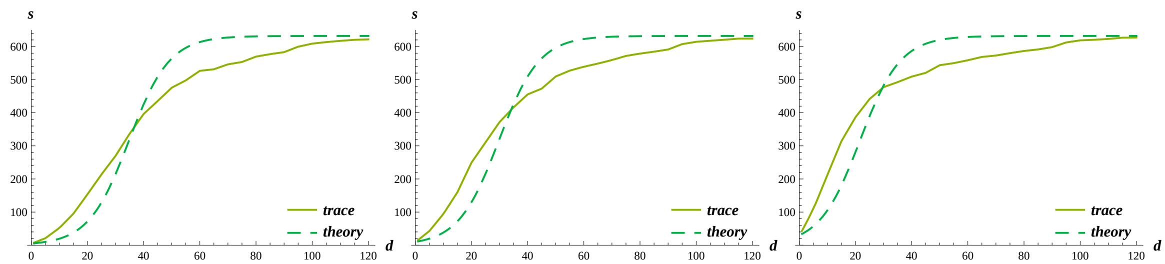

(a) k=5 (b) k=10 (c) k=30

Figure 6.5: Average number of satisfied nodes vs. tolerable delay

6.5.3 Inter-Encounter Time

In this section, we analyze on the inter-encounter time of a pair of nodes in order to verify the Exponential assumption of the inter-encounter time and to obtain its rate for evaluating our model.

Although the trace data is fine-grained and covers 24 hours of a day, many pairs of nodes have only a few encounters, which is too small to have a good statistical meaning if we focus on the per-pair distribution. So, we hypothesize that the inter-encounter time of every pair follows the identical and independent distribution, particularly, the Exponential distribution as we assume in the analysis in Section 6.2.

We first examine the aggregate inter-encounter time collecting the available inter-encounter times of every consecutive encounters of all pairs of nodes. The number of samples is 24,205, and their sample mean is 150.005 minutes. Figure 6.4c shows the tail distribution of the samples and the Exponential distribution with mean 150.005 minutes. As can be seen, they do not show big disparities. Because we assume IID Exponential distributions for per-pair inter-encounter times, their aggregate inter-encounter time has the identical distribution to the per-pair ones, which can be proved easily.

However, the above sample mean for the inter-encounter time is actually an underestimate of the true mean because we ignore many incomplete samples, which is the time from the beginning of the trace to the first encounter and the time from the last encounter to the end of the trace for each pair of nodes. For each of those samples of time duration, we know that its associated realization of the inter-encounter time is larger than the time duration, but we do not know the exact value. That is why we exclude them from the above estimation. But, now that we have the reason (*i.e.* Figure 6.4c) to believe that it is fine to assume the Exponential distribution for the inter-encounter time, we can use the incomplete information to obtain a more accurate estimate.

We use the fact that the number of encounters in a time interval T follows the Poisson distribution with mean βT, when the inter-encounter time is Exponential with rate β. Suppose N_i and T_i are the number of encounters and the whole time duration of the trace, respectively, for i-th pair of nodes, and η the number of the pairs that have at least one encounter in the trace. Then, the following equation gives the maximum likelihood estimate β^* of β.

$$\beta^* = \arg\max_\beta \Pr(N_1, N_2, ..., N_\eta | \beta, T_1, ..., T_\eta) \tag{6.35}$$

where

$$\begin{aligned} \Pr(N_1, N_2, ..., N_\eta | \beta, T_1, ..., T_\eta) &= \prod_{i=1}^{\eta} \Pr(N_i | \beta T_i) = \prod_{i=1}^{\eta} \frac{(\beta T_i)^{N_i} e^{-\beta T_i}}{N_i!} \\ &= \left(\prod_{i=1}^{\eta} \frac{T_i^{N_i}}{N_i!}\right) e^{-\beta \sum_{i=1}^{\eta} T_i} \beta^{\sum_{i=1}^{\eta} N_i} \end{aligned} \tag{6.36}$$

Note that (6.36) holds because the inter-encounter times of every pair are assumed to be jointly independent.

After some calculations, we can obtain the maximum likelihood estimate of the rate of the inter-encounter time of a pair of nodes that ever encounter, as follows:

$$\beta^* = \sum_{i=1}^{\eta} N_i \,/\, \sum_{i=1}^{\eta} T_i \tag{6.37}$$

We shall use this quantity as a parameter value to evaluate our analytical model and compare with the real-trace-based simulation results.

6.5.4 Simulation Methodology

From the time-ordered traces of the encounters of the Beijing traces, produced by the method in Section 6.5.2, we have performed the simulations by running Algorithm 2 multiple times until the sample mean of the number of returned satisfied nodes has its error no more than 5% of its value with 97% confidence. Algorithm 2 takes several input arguments; E is a time-ordered list of encounters, N is the set of vehicles, $S \subset N$ is the set of seed nodes, t_s is the time when S are deployed, and d is the delay budget. We have performed the simulations for various choices for the number of seeds k and the tolerable delay d, letting the seeds be deployed at time $t_s = 9AM$. For particular k and d, we have chosen the seed nodes S uniformly at random at each round.

Algorithm 2 SATISFIEDNODES(E, N, S, t_s, d)

1: Mark every $v \in S$ as satisfied.
2: **for all** $e \in E$ in order s.t. $t_s \leq time(e) \leq t_s + d$ **do**
3: Let v_1 and v_2 be the pair of vehicles for e.
4: **if** only one of v_1 and v_2 is marked satisfied **then**
5: Mark the other node as satisfied.
6: **return** the set of all marked nodes

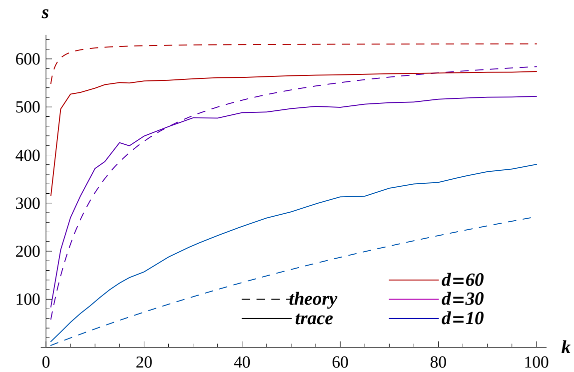

Figure 6.6: Avg. number of satisfied nodes vs. number of seeds

6.5.5 Number of Satisfied Nodes

Figure 6.6 shows the average number of satisfied nodes with respect to the number of seeds when the delay constraints are 10, 30, and 60 minutes. When the delay is small (*i.e.* 10 minutes), the real traces suggest more nodes are expected to be satisfied than the theory predicts. When the delay is medium (*i.e.* 30 minutes), the real traces and the theory suggest similar behavior of the dissemination, while the theory overestimates the number of satisfied nodes when the delay is 60 minutes. But, the figure shows qualitatively similar behavior of the average number of satisfied nodes as the number of seeds increases.

Figure 6.5 shows in more detail how the gap between the theory and the trace suggest changes as the delay constraint increases. The numbers of seeds considered are 5, 10, and 30. And all the cases indicate similar trends of the content dissemination; the real traces suggest that the dissemination is faster than the theory predicts in the early phase, but loses its momentum as more portion of nodes are infected. This difference may be because of the movement dependencies between groups of vehicles in reality. Suppose there is some dependency among the pair-wise encounter processes that is caused by the movement dependency. It is easy to see that the content

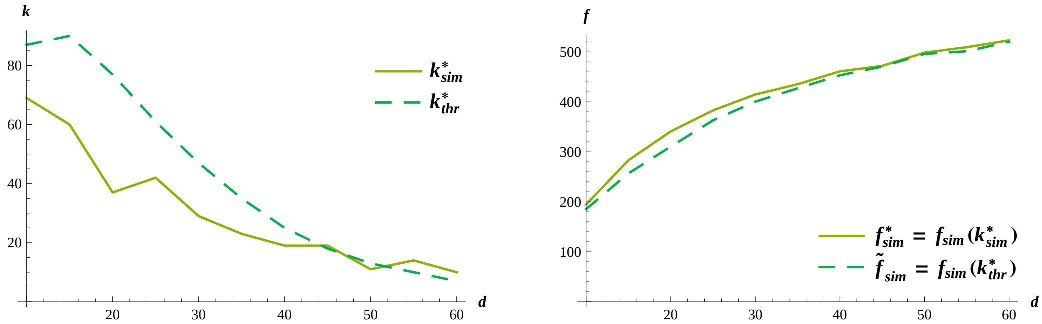

(a) Optimal Seed Number (b) System utility

Figure 6.7: System behaviors in optimal regime w.r.t the delay budget

spread faster to the other nodes of positive correlation than the average, and slower to the nodes of negative correlation. Hence, in the early phase of the dissemination, the content spreads fast to positively correlated nodes, and after consuming most of them, it spreads slowly to the nodes of negative correlation. This can partly address the gap in Figure 6.5. But, more accurate analysis calls for further investigation, which is out of scope of this dissertation and the subject of future research.

Nevertheless, the system behavior with respect to the number of seeds is more important for our problem because it is the parameter to optimize on. And, Figure 6.6 suggests comparable numbers of seeds for the knees of plots from the theory and the real traces.

6.5.6 Optimal Number of Seeds

Now we look into the system utility f with respect to the number of seeds. We have compared the system utilitiesthat our model predicts and the Beijing traces suggest, with various delay constraints and cost weights. It turns out they show similar behaviors as in Figure 6.6; the real traces suggest larger utility values than what the theory predicts when the delay is small. Their difference decreases as the delay budget increases up to some point, after which the difference increases again. In this case the real traces suggest smaller utility values than that of theory. They however share similarities in the shape and trends in the similar manner as in Figure 6.6.

We also examine how good our analytic solution of the optimal number of seeds, k^*_{thr}, would be in the realistic setting induced from the Beijing traces. Figure 6.7 shows the optimal number of seeds and the corresponding empirical system utility with respect to the delay budget. Figure 6.7a compares the empirical optimal number of seeds k^*_{sim} and its analytical counterpart k^*_{thr}. We can see from the figure that k^*_{sim} and k^*_{thr} are getting closer to each other as the delay budget d increases. Although k^*_{sim} and k^*_{thr} have big differences when the delay budget is small, we note that the utility function has a very gentle slope near its optimum in this small delay regime (see Figure 6.6). This is why our analytical solution provides near-optimal performance even in the small delay regime as can be seen in Figure 6.7b.

Figure 6.7b compares the best possible system utility values f^*_{sim} of the trace-based simulations and the empirical utility values $\widetilde{f}_{sim}$ when our solution k^*_{thr} is used. In other words, the figure shows how close the system utility of the real system would be to the system's best possible if the system uses our analytic solution. As can be seen, the system utilities in the real world would be within 95% of their real maximums over the entire delay regime if our theoretical optimizers are used. Therefore, these results support the usefulness of our model.

Chapter 7

Conclusions and Future Work

In this chapter, we present the conclusion of this dissertation and possible directions for future investigations.

7.1 Communication Cost Modeling in Wireless Sensor Networks

We have derived minimum expected search energy costs for several kinds of data-centric wireless sensor networks in Chapter 3. In particular, we have considered structured and unstructured networks deployed in d-dimensional area with a constant node density. In structured networks, the search cost of the FTP deployment of nodes is proportional to $\sqrt[d]{N}/\sqrt[d]{r}$, while that of the RGG deployment is proportional to $\frac{\sqrt[d]{N(\log N)^{\eta-1}}}{\sqrt[d]{r}}$. In unstructured networks, the search cost of the FTP deployment is proportional to $\frac{N}{r+1}$ regardless of the spatial dimension d of the network, while that of the RGG deployment is proportional to $\frac{N(\log N)^{\frac{\eta}{d}}}{r+1}$.

Although we assume constant spatial node density and have presented two specific cases of neighbor density scaling – constant and logarithmic, the approach presented here can be easily extended to consider other kinds of spatial and neighbor density scaling. For example, if we fix the network radius L and the radio range R and let the node density increase as N grows, it is easy to obtain that the search cost of structured networks under the FTP deployment is proportional to $\frac{L}{\sqrt[d]{r}}$ regardless of N, while that of unstructured networks is kept proportional to $\frac{N}{r+1}$.

One caveat to our models originates from the fact that we have resorted to approximating summations in both structured and unstructured cases using integrations since the summations fail to produce tractable closed-from expressions. When the radius of the network L is small or the number of copies r is very large compared to N, the approximations exhibit poor performance. The reason for the latter case is that larger r makes the curves of the integrands sharper.

We believe that the results will be useful analytical tools for exploring the general performance of data-centric wireless sensor networks. For example, the results are used as building blocks to derive optimum data replication for expanding ring search in Chapter 4 and to derive scaling laws in data-centric wireless sensor networks in Chapter 5.

7.2 Optimum Data Replication for Expanding Ring Search

In Chapter 4, we have shown how the number of replicas of event information can be optimized for expanding ring-based queries in wireless sensor networks. We have found that a square-root-proportional replication strategy provides optimal performance both with and without storage constraints. Detailed realistic simulations have validated the analysis.

There are several directions in which these results can be extended. The analysis could be extended to other querying mechanisms, including structured storage, since there is a similar trade-off between search and replication costs in many other settings. The analysis could also be extended to consider more irregular deployment areas, including three-dimensional deployments.

The results have been used to investigate the scaling behavior of querying in storage-constrained sensor networks in Chapter 5. We also plan to develop distributed implementations which allow for optimal or near-optimal replication without global knowledge of the relative query rates for all events.

7.3 Scaling Laws in Data-Centric Wireless Sensor Networks

In Chapter 5, we have investigated the scaling behavior of the data-centric storage and querying in wireless sensor networks. During the investigation, we have derived the communication costs of searching and replication in terms of the energy consumption, and have found out that the square-root-proportional replication optimizes the total communication cost for 2D networks. The main take away from this scalability study is that the event and query rates must scale sufficiently slowly with the network size if scalable performance is desired.

In particular, an important scaling condition is ensuring that $q^{1/2} \cdot m$ be $O(N^{\frac{d-1}{2d}})$ for unstructured networks, and that $q^{\frac{d}{d+1}} \cdot m$ be $O(N^{\frac{d-1}{d}})$ for structured networks. Satisfying this condition ensures that adding nodes to the network is beneficial in that the energy and storage resources they bring outweigh the additional event and query activity they induce. This can be seen from many perspectives: satisfying this condition implies that (i) sensor networks require bounded energy and storage per node, (ii) arbitrarily large networks can be operated successfully with a limited energy budget, and (iii) that the network lifetime increases with network size for a given energy budget.

We have also provided necessary conditions for scalability to handle potentially more sophisticated replication strategies than those considered in our basic analysis. Further, while our analysis is primarily focused on the total energy consumption, we have also considered the hot-spot problem to handle per-node energy constraints. In this context, we have shown that with an appropriate load-balancing scheme, the ratio of the peak energy consumption to average energy consumption remains bounded, implying that our results still remain meaningful.

7.4 Content Dissemination in Heterogeneous Vehicular Networks

We have investigated the optimum content dissemination in the heterogeneous vehicular network in Chapter 6. In this network, each vehicle is equipped with two radios; one is the costly long-range low-bandwidth radio for direct communication with the infrastructure, and the other is the low-cost short-range high-bandwidth radio for communication with peer vehicles. We have considered the problem of how to spread relevant content to more vehicles with smaller cost. We have developed the relevant optimization formulation, derived their analytical solutions with some relaxation, and examined the behaviors of the system under the optimum regime. One interesting takeaway point is that the contents can be disseminated to a large number of vehicles with a few costly access to the infrastructure, if some delay, on the order of an hour, can be tolerated. We have also developed a polynomial algorithm to calculate the exact optimum seed vector with no relaxation.

In order to verify our analysis and justify our assumptions and approximations, we have performed simulations based on the real GPS traces of 632 taxis gathered in Beijing, China. We have found that the real traces show the aggregate inter-encounter time of vehicles is close to the exponential distribution agreeing with our assumption, and that their performance of contents dissemination exhibits similarities to what our model predicts.

In this work, we have assumed a low density of subject vehicles to avoid further level of complexity to the problem, for example, radio interference and packet collisions. Although the low density assumption is not so unrealistic, especially for the early phase of vehicular networks, more extensive investigation is a subject of future work. We have also assumed i.i.d. pair-wise inter-encounter times, and we have pointed out in Section 6.5.5 that the mismatched increase rate of the number of satisfied nodes may be attributed to this assumption. Relaxing this assumption is also a topic of future research.

References

[1] Sensor Networking with Delay Tolerance (SeNDT). `http://down.dsg.cs.tcd.ie/sendt/`.

[2] J. Ahn, S. Kapadia, S. Pattem, A. Sridharan, M. Zuniga, J.-H. Jun, C. Avin, and B. Krishnamachari. Empirical evaluation of querying mechanisms for unstructured wireless sensor networks. *SIGCOMM Comput. Commun. Rev.*, 38:17–26, July 2008.

[3] J. Ahn and B. Krishnamachari. Derivations of the Expected Energy Costs of Search and Replication in Wireless Sensor Networks. Technical Report CENG-2006-3, USC CENG, Apr. 2006.

[4] J. Ahn and B. Krishnamachari. Fundamental scaling laws for energy-efficient storage and querying in wireless sensor networks. In *MobiHoc '06: Proceedings of the 7th ACM international symposium on Mobile ad hoc networking and computing*, 2006.

[5] J. Ahn and B. Krishnamachari. Modeling Search Costs in Wireless Sensor Networks. In *SpaSWiN '07: Workshop on Spatial Stochastic Models in Wireless Networks*, 2007.

[6] J. Ahn and B. Krishnamachari. Scaling Laws for Data-Centric Storage and Querying in Wireless Sensor Networks. *IEEE/ACM Transactions on Networking*, 17:1242–1255, August 2009.

[7] J. Ahn, B. Krishnamachari, F. Bai, and L. Zhang. Optimizing Content Dissemination in Heterogeneous Vehicular Networks. Technical Report CENG-2010-2, USC CENG, 2010.

[8] I. Akyildiz, W. Su, Y. Sankarasubramaniam, and E. Cayirci. A Survey on Sensor Networks. *Communications Magazine, IEEE*, 40(8):02–114, aug 2002.

[9] C. Avin and C. Brito. Efficient and Robust Query Processing in Dynamic Environments Using Random Walk Techniques. In *IPSN '04: The 3rd ACM international symposium on Information processing in sensor networks*, 2004.

[10] F. Bai and A. Helmy. Impact of Mobility on Last Encounter Routing Protocols. In *SECON '07: The 4th Annual IEEE Communications Society Conference on Sensor, Mesh and Ad Hoc Communications and Networks*, 2007.

[11] F. Bai and B. Krishnamachari. Spatio-temporal variations of vehicle traffic in VANETs: facts and implications. In *VANET '09: The 6th ACM International Workshop on Vehicular Internetworking*, 2009.

[12] F. Bai and B. Krishnamachari. Exploiting the Wisdom of the Crowd: Localized, Distributed Information-Centric VANETs. *IEEE Communications Magazine*, 48(5), 2010.

[13] F. Bai and H. Krishnan. Reliability Analysis of DSRC Wireless Communication for Vehicle Safety Applications. In *ITSC '06: The 9th International IEEE Conference on Intelligent Transportation Systems*, 2006.

[14] M. Bathula, M. Ramezanali, I. Pradhan, N. Patel, J. Gotschall, and N. Sridhar. A Sensor Network System for Measuring Traffic in Short-Term Construction Work Zones. In *DCOSS '09: International Conference on Distributed Computing in Sensor Systems*. 2009.

[15] C. Bettstetter. Mobility Modeling in Wireless Networks: Categorization, Smooth Movement, and Border Effects. *SIGMOBILE Mob. Comput. Commun. Rev.*, 5:55–66, July 2001.

[16] C. Bettstetter and C. Wagner. The Spatial Node Distribution of the Random Waypoint Mobility Model. In *WMAN '02: Mobile Ad-Hoc Netzwerke, 1. deutscher Workshop uber Mobile Ad-Hoc Netzwerke*, 2002.

[17] M. Bhardwaj and A. P. Chandrakasan. Bounding the Lifetime of Sensor Networks Via Optimal Role Assignments. In *INFOCOM '02: Proceedings of the 21st Annual Joint Conference of the IEEE Computer and Communications Societies*, 2002.

[18] B. Bhargava, X. Wu, Y. Lu, and W. Wang. Integrating heterogeneous wireless technologies: a cellular aided mobile Ad Hoc network (CAMA). *Mob. Netw. Appl.*, 9(4), 2004.

[19] D. Braginsky and D. Estrin. Rumor routing algorthim for sensor networks. In *WSNA '02: The 1st ACM international workshop on Wireless sensor networks and applications*, 2002.

[20] J. Broch, D. A. Maltz, D. B. Johnson, Y.-C. Hu, and J. Jetcheva. A performance comparison of multi-hop wireless ad hoc network routing protocols. In *MobiCom '98: In Proceedings of the 4th Annual international Conference on Mobile Computing and Networking*, 1998.

[21] J. Burgess, B. Gallagher, D. Jensen, and B. N. Levine. MaxProp: Routing for Vehicle-Based Disruption-Tolerant Networks. In *INFOCOM '06: The 25th IEEE International Conference on Computer Communications*, 2006.

[22] B. Burns, O. Brock, and B. Levine. MV Routing and Capacity Building in Disruption Tolerant Networks. In *INFOCOM '05: The 24th IEEE Annual Joint Conference of the IEEE Computer and Communications Societies*, 2005.

[23] A. Chaintreau, P. Hui, J. Crowcroft, C. Diot, R. Gass, and J. Scott. Impact of Human Mobility on the Design of Opportunistic Forwarding Algorithms. In *INFOCOM '06: The 25th Annual Joint Conference of the IEEE Computer and Communications Societies*, 2006.

[24] A. Chaintreau, J.-Y. Le Boudec, and N. Ristanovic. The age of gossip: spatial mean field regime. In *SIGMETRICS '09: Proceedings of the 11th ACM international joint conference on measurement and modeling of computer systems*, 2009.

[25] A. Chaintreau, J.-Y. Le Boudec, and N. Ristanovic. The age of gossip: spatial mean field regime. In *SIGMETRICS '09: Proceedings of the 11th ACM international joint conference on measurement and modeling of computer systems*, 2009.

[26] C. Chan and G. Wu. Pivotal Role of Heterogeneous Networks in 4G Deployment. In *ZTE Technologies, China*, January 2010.

[27] J. Chang and L. Tassiulas. Maximum Lifetime Routing In Wireless Sensor Networks. *IEEE/ACM Transactions on Networking*, 12(4):609–619, Aug. 2004.

[28] N. Chang and M. Liu. Revisiting the TTL-based Controlled Flooding Search: Optimality and Randomization. *MobiCom '04: Proceedings of the 10th annual international conference on Mobile computing and networking*, 2004.

[29] K. Chebrolu, B. Raman, N. Mishra, P. K. Valiveti, and R. Kumar. BriMon: A Sensor Network System for Railway Bridge Monitoring. In *MobiSys '08: The 6th international conference on Mobile systems, applications, and services*, 2008.

[30] Z. Cheng and W. B. Heinzelman. Flooding Strategy for Target Discovery in Wireless Networks. *Wireless Networks*, 11:607–618, 2005.

[31] J. Cho and Z. J. Hass. On the throughput enhancement of the downstream channel in cellular radio networks through multihop relaying. In *IEEE JSAC*, 2004.

[32] CISCO. Cisco Visual Networking Index Forecast Predicts Continued Mobile Data Traffic Surge. Feb. 2010. available online at http://www.cisco.com/web/MT/news/10/news_220210.html.

[33] E. Cohen and S. Shenker. Replication strategies in unstructured peer-to-peer networks. In *ACM SIGCOMM*, 2002.

[34] D. D. Couto, D. Aguayo, J. Bicket, and R. Morris. A High-Throughput Path Metric for Multi-Hop Wireless Routing. In *MobiCom '03: In Proceedings of the 9th Annual international Conference on Mobile Computing and Networking*, 2003.

[35] D. Daley and J. Gani. *Epidemic Modelling*. Cambridge University Press, 1999.

[36] J. Eriksson, H. Balakrishnan, and S. Madden. Cabernet: vehicular content delivery using WiFi. In *MobiCom '08: In Proceedings of the 14th Annual international Conference on Mobile Computing and Networking*, 2008.

[37] K. Fall. A delay-tolerant network architecture for challenged internets. In *ACM SIGCOMM*, 2003.

[38] L. Filipponi, S. Santini, and A. Vitaletti. Data Collection in Wireless Sensor Networks for Noise Pollution Monitoring. In *DCOSS '08: International Conference on Distributed Computing in Sensor Systems*. 2008.

[39] A. Ganesh, L. Massouli, and D. Towsley. The effect of network topology on the spread of epidemics. In *INFOCOM '05: The 24th Annual Joint Conference of the IEEE Computer and Communications Societies*, 2005.

[40] T. Gao, T. Massey, M. Sarrafzadeh, L. Selavo, and M. Welsh. Participatory User Centered Design Techniques for a Large Scale Ad-Hoc Health Information System. In *HealthNet '07: The 1st ACM SIGMOBILE international workshop on Systems and networking support for healthcare and assisted living environments*, 2007.

[41] S. Ghandeharizadeh, S. Kapadia, and B. Krishnamachari. Comparison of replication strategies for content availability in C2P2 networks. In *MDM '05: The 6th International Conference on Mobile Data Management*, 2005.

[42] R. Govindan. Data-centric Routing and Storage in Sensor Networks. In C. Raghavendra, K. Sivalingam, and T. Znati, editors, *Wireless Sensor Networks*, chapter 9, pages 185–206. Kluwer Academic Publishers, 2004.

[43] B. Greenstein, S. Ratnasamy, S. Shenker, R. Govindan, and D. Estrin. DIFS: a distributed index for features in sensor networks. *Ad Hoc Networks*, 1(2-3):333 – 349, 2003.

[44] R. Groenevelt, P. Nain, and G. Koole. The Message Delay in Mobile Ad Hoc Networks. *Performance Evaluation*, 62(1-4):210 – 228, 2005.

[45] R. Groenevelt, P. Nain, and G. Koole. The Message Delay In Mobile Ad Hoc Networks. *Elsevier Journal of Performance Evaluation*, 2005.

[46] M. Grossglauser and D. N. C. Tse. Mobility increases the capacity of ad hoc wireless networks. *IEEE/ACM Transactions on Networking*, 10:477–486, August 2002.

[47] I. . W. Group. http://www.ieee802.org/21/.

[48] R. Guerin. Channel Occupancy Time Distribution in a Cellular Radio System. *IEEE Transactions on Vehicular Technology*, 36(3):89–99, aug 1987.

[49] P. Gupta and P. Kumar. Critical Power for Asymptotic Connectivity in Wireless Networks. *Stochastic Analysis, Control, Optimization and Applications: A Volume in Honor of WH Fleming*, 3(20):547–566, 1998.

[50] P. Gupta and P. Kumar. Internets in the sky: capacity of 3D wireless networks. In *CDC '00: Proceedings of the 39th IEEE Conference on Decision and Control*, volume 3, pages 2290–2295, 2000.

[51] P. Gupta and P. Kumar. The Capacity of Wireless Networks. *IEEE Transactions on Information Theory*, 46(2), Mar. 2000.

[52] Z. Haas and T. Small. A New Networking Model For Biological Applications Of Ad Hoc Sensor Networks. *IEEE/ACM Transactions on Networking*, 2006.

[53] K. Harras, K. Almeroth, and E. Belding-Royer. Delay Tolerant Mobile Networks (DTMNs): Controlled Flooding in Sparse Mobile Networks. In *NETWORKING '05: Networking Technologies, Services, and Protocols; Performance of Computer and Communication Networks; Mobile and Wireless Communications Systems*, volume 3462, pages 41–91. 2005.

[54] C. Hartung, R. Han, C. Seielstad, and S. Holbrook. FireWxNet: A Multi-Tiered Portable Wireless System for Monitoring Weather Conditions in Wildland Fire Environments. In *MobiSys '06: The 4th ACM international conference on Mobile systems, applications and services*, 2006.

[55] T. He, S. Krishnamurthy, J. A. Stankovic, T. Abdelzaher, L. Luo, R. Stoleru, T. Yan, L. Gu, J. Hui, and B. Krogh. Energy-Efficient Surveillance System Using Wireless Sensor Networks. In *MobiSys '04: The 2nd ACM international conference on Mobile systems, applications, and services*, 2004.

[56] W. Heinzelman, A. Chandrakasan, and H. Balakrishnan. An application-specific protocol architecture for wireless microsensor networks. *IEEE Transactions on Wireless Communications*, 1(4):660–670, Oct. 2002.

[57] W. Hu, N. Bulusu, C. T. Chou, S. Jha, A. Taylor, and V. N. Tran. Design and Evaluation of a Hybrid Sensor Network for Cane Toad Monitoring. *ACM Transactions on Sensor Networks*, 5:4:1–4:28, February 2009.

[58] Z. Hu and B. Li. Fundamental Performance Limits of Wireless Sensor Networks. In Y. Xiao and Y. Pan, editors, *Ad Hoc and Sensor Networks*. Nova Science Publishers, 2004.

[59] M. Imase and B. Waxman. Dynamic Steiner Tree Problem. *SIAM Journal on Discrete Mathematics*, 4:369, 1991.

[60] C. Intanagonwiwat, D. Estrin, R. Govindan, and J. Heidemann. Impact of Network Density on Data Aggregation in Wireless Sensor Networks. In *ICDCS '02: The 22nd International Conference on Distributed Computing Systems*, 2002.

[61] C. Intanagonwiwat, R. Govindan, and D. Estrin. Directed Diffusion: a Scalable and Robust Communication Paradigm for Sensor Networks. In *MobiCom '00: In Proceedings of the 6th Annual international Conference on Mobile Computing and Networking*, 2000.

[62] D. B. Johnson and D. A. Maltz. Dynamic Source Routing in Ad Hoc Wireless Networks. In *Mobile Computing*, volume 353 of *The Kluwer International Series in Engineering and Computer Science*, pages 153–181. 1996.

[63] D. B. Johnson, D. A. Maltz, and J. Broch. Ad hoc networking. chapter DSR: the dynamic source routing protocol for multihop wireless ad hoc networks, pages 139–172. 2001.

[64] P. Juang, H. Oki, Y. Wang, M. Martonosi, L. S. Peh, and D. Rubenstein. Energy-Efficient Computing for Wildlife Tracking: Design Tradeoffs and Early Experiences With ZebraNet. In *ASPLOS-X '02: The 10th ACM international conference on Architectural support for programming languages and operating systems*, 2002.

[65] K. Kalpakis, K. Dasgupta, and P. Namjoshi. Efficient algorithms for maximum lifetime data gathering and aggregation in wireless sensor networks. *Computer Networks: The International Journal of Computer and Telecommunications Networking*, 42(6):697–716, Aug. 2003.

[66] S. Kapadia and B. Krishnamachari. Comparative Analysis of Push-Pull Query Strategies for Wireless Sensor Networks. In *DCOSS '06: International Conference on Distributed Computing in Sensor Systems*, 2006.

[67] S. Kim, S. Pakzad, D. Culler, J. Demmel, G. Fenves, S. Glaser, and M. Turon. Health Monitoring of Civil Infrastructures Using Wireless Sensor Networks. In *IPSN '07: The 6th ACM international conference on Information processing in sensor networks*, 2007.

[68] B. Krishnamachari and J. Ahn. Optimizing Data Replication for Expanding Ring-based Queries in Wireless Sensor Networks. In *WiOpt '06: Proceedings of the 4th International Symposium on Modeling and Optimization in Mobile, Ad Hoc and Wireless Networks*, 2006.

[69] L. Krishnamurthy, R. Adler, P. Buonadonna, J. Chhabra, M. Flanigan, N. Kushalnagar, L. Nachman, and M. Yarvis. Design and Deployment of Industrial Sensor Networks: Experiences from a Semiconductor Plant and the North Sea. In *SenSys '05: The 3rd ACM international conference on Embedded networked sensor systems*, pages 64–75, 2005.

[70] F. Kuhn, T. Moscibroda, and R. Wattenhofer. Initializing Newly Deployed Ad Hoc and Sensor Networks. In *MobiCom '04: In Proceedings of the 10th Annual international Conference on Mobile Computing and Networking*, 2004.

[71] L. Kllstrma, S. Leggiob, J. Mannerb, T. Mikkonenc, K. Raatikainenb, J. Saarinenc, S. Suorantaa, and A. Yl-Jskia. A Framework for Seamless Service Interworking in Ad-Hoc Networks. *Elsevier Journals on Computer Communications*, 2006.

[72] L. K. Law, S. V. Krishnamurthy, and M. Faloutsos. Capacity of Hybrid Cellular-Ad Hoc Data Networks. In *INFOCOM '09: Proceedings of the 28th Annual Joint Conference of the IEEE Computer and Communications Societies*, 2009.

[73] J. LeBrun, C.-N. Chuah, D. Ghosal, and M. Zhang. Knowledge-Based Opportunistic Forwarding in Vehicular Wireless Ad Hoc Networks. In *VTC '05: IEEE Vehicular Technology Conference*, 2005.

[74] K. Lee, S.-H. Lee, R. Cheung, U. Lee, and M. Gerla. First Experience with CarTorrent in a Real Vehicular Ad Hoc Network Testbed. In *MOVE '07: The IEEE Workshop on MObile Networks for Vehicular Environments*, 2007.

[75] J. Leguay, T. Friedman, and V. Conan. Evaluating Mobility Pattern Space Routing for DTNs. In *INFOCOM '06: The 25th IEEE International Conference on Computer Communications*, 2006.

[76] O. Leveque and E. Preissmann. Scaling laws for one-dimensional ad Hoc Wireless networks. *IEEE Transactions on Information Theory*, 51(11):3987–3991, Nov. 2005.

[77] O. Leveque and I. Telatar. Information-theoretic upper bounds on the capacity of large extended ad hoc wireless networks. *IEEE Transactions on Information Theory*, 51(3):858–865, Mar. 2005.

[78] X. Li, Y. Kim, R. Govindan, and W. Hong. Multi-dimensional Range Queries in Sensor Networks. In *SenSys '03: The First ACM Conference on Embedded Networked Sensor Systems*, 2003.

[79] L. Lima and J. Barros. Random Walks on Sensor Networks. In *WiOpt 2007: The 5th International Symposium on Modeling and Optimization in Mobile, Ad Hoc and Wireless Networks and Workshops*, 2007.

[80] Y.-D. Lin and Y.-C. Hsu. Multihop Cellular: A New Architecture for Wireless Communication. In *INFOCOM '00: The 19th Annual Joint Conference of the IEEE Computer and Communications Societies*, 2000.

[81] A. Lindgren, A. Doria, and O. Schelén. Probabilistic routing in intermittently connected networks. *SIGMOBILE Mob. Comput. Commun. Rev.*, 7:19–20, July 2003.

[82] B. Liu, Z. Liu, and D. Towsley. On the Capacity of Hybrid Wireless Networks. In *INFOCOM '03: Proceedings of the 22nd Annual Joint Conference of the IEEE Computer and Communications Societies*, 2003.

[83] X. Liu, Q. Huang, and Y. Zhang. Combs, needles, haystacks: balancing push and pull for discovery in large-scale sensor networks. In *SenSys '04: The 2nd international conference on Embedded networked sensor systems*, 2004.

[84] Q. Lv, P. Cao, E. Cohen, K. Li, and S. Shenker. Search and replication in unstructured peer-to-peer networks. In *ICS '02: The 16th International Conference on Supercomputing*, 2002.

[85] A. Mainwaring, D. Culler, J. Polastre, R. Szewczyk, and J. Anderson. Wireless Sensor Networks for Habitat Monitoring. In *WSNA '02: The 1st ACM international workshop on Wireless sensor networks and applications*, 2002.

[86] A. Milenkovic, C. Otto, and E. Jovanov. Wireless Sensor Networks for Personal Health Monitoring: Issues and an Implementation. *Computer Communications*, 29(13-14):2521 – 2533, 2006. Wirelsess Senson Networks and Wired/Wireless Internet Communications.

[87] L. Nachman, R. Kling, R. Adler, J. Huang, and V. Hummel. The Intel Mote Platform: A Bluetooth-Based Sensor Network for Industrial Monitoring. In *IPSN '05: The 4th IEEE international symposium on Information processing in sensor networks*, 2005.

[88] P. Nain, D. Towsley, B. Liu, and Z. Liu. Properties of Random Direction Models. In *INFOCOM '05: The 24th Annual Joint Conference of the IEEE Computer and Communications Societies*, 2005.

[89] A. Nandan, S. Das, B. Zhou, G. Pau, and M. Gerla. AdTorrent: Digital Billboards for Vehicular Networks. In *V2VCOM '05: The First International Workshop on Vehicle-to-Vehicle Communications*, 2005.

[90] NYTimes. Customers Angered as iPhones Overload AT&T. september 2009.

[91] J. Paek, K. Chintalapudi, R. Govindan, J. Caffrey, and S. Masri. A Wireless Sensor Network for Structural Health Monitoring: Performance and Experience. In *EmNetS-II '05: The Second IEEE Workshop on Embedded Networked Sensors*, 2005.

[92] K. Pahlavan, P. Krishnmaurthy, A. Hatami, M. Ylianttila, J. Makela, R. Pichna, and J. Vallstron. Handoff in Hybrid Mobile Networks. *IEEE Personal Communication*, 2000.

[93] M. Penrose. The Longest Edge of the Random Minimal Spanning Tree. *The Annals of Applied Probability*, 7(2):340–361, 1997.

[94] M. Penrose. A Strong Law for the Longest Edge of the Minimal Spanning Tree. *The Annals of Probability*, 27(1):246–260, 1999.

[95] C. E. Perkins and E. M. Royer. Ad-hoc On-Demand Distance Vector Routing. *IEEE Workshop on Mobile Computing Systems and Applications*, 1999.

[96] H. Ramamurthy, B. Prabhu, R. Gadh, and A. Madni. Wireless Industrial Monitoring and Control Using a Smart Sensor Platform. *IEEE Sensors Journal*, 7(5):611 –618, may 2007.

[97] A. Rath, S. Hua, and S. Panwar. Femtohaul: Using Femtocells with Relays to Increase Macrocell Backhaul Bandwidth. In *INFOCOM '10: Proceedings of the 29th Annual Joint Conference of the IEEE Computer and Communications Societies*, 2010.

[98] S. Ratnasamy, B. Karp, S. Shenker, D. Estrin, R. Govindan, L. Yin, and F. Yu. Data-Centric Storage in Sensornets with GHT, a Geographic Hash Table. *Mobile Networks and Applications*, 8:427–442, 2003.

[99] J. Reich and A. Chaintreau. The age of impatience: optimal replication schemes for opportunistic networks. In *CoNEXT '09: The 5th ACM International Conference on emerging Networking EXperiments and Technologies*, 2009.

[100] I. Rhee, M. Shin, S. Hong, K. Lee, and S. Chong. On the Levy-Walk Nature of Human Mobility. In *INFOCOM '08: The 27th Annual Joint Conference of the IEEE Computer and Communications Societies*, 2008.

[101] H. Robbins. Remark of Stirling's Formula. *Amer. Math. Monthly 62*, pages 26–29, 1955.

[102] N. Sadagopan, B. Krishnamachari, and A. Helmy. The acquire mechanism for efficient querying in sensor networks. In *The 1st IEEE International Workshop on Sensor Network Protocols and Applications*, 2003.

[103] A. Salkintzis, C. Fors, and R. Pazhyannur. WLAN-GPRS Integration for Next-Generation Mobile Data Networks. *IEEE Comm. Mag.*, 2002.

[104] R. C. Shah, S. Roy, S. Jain, and W. Brunette. Data mules: modeling and analysis of a three-tier architecture for sparse sensor networks. *Ad Hoc Networks*, 1(2-3):215 – 233, 2003.

[105] S. Shakkottai. Asymptotics of Query Strategies over a Sensor Network. In *INFOCOM '04: The 23rd Annual Joint Conference of the IEEE Computer and Communications Societies*, 2004.

[106] G. Sharma and R. Mazumdar. Scaling Laws For Capacity And Delay In Wireless Ad Hoc Networks With Random Mobility. In *ICC '04: The IEEE International Conference on Communications*, 2004.

[107] S. Shenker, S. Ratnasamy, B. Karp, R. Govindan, and D. Estrin. Data-centric storage in sensornets. *SIGCOMM Comput. Commun. Rev.*, 33:137–142, January 2003.

[108] T. Small and Z. J. Haas. Resource and performance tradeoffs in delay-tolerant wireless networks. In *WDTN '05: The ACM SIGCOMM workshop on Delay-tolerant networking*, 2005.

[109] T. Spyropoulos, K. Psounis, and C. S. Raghavendra. Spray and wait: an efficient routing scheme for intermittently connected mobile networks. In *WDTN '05: The ACM SIGCOMM workshop on Delay-tolerant networking*, 2005.

[110] T. Spyropoulos, K. Psounis, and C. S. Raghavendra. Efficient routing in intermittently connected mobile networks: the multiple-copy case. *IEEE/ACM Transactions on Networking*, 16(1), 2008.

[111] I. Stoianov, L. Nachman, S. Madden, and T. Tokmouline. PIPENET: A Wireless Sensor Network for Pipeline Monitoring. In *IPSN '07: The 6th ACM international conference on Information processing in sensor networks*, 2007.

[112] R. Szewczyk, E. Osterweil, J. Polastre, M. Hamilton, A. Mainwaring, and D. Estrin. Habitat Monitoring With Sensor Networks. *Commun. ACM*, 47:34–40, June 2004.

[113] B. Thorstensen, T. Syversen, T.-A. Bjørnvold, and T. Walseth. Electronic Shepherd - a Low-Cost, Low-Bandwidth, Wireless Network System. In *MobiSys '04: The 2nd ACM international conference on Mobile systems, applications, and services*, 2004.

[114] H. Tian, H. Shen, and T. Matsuzawa. RandomWalk Routing for Wireless Sensor Networks. *International Conference on Parallel and Distributed Computing Applications and Technologies*, 2005.

[115] O. Tipmongkolsilp, S. Zaghloul, and A. Jukan. The Evolution of Cellular Backhaul Technologies: Current Issues and Future Trends. In *IEEE Communications Surveys & Tutorials*, 2010.

[116] G. Tolle, J. Polastre, R. Szewczyk, D. Culler, N. Turner, K. Tu, S. Burgess, T. Dawson, P. Buonadonna, D. Gay, and W. Hong. A Macroscope in the Redwoods. In *SenSys '05: The 3rd ACM international conference on Embedded networked sensor systems*, 2005.

[117] S. Toumpis. Capacity Bound for Three Classes of Wireless Networks: Asymmetric, Cluster and Hybird. In *MobiHoc '04: Proceedings of the 5th ACM international symposium on Mobile ad hoc networking and computing*, 2004.

[118] Y.-C. Tseng, S.-Y. Ni, Y.-S. Chen, and J.-P. Sheu. The broadcast storm problem in a mobile ad hoc network. *Wirel. Netw.*, 8:153–167, March 2002.

[119] A. Vahdat and D. Becker. Epidemic Routing for Partially Connected Ad Hoc Networks. Technical Report CS-200006, Duke University, Apr. 2000.

[120] A. Vahdat and D. Becker. Epidemic Routing For Partially-Connected Ad Hoc Networks. Technical Report CS-2000-06, UCSD, 2000.

[121] Y. Wang, D. Chakrabarti, C. Faloutsos, C. Wang, and C. Wang. Epidemic spreading in real networks: An eigenvalue viewpoint. In *SRDS '03: The 22nd Symposium on Reliable Distributed Systems*, 2003.

[122] T. Wark, C. Crossman, W. Hu, Y. Guo, P. Valencia, P. Sikka, P. Corke, C. Lee, J. Henshall, K. Prayaga, J. O'Grady, M. Reed, and A. Fisher. The Design and Evaluation of a Mobile Sensor/Actuator Network for Autonomous Animal Control. In *IPSN '07: The 6th ACM international conference on Information processing in sensor networks*, 2007.

[123] E. W. Weisstein. Disk Line Picking. MathWorld–A Wolfram Web Resource. available online at http://mathworld.wolfram.com/DiskLinePicking.html.

[124] G. Werner-Allen, J. Johnson, M. Ruiz, J. Lees, and M. Welsh. Monitoring Volcanic Eruptions With a Wireless Sensor Network. In *Proceedings of the 2nd European Workshop on Wireless Sensor Networks*, 2005.

[125] J. Widmer and J.-Y. Le Boudec. Network coding for efficient communication in extreme networks. In *WDTN '05: The ACM SIGCOMM workshop on Delay-tolerant networking*, 2005.

[126] E. Woodrow and W. Heinzelman. SPIN-IT: a data centric routing protocol for image retrieval in wireless networks. In *International Conference on Image Processing*, 2002.

[127] H. Wu, C. Qiao, S. De, and O. Tonguz. Integrated Cellular and Ad Hoc Relaying Systems: iCAR. In *IEEE Journal on Selected Areas in Communications*, 2001.

[128] L. Xie and P. Kumar. A network information theory for wireless communication: scaling laws and optimal operation. *IEEE Transactions on Information Theory*, 50(5):748–767, May 2004.

[129] Y. Xu, J. Heidemann, and D. Estrin. Geography-Informed Energy Conservation for Ad Hoc Routing. In *MobiCom '01: In Proceedings of the 7th Annual international Conference on Mobile Computing and Networking*, 2001.

[130] M. Ylianttila, M. Pande, J. Makela, and P. Mahonen. Optimization Scheme for Mobile Users Performing Vertical Handoffs between IEEE 802.11 and GPRS/EDGE Networks. In *IEEE Proceeding of Global Telecommunication Conferences*, 2001.

[131] J. Yoon, M. Liu, and B. Noble. Random Waypoint Considered Harmful. In *INFOCOM '03: The 22nd Annual Joint Conference of the IEEE Computer and Communications*, 2003.

[132] O. Younis and S. Fahmy. Distributed clustering in ad-hoc sensor networks: a hybrid, energy-efficient approach. In *INFOCOM '04: Twenty-third Annual Joint Conference of the IEEE Computer and Communications Societies*, 2004.

[133] L. Yu, N. Wang, and X. Meng. Real-Time Forest Fire Detection With Wireless Sensor Networks. In *WCNM '05: The International Conference on Wireless Communications, Networking and Mobile Computing*, 2005.

[134] Q. Yuan, I. Cardei, and J. Wu. Predict and relay: an efficient routing in disruption-tolerant networks. In *MobiHoc '09: Proceedings of the 10th ACM international symposium on Mobile ad hoc networking and computing*, 2009.

[135] T. Zahn, G. O'Shea, and A. Rowstron. Feasibility of content dissemination between devices in moving vehicles. CoNEXT '09: The 5th ACM International Conference on emerging Networking EXperiments and Technologies, 2009.

[136] P. Zhang, C. M. Sadler, S. A. Lyon, and M. Martonosi. Hardware Design Experiences in ZebraNet. In *SenSys '04: The 2nd ACM international conference on Embedded networked sensor systems*, 2004.

[137] X. Zhang, G. Neglia, J. Kurose, and D. Towsley. Performance modeling of epidemic routing. *Computer Networks*, 51(10):2867 – 2891, 2007.

[138] M. Zuniga and B. Krishnamachari. A Realistic Wireless Link Quality Model and Generator. *available online at http://anrg.usc.edu/www/index.php/Downloads*, 2005.

Appendix: Lemmas for Search Cost Modeling

Lemma A.1. *For $r \geq 1$ and $1 \leq d \leq 12$, the following double inequality holds:*

$$\left(\frac{d}{d+1}\right)^{\frac{2+3d}{2d}} \frac{exp\left(\frac{1}{d}\right)}{\sqrt[d]{r}} \;<\; \frac{\Gamma(r+1)}{\Gamma(r+\frac{1}{d}+1)} \;<\; \frac{exp\left(\frac{1}{d}+\frac{12+d}{12(12+13d)}\right)}{\sqrt[d]{e}} \cdot \frac{1}{\sqrt[d]{r}}$$

Proof. From Robbins 1955 [101], Stirling's approximation can be extended to the following double inequality:

$$\Gamma(r+1) \quad > \quad \sqrt{2\pi} r^{r+\frac{1}{2}} e^{-r+\frac{1}{12r+1}} \tag{A.1}$$

$$\Gamma(r+1) \quad < \quad \sqrt{2\pi} r^{r+\frac{1}{2}} e^{-r+\frac{1}{12r}} \tag{A.2}$$

Using Equation (A.2),

$$\Gamma(r+\frac{1}{d}+1) \quad < \quad \sqrt{2\pi}(r+\frac{1}{d})^{r+\frac{1}{d}+\frac{1}{2}}\ e^{-r-\frac{1}{d}+\frac{d}{12rd+12}}$$

From the above equation and (A.1),

$$\begin{aligned}
\frac{\Gamma(r+1)}{\Gamma(r+\frac{1}{d}+1)} &> \frac{1}{\sqrt[d]{r}}\left(\frac{rd}{rd+1}\right)^{\frac{2rd+d+2}{2d}} \quad e^{\left(\frac{1}{d}+\frac{12-d}{12(12r+1)(rd+1)}\right)} \\
&\geq \frac{1}{\sqrt[d]{r}}\left(\frac{d}{d+1}\right)^{\frac{3d+2}{2d}} \quad e^{\left(\frac{1}{d}+\frac{12-d}{12(12r+1)(rd+1)}\right)} \\
&\geq \frac{1}{\sqrt[d]{r}}\left(\frac{d}{d+1}\right)^{\frac{3d+2}{2d}} \quad e^{\frac{1}{d}}
\end{aligned}$$

Note that the second inequality holds since $\left(\frac{rd}{rd+1}\right)^{\frac{2rd+d+2}{2d}}$ is increasing with respect to r for $r \geq 1$ so that it has its minimum value at $r = 1$. And the third inequality holds since $\frac{12-d}{12(12r+1)(rd+1)} \geq 0$ for $r \geq 1$ and $d \leq 12$.

In the other hand, using the Robbins' double inequality in the other way around produces the following:

$$\frac{\Gamma(r+1)}{\Gamma(r+\frac{1}{d}+1)} < \frac{1}{\sqrt[d]{r}}\left(\frac{rd}{rd+1}\right)^{\frac{2rd+d+2}{2d}} \quad e^{\left(\frac{1}{d}+\frac{d+12}{12r(12rd+d+12)}\right)} \tag{A.3}$$

Let $p(r) = \left(\frac{rd}{rd+1}\right)^{\frac{2rd+d+2}{2d}}$ and $q(r) = e^{\left(\frac{1}{d}+\frac{d+12}{12r(12rd+d+12)}\right)}$. Then, let's calculate the supremum of each of them.

$$\begin{aligned}
\sup_{r\geq 1} p(r) &= \lim_{r\to\infty}\left(\left(1-\frac{1}{rd+1}\right)^{rd+1}\right)^{\frac{1}{d}}\left(\frac{rd}{rd+1}\right)^{-\frac{1}{d}} \\
&\quad (\because p(r) \text{ is increasing w.r.t } r \text{ for } r \geq 1) \\
&= \lim_{t\to\infty}\left(\left(1-\frac{1}{t}\right)^{t}\right)^{\frac{1}{d}} \cdot \lim_{r\to\infty}\left(\frac{rd}{rd+1}\right)^{-\frac{1}{d}} \\
&\quad (\because \text{substituting } t \doteq rd+1) \\
&= e^{-\frac{1}{d}}
\end{aligned} \tag{A.4}$$

$$\begin{aligned}\sup_{r\geq 1} q\left(r\right) &= \exp\left(\frac{1}{d}+\frac{d+12}{12r(12rd+d+12)}\right)\Bigg|_{r=1} \\ &\quad (\because \text{ the exponent is decreasing w.r.t } r \text{ for } r\geq 1) \\ &= \exp\left(\frac{1}{d}+\frac{d+12}{12(13d+12)}\right)\end{aligned}$$

Hence, the RHS of inequality (A.3) can be further upper-bounded using the above supremums resulting in the following:

$$\frac{\Gamma(r+1)}{\Gamma(r+\frac{1}{d}+1)} < \frac{exp\left(\frac{1}{d}+\frac{12+d}{12(12+13d)}\right)}{\sqrt[d]{e}}\cdot\frac{1}{\sqrt[d]{r}}$$

□

Lemma A.2. *Suppose* $h_1(x) > 0$, $h_2(x) > 0$ *for every* $x > 0$, $g_1(y) > 0$, $g_2(y) > 0$ *for every* $y > 0$, *and* $f(x, y) > 0$ *for every* $x > 0$, $y > 0$. *And suppose*

1. $f(x, y) \leq \frac{h_1(x)}{g_1(y)}$ *for every* $x > 0$, $y > 0$

2. $f(x, y) \leq \frac{h_2(x)}{g_2(y)}$ *for every* $x > 0$, $y > 0$

3. $h_1(x) = O(x^n)$ *and* $h_2(x) = O(x^m)$, *where* $n > m > 0$

4. $g_1(y) = \Omega(y^a)$ *and* $g_2(y) = \Omega(y^b)$, *where* $a > b > 0$

Then,

$$f(x, y) = O\left(\frac{x^m}{y^a}\right) \tag{A.5}$$

Proof. From 3) and 4), there exist $c_1 > 0$ and $c_2 > 0$ such that

$$h_2(x) \leq c_1 \cdot x^m, \quad \text{for } \forall x \tag{A.6}$$

$$g_1(y) \geq c_2 \cdot y^a, \quad \text{for } \forall y \tag{A.7}$$

Suppose $f(x, y) = \Theta(x^{m+p} \cdot y^{-a+q})$ where $p, q \in \mathbb{R}$. Then, there exists $c > 0$ such that

$$f(x, y) \geq c \cdot x^{m+p} \cdot y^{-a+q}, \quad \text{for } \forall x, \forall y \tag{A.8}$$

If $p > 0$, then for every $y > 0$,

$$x^p > \frac{c_1}{cy^{-a+q} g_2(y)}$$

for sufficiently large x due to the archimedean property.

$$\Rightarrow f(x, y) \geq cx^{m+p} y^{-a+q} > \frac{c_1 x^m}{g_2(y)} \geq \frac{h_2(x)}{g_2(y)} \quad (\because \text{(A.6)})$$

which is contradiction to 2). Hence, $p \leq 0$.

If $q > 0$, then for every $x > 0$,

$$y^q > \frac{h_1(x)}{cc_2 x^{m+p}}$$

for sufficiently large y due to the archimedean property.

$$\Rightarrow f(x, y) \geq cx^{m+p} y^{-a+q} > \frac{h_1(x)}{c_2 y^a} \geq \frac{h_1(x)}{g_1(y)} \quad (\because \text{(A.7)})$$

which is contradiction to 1). Hence, $q \leq 0$.

From $p \leq 0$ and $q \leq 0$, we conclude that $f(x, y) = O(x^m \cdot y^{-a})$. $\square$